



The University of
Nottingham

*Investigating the role of Proteins in Melanosome
Transport*

Submitted by

Kajana Sivarasa

For the MRes in Bio Medical Science

University of Nottingham

Faculty of Life Science

June 2018

Abstract

The specialized epidermal cells produce melanin within the organelles referred to as melanosomes. These melanosomes are believed to be transported along the microtubules from the perinuclear region to the actin and then the tri-partile complex of myosin Va, Melanophilin and Rab27a move the melanosomes along the actin filaments to the plasma membrane. Any defectiveness or disruption of these proteins leads to several disorders such as Hermansky-Pudlak Syndrome (HPS), Chediak-Higashi Syndrome and Griscelli Syndrome which are caused due to defects in genes that control organelle biogenesis, organelle motility or cargo transport within cells.

The key aim of this project is to study the involvement of the proteins myosin Va, Rab27a and its effector proteins melanophilin and slp2-a. The experiment fluorescence Recovery after photobleaching(FRAP) was performed in different mutant cell lines such as melan-leaden (lacks melanophilin), melan-d (lacks myosin Va) and melan-ash (lacks Rab27a). We then transfected members of the tri-partile complex into these cell cells to observe their effect on melanosome transport. A mutant Rab27a which highly reduces the binding of its effectors slp2 and melanophilin was also used to investigate the binding dynamics of these effector proteins with Rab27a. Finally, these findings led to the idea of constructing a chimeric molecule where the RBD region of melanophilin been replaced with the RBD region of Slp2 and was expected to have a stable interaction with Rab27a.

From these experiments, it was identified that melanophilin has a dynamic interaction with Rab27a and Slp2 has a stable interaction. It was understood that the Rab binding region(RBD) of slp2 and melanophilin perform a major part in controlling the nature of movement with Rab27a.

Acknowledgements

This work has been completed during my studies as a student in MRes in Bio Medical Science in the Faculty of School of Life Sciences at the University of Nottingham.

First of all, I wish to thank Assistant Professor Alistair Hume who has provided continuous guidance throughout this study. His vast experience in bio medical science and his readiness to share that experience have been an ever-reliable resource when I was faced with difficulties in the research. I am grateful for his abundant advises valuable suggestions.

I also wish to express my appreciations to the direct or indirect support for this work from all the colleagues and friends. Finally, I would like to express my sincere gratitude to my family who have stood by me and supported me throughout my education and career. Finally, I would like to thank my husband for encouraging and supporting with all my decisions to complete my MRes project successfully.

Table of Contents

Abstract	I
Acknowledgements	II
List of Figures	VI
List of Tables	IX
Abbreviations	X

1. Introduction

1.1 Cell signalling and vesicle transport	02
1.1.1 Membrane trafficking	02
1.1.2 Exocytosis.....	03
1.1.3 Endocytosis.....	06
1.1.4 Intracellular membrane trafficking of organelles	10
1.1.5 Proteins involved in organelle trafficking.....	10
1.1.6 Dynamics of organelle trafficking involving microtubules	14
1.1.7 Dynamics of organelle trafficking involving actin filaments	18
1.2 Overview: Melanocytes and melanosomes	22
1.3 Melanosome transport.....	24
1.3.1 Melanosome biogenesis and maturation.....	24
1.3.2 Microtubule-dependent anterograde transport from MTOC along tubulin	26
1.3.3 Transfer to actin at cell periphery ready for exocytosis, and actin dependent anterograde melanosome transport	27
1.3.4 Rab proteins and their roles.....	29
1.3.5 Roles of Slp2-a	31
1.3.6 Transfer of melanosome to keratinocyte	32
1.3.7 Comparison of melanosome transport to secretion	35
1.4 Fluorescence Microscopy	36
1.4.1 Introduction	36
1.4.2 Fluorescence Recovery after photo bleaching	37
1.4.3 Applications of FRAP.....	39
1.4.4 Limitations of FRAP	41

1.5 Scope of study	42
1.5.1 Use of mutant cell lines	42
1.5.2 Aim of study	42
1.5.3 Hypotheses.....	42

2. Materials and Methods

2.1 Analysis of the interaction of the proteins	44
2.1.1 Cell Culture.....	44
2.1.2 Transfection	44
2.1.3 Fluorescence Recovery After Photo-bleaching.	45
2.1.4 Image Processing in Image J.....	46
2.1.5 Volocity and Prism Image analysis.....	46
2.2 Further Investigation on the dynamic interaction of Slac2-a.....	49
2.2.1 PCR.....	50
2.2.2 Agarose Gel Electrophoresis.....	51
2.2.3 Restriction Digest Protocol.....	52
2.2.4 De-Phosphorylation	52
2.2.5 DNA Purification and Ligation.....	53
2.2.6 Transformation	54
2.2.7 Preparing agar plates.....	56
2.2.8 Inoculating Overnight Cultures.....	56
2.2.9 DNA Isolation (Mini prep)	57

3. Results

3.1 Rab27-a in different cell lines - Frap analysis of the dynamics of rab 27A in the cell lines melan- a, melan-ln and melan-ash	59
3.1.1 Introduction	59
3.1.2 Rab27a in melan-a	62
3.1.3 Rab27a in melan-ashen.....	63
3.1.4 Rab27a in melan-ln.....	64
3.1.5 Rab27a chimera in melan-a	65
3.1.6 Rab 27a comparison graph in different cell lines.....	66
3.2 Rab27a effectors in different cell lines - Frap analysis of the dynamics of Slac2-a in the cell lines melan-a, melan-ln and melan-d	67
3.2.1 Slac2-a(full) in melan-a	69
3.2.2 Slac2-a RBD in melan-a	70
3.2.3 Slac2-a RBD in melan-ln.....	71
3.2.4 Slac2-a RBD in melan-d.....	72

3.3 Frap analysis of the dynamics of Slp2 in the cell line melan-a	73
3.4 Chimeric Molecule (slp2-mlph Chimera) in Melan-ln	74
3.5 Summary	77
4 Conclusion & Discussion	80
5 References	84

List of figures

1.1 Neurotransmitter exocytosis in neurones.....	5
1.2 The general mechanism involved in regulated secretory granule release.....	6
1.3 Trafficking of molecules between the nucleus, endoplasmic reticulum, Golgi complex, endosomes and the extracellular environment.....	8
1.4 Bidirectional transport of vesicles in cells via microtubule binding.....	10
1.5 Microtubule structure. Protofilaments form from α -tubulin and β -tubulin dimers.....	11
1.6 Intermediate filament structure.....	13
1.7 Polymerisation of G-actin to form F-actin	13
1.8 The dynein and kinesin motor proteins.....	14
1.9 The steps involved in the processivity of (a) kinesin and (b) dynein along the microtubule	15
1.10 Representation of how myosins, kinesin, and dynein are involved in transport of vesicles/ organelles in the cell	17
1.11 The structure and function of the myosin Va molecule.....	20
1.12 The melanocyte	23
1.13 Melanosome maturation	25
1.14 Synthesis of eumelanin and pheomelanin	26
1.15 The proposed structure of the tripartite Rab27a, Slac-2a and myosin Va complex.....	27

1.16 The SNARE protein hypothesis in relation to Rab GTPases	29
1.17 Examples of proteins recruited by Rab GTPases in the four general stages of membrane trafficking.....	30
1.18 Melanosome transfer from the microtubules	31
1.19 Microtubule-based transport	32
1.20 The four proposed mechanisms of melanosome transfer from melanocytes to keratinocytes	34
1.21 Representation of a. late endosomal transport in secretory cells, b. melanosome transport in melanocytes.....	35
1.22 Bohr Model.....	38
1.23 Principles of FRAP	40
1.24 Detail of Fluorescence Recovery curve.....	41
2.1 Percentage Recovery calculation	48
3.1 FRAP analysis of the dynamics of melanosomal GFP-Rab27a in melan-a cells	61
3.2 FRAP analysis of the dynamics of melanosomal GFP-Rab27a in melan-ashen cells.....	62
3.3 FRAP analysis of the dynamics of melanosomal GFP- Rab27a in melan-ln cells.....	63
3.4 FRAP analysis of the dynamics of melanosomal GFP- mutated Rab27 chimeric molecule in melan-a cells	64
3.5 Rab27a recovery comparison graph in different cell lines	65
3.6 FRAP analysis of the dynamics of melanosomal GFP-mlph in melan-a cells.....	68
3.7 FRAP analysis of the dynamics of melanosomal GFP-mlph RBD in melan-a cells	69
3.8 FRAP analysis of the dynamics of melanosomal GFP-mlph RBD in melan-ln cells.....	70

3.9 FRAP analysis of the dynamics of melanosomal GFP-mlph RBD in melan-d cells.....	71
3.10 FRAP analysis of the dynamics of melanosomal GFP-SLP2 in melan-a cells.....	72
3.11 Construction of Chimera	74
3.12 FRAP analysis of the dynamics of melanosomal GFP-Slp2- Mlph chimera in melan-ln cells.....	75
3.13 Average percentage recovery.....	76

List of Tables

2.1 PCR	50
2.2 The primers used for the construction of the chimera slp2- mlph	50
2.3 PCR cycle conditions.....	51
2.4 Components of restriction Digest Protocol.....	52
2.5 Components used in DNA ligation	53
2.6 Choice of vector, insert combination	55
3.1 Average Percentage recovery (mean \pm SD).....	73

Abbreviations

CHS	Chediaki Higashi syndrome
DCT	Dopa Chrome Tautomerase
F-actin	Filamentous actin
FRAP	Fluorescence Recovery After Photobleaching
G-actin	Globular actin
GFP	Green Fluorescent protein
HPS	Hermansky-Pudlak Syndrome
KLC2	Kinesin light chain 2 protein
Kif5b	Kinesin heavy chain
LB	Lysogeny broth
MDCK	Madin–Darby canine kidney
Mlph	Melanophilin
MTOC	Microtubule organising centre
MVB	Multivesicular body
MyoVa	MyosinVa
NSF	N-ethylmaleimide-sensitive factor
PBS	Phosphate Buffered Saline
PMA	Phorbol 12-myristate 13-acetate
P/S	Penicillin/streptomycin
Pi	Inorganic phosphate
RBD	Rab Binding Domain
RGB	Red Green Blue
ROI	Region of Interest
SAP	Shrimp Alkaline phosphatase
SED1	Spondyloepiphyseal dysplasia tarda
TGN	Trans-Golgi network
TI	Transport intermediaries
TYR	Tyrosinase
TYRP1	Tyrosine-related protein 1

Chapter 1

Introduction

1.1 Cell signalling and vesicle transport

Complex multi-cellular organisms have eukaryotic cells containing membrane-bound organelles. In order to achieve homeostasis and effectively respond to stimuli, the process of communication within, and between cells, must be continuous. Organelles including the nucleus, the endoplasmic reticulum, and the Golgi system achieve this via membrane trafficking. This process is used by secretory cells, as well pigment producing melanocytes to perform their major functions. While these cells are specialised to produce material that will be ultimately transported in large quantities outside the cell, other types of cells adopt to use the same methods for smaller volumes of transfer such as transport of molecules from the nucleus to the cytoplasm. Thus the identification of the major cytoskeletal components, vesicular markers, and other proteins becomes important (Andrei, Aixa, and Nava Segev. 2009).

1.1.1 Membrane trafficking

The movement of macromolecules and proteins from the site of synthesis to their ultimate destination within the cell, and to the outside of the cell, is performed through membrane trafficking. This involves the transfer of these molecules into membrane-enclosed organelles, termed transport intermediaries (TI) or vesicles, upon production. This is followed by the targeting of the TI for their destination, via membrane-bound and membrane associated proteins, and their effectors. Transfer of molecules can be between organelles in a specific direction; for example, for the purpose of secretion (Costaguta G, Payne G, 2009).

The major pathways of membrane trafficking are between organelles, to the external environment via exocytosis, and from the outside into the cell by endocytosis (Segev N, 2009).

Each of these needs to be tightly regulated in order to ensure that the correct target is reached through the complex network of linked pathways efficiently. This needs a correct selection of the molecule to be

transported and its increase in concentration in a region of the membrane (Hua Z, Graham T, 2009). This is followed by the emergence of the TI/vesicle as a bud from the membrane, with or without the insertion or attachment of specific proteins markers which serve as tags on the bud. The vesicles then move along cytoskeletal components and dock with the target membrane, via protein complexes involved in “tethering” (Hutagalung & Novick, 2011). After this untethering or removal of any protein, tags can take place. Lastly, the vesicle fuses with the correct compartment to release its contents by the activity of SNARE proteins. The SNARE hypothesis details the fusion of vesicular membranes to other organelle or with the plasma membrane. This involves SNAREs from both the vesicle and the target membrane binding to form a tight complex. SNAREs are transmembrane receptors whose ligands are containing an N-ethylmaleimide-sensitive factor (NSF) domain. The SNARE ligand is termed SNAP; so called as SNAPS are soluble NSF attachment proteins. The NSF is an ATPase which enables the fusion event. This is shown in figure 1.1. The individual pathways have different factors or proteins involved but the master regulator is always a Rab protein (Hutagalung & Novick, 2011).

1.1.2 Exocytosis

It is known that all cells carry out exocytosis as a normal part of their function in order to transport by substances to the outside of the cell or to insert membrane protein into the cell membrane after synthesis, this is termed constitutive exocytosis. However, exocytosis in response to external stimuli, termed regulated exocytosis, is tightly controlled and has been observed as requiring elevation of intracellular calcium ion concentration. Regulated exocytosis involves communication of the cell performing the exocytosis with other cells at a distance, or neighbouring cells respectively through endocrine or paracrine signalling (Nagarajan N, Custer K, Bajjalieh S, 2009).

The general picture of exocytosis shows a multi-step process involving the docking of the vesicle to be exocytosed with the plasma

membrane, priming of the vesicle for exocytosis, which can be enhanced by a super-priming step; with a fusion of the vesicular membrane with the plasma membrane being the last step.

However, in order to understand exocytosis, it is important to be aware that while exocytosis is similar in all cells, it has been studied in specific types of cells, and exocytosis has been found to differ by cell type in terms of which protein are involved in the general steps.

In neurones, an action potential opens voltage gated calcium channels in the presynaptic membrane, and the increase in intracellular calcium triggers the transport of the vesicle towards the cell membrane (Hurst, 2013). Exocytosis in neurones allows neurotransmitter release, as shown in figure 1.1.

Secretory cells have granules and include dendritic cells, such as melanocytes; lymphocytes and natural killer cells. The latter can secrete cytokines by either regulated (as shown in figure 1.2) or constitutive exocytosis. Regulated release involves primary messenger signalling at the plasma membrane by a ligand docking in its receptor. This appears to be similar for all granulocytes.

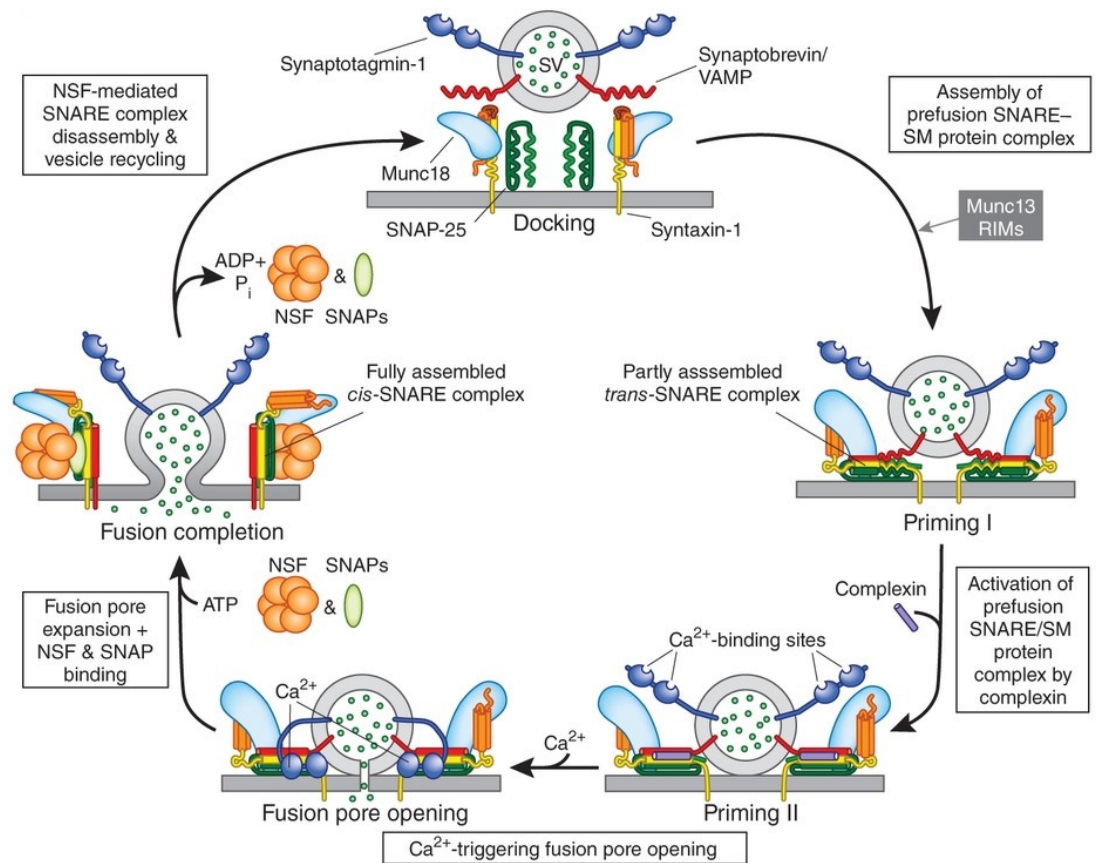


Figure 1.1. Neurotransmitter exocytosis in neurones. The vesicle docks with the cell membrane by synaptobrevin/VAMP in the vesicular associating with proteins at the inner face of the plasma membrane. The vesicle is then primed for exocytosis by the formation of the *trans*-SNARE complex which includes synaptobrevin/VAMP, Munc18, SNAP-25, complexin and syntaxin. Super-priming (shown as priming II) involves zipping of the SNARE complex by complexin. The fusion pore opens upon synaptotagmin in the vesicular membrane binding calcium ions at its C2 domain. In an ATP-driven process vesicular fusion with the plasma membrane is completed when binding of NSF and SNAP proteins in the SNARE complex forms the *cis*-SNARE complex. The vesicle is then recycled and the SNARE complex disassembled. Reprinted from Südhof (2013).

to increasing additional oligomerization of caveolin and is released from the membrane by the action of the GTPase dynamin II.

(iv) Clathrin-mediated endocytosis. Clathrin coats vesicles, by binding to lipo in order to aid vesicular trafficking. It is a protein which polymerises to form a cage structure composed of monomers of 3 light and 3 heavy chains of clathrin.

Receptor-mediated endocytosis can be aided by the presence of *caveolae* and / or clathrin. When clathrin is present the membrane forms clathrin-coated pits. This makes use of the presence of cell surface receptors to bring selected substances into the cell as ligands only bind specific to receptors. Upon binding, the region of the membrane containing the receptor-ligand complex pinches off, to form an endocytic vesicle (Conibear E, Tam Y, 2009).

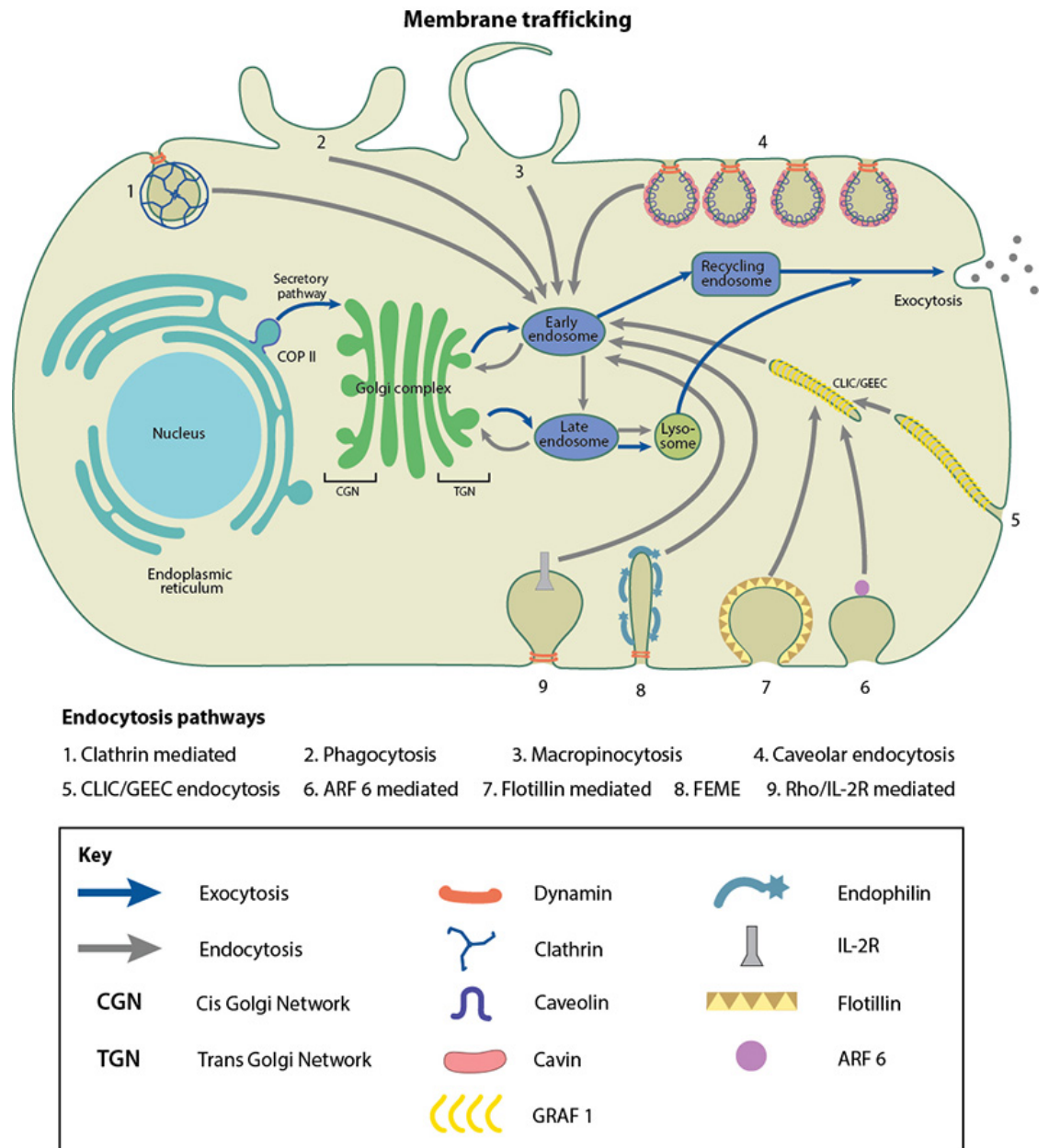


Figure 1.3. Trafficking of molecules between the nucleus, endoplasmic reticulum, Golgi complex, endosomes and the extracellular environment. The blue arrows indicate the process of exocytosis and grey arrows endocytosis. Reprinted from MBInfo contributors. Membrane trafficking pathways. In MBInfo Wiki, Retrieved 10/21/2014 from <http://mbinfo.mbi.nus.edu.sg/figure/membrane-trafficking-pathways/>

Endosomes are formed as a result of vesicular import, often from several vesicles fusing together. Close to the plasma membrane early endosomes function to allow separation of contents for onward transport, for example, dissociation of ligand-receptor complexes and recycling of receptors.

These can be spherical with tube-like projections and have a slightly acidic pH. In contrast, late endosomes have a lower pH and are postulated to be involved in moving material from the early endosome to the lysosome. They can also transport materials from phagosome and newly synthesised products from the Golgi. The material brought into the cell by endocytosis terminates at the lysosome which has the lowest pH of all organelles, and in these large molecules are hydrolyzed by enzyme action into monomers which can then be used by the cell once the endosome releases these to the cytosol (Pruess M, Weidman P, Nielsen E., 2009).

The current major focus of research divides endocytosis into clathrin-depend versus clathrin-independent pathways. Studying membrane trafficking is an intricate process and often difficult to study *in vivo*. However, melanosomes, the organelles specialised for melanin synthesis in melanocytes, have been extensively studied to elucidate some of the actions involved in this function.

1.1.4 Intracellular membrane trafficking of organelles

In many cells cargo is transported in two directions- away from the nucleus towards the cell membrane, termed anterograde transport; and towards the nucleus, termed retrograde transport (as shown in figure 1.4). The complete picture of how this works and the molecules involved is the subject of ongoing research.

1.1.5 Proteins involved in organelle trafficking

It is known that cell contains three major polymeric proteins which make up the cytoskeleton – microtubules, intermediate filaments, and actin filaments. These are able to extend and shorten in response to the needs of the cell (Wickstead & Gull, 2011). The cytoskeletal proteins serve as the scaffold along which motor proteins move while carrying cargo from the intracellular origin to the destination (Fletcher & Mullins, 2010). The larger of proteins these are the microtubule which stretches across the cell from the edge of the nucleus to close cell membrane, where actin filaments are able to accept the cargo.

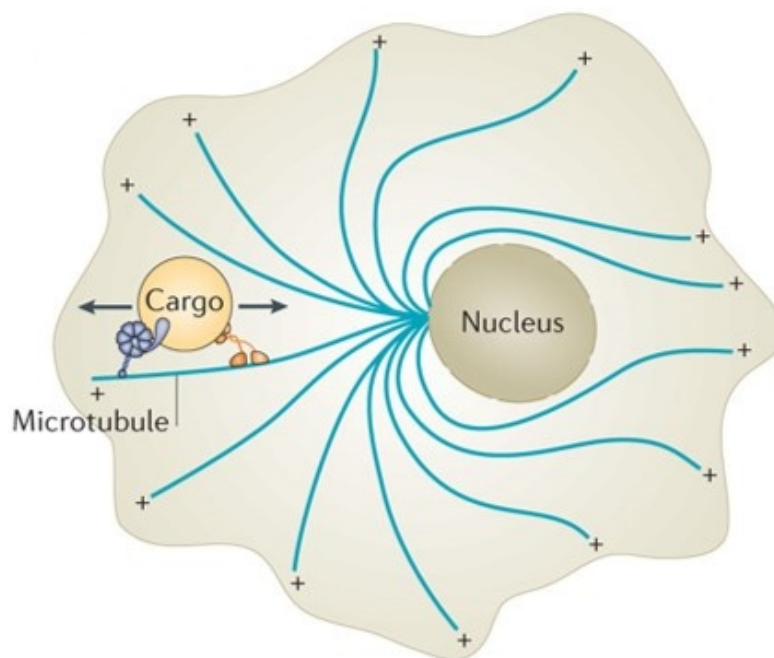


Figure 1.4. Bidirectional transport of vesicles in cells via microtubule binding. (Reprinted from Hancock, 2014). Anterograde transport is from the nucleus towards the cell membrane, via the walking of motor proteins on microtubules. The motor proteins carry vesicular or organelle cargo towards the cell membrane, where the plus (+) end of the microtubule lies. Retrograde transport is in the opposite direction.

Microtubules adopt a tube-like formation, so that it is hollow on the inside, with the polymer having an outer diameter of around 25 nm (Ikegami & Setou, 2010), as shown in figure 1.5. Each microtubule is made up by 13 protofilaments, and each protofilament is composed of dimers of α -tubulin and β -tubulin (Ikegami & Setou, 2010).

These protofilaments form a parallel bundle with β -tubulin of one terminal dimer present at the plus (+) end, and α -tubulin of the other terminal dimer present at the minus (-) end. Microtubules can lengthen faster from the plus (+) end compared to the minus (-) end.

Each microtubule can extend up to 50 μ M. They are generated at the microtubule organising centre (MTOC), which is located close to the nucleus (Klok *et al.*, 2014). After formation within the nucleus the microtubules are released into the cytoplasm, and the MTOC anchors microtubules into place (Klok *et al.*, 2014). Microtubules are dynamic, with the ends constantly under flux as required by the cell to perform transport and motility functions (Ikegami & Setou, 2010).

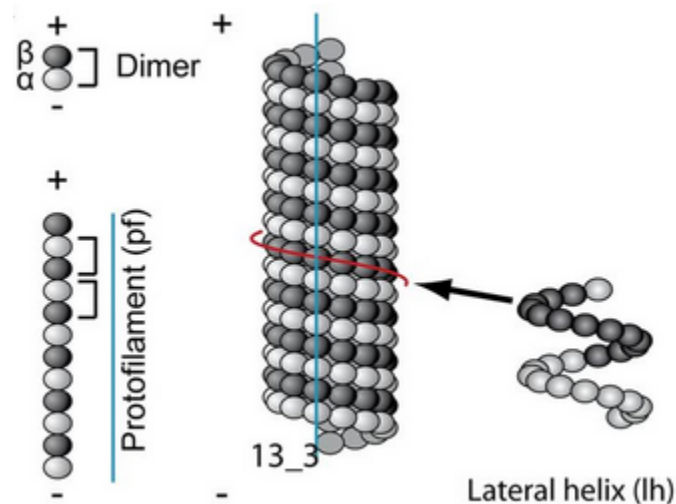


Figure 1.5. Microtubule structure. Protofilaments form from α -tubulin and β -tubulin dimers. These assemble forming a protofilament. The protofilaments arrange in a parallel manner to form the bundle, having a 13_3 structure. The lateral helix shows how each turn of the microtubule has either only α -tubulin or β -tubulin. Reprinted from Coquelle, Vitre, & Arnal (2009).

The intermediate filaments, whose diameter is between that of microtubules and actin filaments, at 10nm, are present both in the cytoplasm and the nucleus (Cooper, 2000). These are polymers of any of at least 50 different proteins that are members of 6 groups (Cooper, 2000). Due to this variability, the intermediate filaments can be thought of as being cell specific. However, each polypeptide adopts a common structure consisting of an N-terminal head, a C-terminal tail; both of varying length, which are joined together by a central region of between 310 and 350 amino acids (Cooper, 2000).

The central domain has an alpha-helix structure so that it resembles a rod, as shown in figure 1.6. In the final filament, four polypeptides come together to achieve a staggered anti-parallel structure, after the formation of two dimers by central rod regions wrapping around each other in a coiled-coil arrangement (Cooper, 2000).

The actin filament, or microfilament, is composed of monomers of globular actin (G-actin), which polymerise to form the filamentous actin (F-actin). F-actin consists of two helical strands which are intertwined forming a single left-handed helix, of approximately 7 nm diameter (Dominguez & Holmes, 2011), as shown in figure 1.7. The structure is polarised with the plus (+) growing end having a 'barbed' shape; and the minus (-), faster monomer releasing end having a pointed shape (Dominguez & Holmes, 2011). The dynamic nature of the filaments aids its function as an enabler of intracellular vesicle transport. In non-muscle cells, these filaments are generated and exist near the cell membrane.

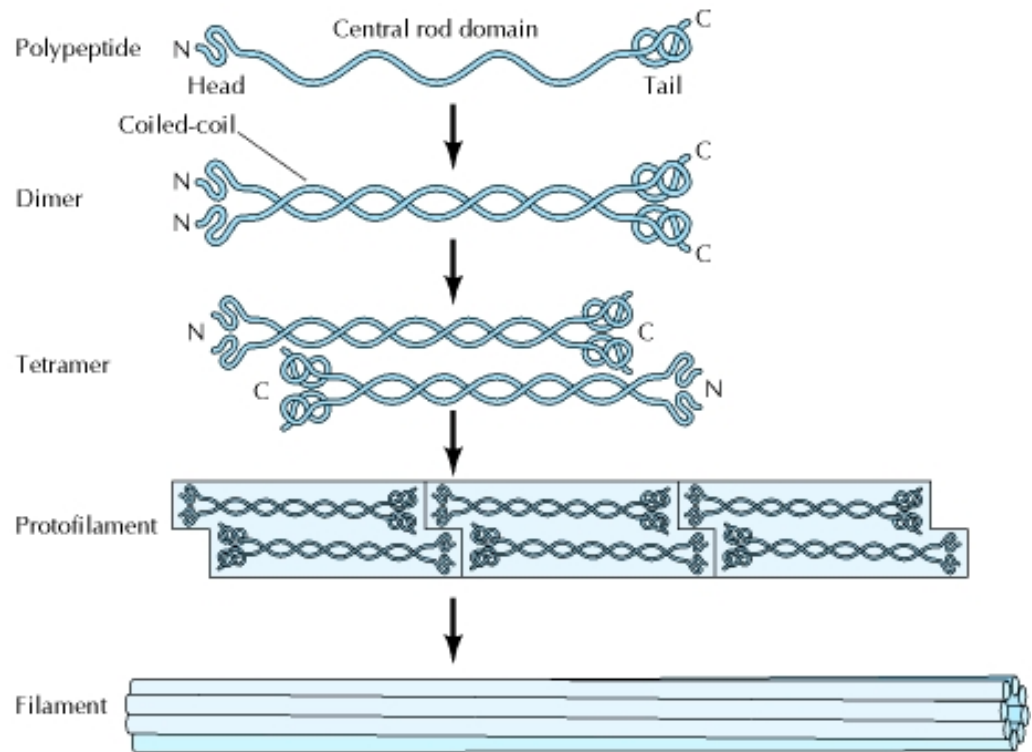


Figure 1.6. Intermediate filament structure. The polypeptide forms 2 dimers, which come together to form a tetramer. The tetramers are staggered and these lineup end to end to form the protofilament. The protofilament comes together to form the intermediate filament. Reprinted from *The cell*, Fourth Edition, Figure 12.37

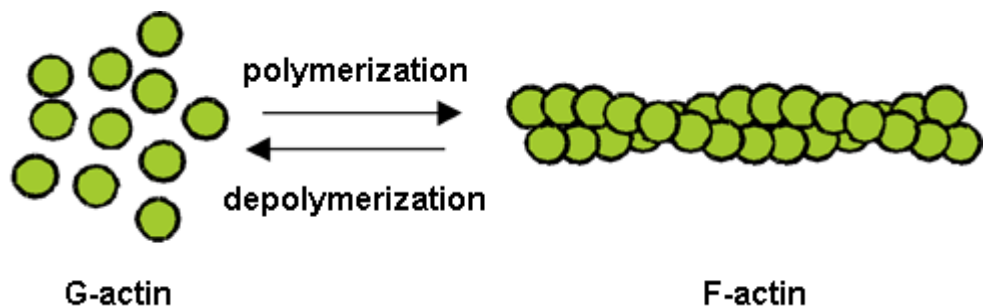


Figure 1.7. Polymerisation of G-actin to form F-actin. The F-actin filament consists of 2 polypeptides which are intertwined forming a left-handed helix. Reprinted from Oda *et al.*, 2009.

Evidence suggests that all three of the major cytoskeletal proteins have a role to play in organelle transport. Intermediate filaments stabilise the location of organelles (Lowery *et al.*, 2015) and which have been observed as regulating the speed of melanosome trafficking (Chang *et al.*, 2009). On the other hand, microtubules and actin filaments associate with motor proteins which use these as ‘tracks’ along which they carry the organelle or vesicle as cargo (Hancock, 2014).

1.1.6 Dynamics of organelle trafficking involving microtubules

Transport of organelles or vesicles bi-directionally from the nucleus towards the cell membrane, or in the opposite direction involves microtubules. Two motor proteins- dynein and kinesin (as shown in figure 1.8)– move along the microtubule track, respectively performing retrograde and anterograde transport in the cell. Each of these has two head domains, and the motor protein ‘walks’ along the microtubules in an unbroken manner, by coordinating the binding of alternate heads with the microtubule, which requires ATP (Gennerich & Vale, 2009). This has been termed ‘processivity’.

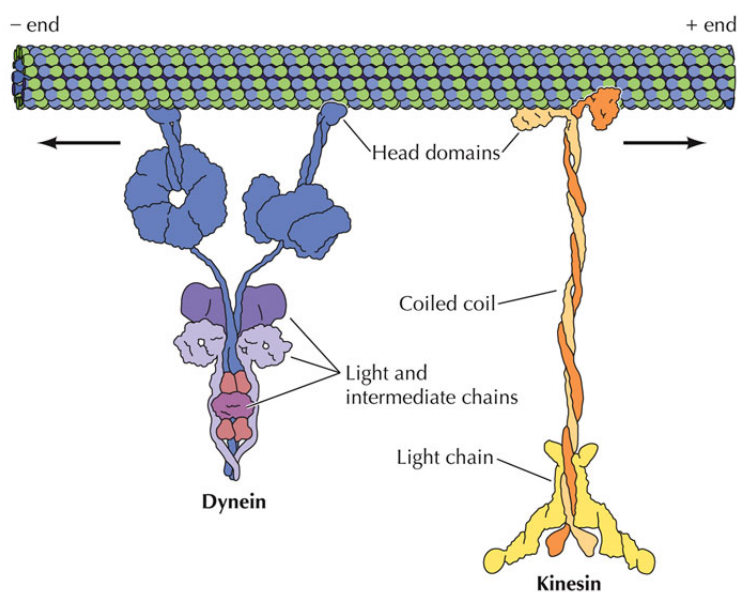


Figure 1.8. The dynein and kinesin motor proteins. Reprinted from Cooper & Hausman (2006). Each has two head domain which binds the microtubule to allow retrograde and anterograde movement, respectively.

The movement of kinesin requires a conformational change in the forward head, which then binds tightly, followed by dissociation and anterograde movement of the other head by 16nm, which then binds tightly to the microtubule. The movement of the centre of the molecule is 8 nm, and this is powered by the concomitant hydrolysis of ATP (Gennerich & Vale, 2009). This is shown in figure 1.9.

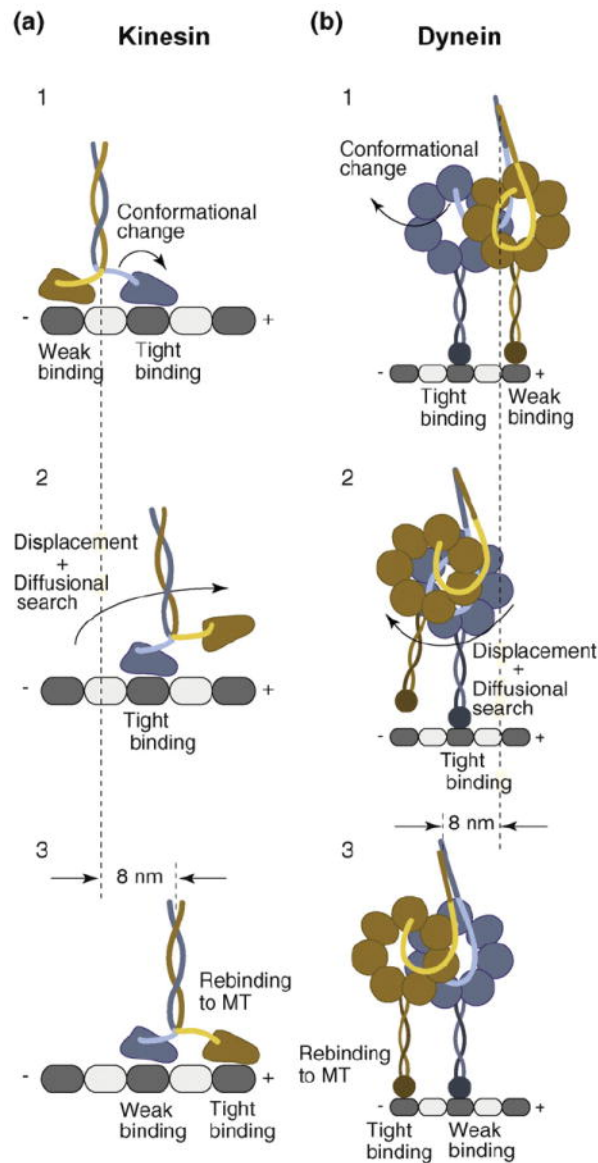


Figure 1.9. The steps involved in the processivity of (a) kinesin and (b) dynein along the microtubule. Both are suggested as having a mechanism which involves alternative weak and strong binding states for the head of the motor proteins. This enables the head with the weaker binding to dissociate from the microtubule, and diffuse forward, using the stronger binding head to remain on the track. The newly bound head now has stronger binding enabling walking of the motor protein. Reprinted from Gennerich & Vale (2009).

The movement of dynein is thought to involve an ATP requiring a change in conformation of the weaker binding head which allows it to dissociate from the microtubule and move retrograde by between 4 to 24 nm, but most often by 8 nm. It then forms a stronger association. Thereafter, the other head adopts weaker binding and processivity continues. This is also shown in figure 1.9.

Recent research has shed some light on the dynamics of organelle trafficking, but this has not been fully clarified. The relationship between dynein and kinesin has in the past been described as a ‘tug-of-war’ (Hancock 2014) whereby the two proteins will associate with the same vesicle or organelle. However, laboratory-based studies using gene knockout and protein inhibition determined when any of the two is inhibited the speed of transport in both directions is reduced. This has been called the ‘paradox of co-dependence’ (Hancock 2014). As a result, a number of models have been put forward to explain this phenomenon (Hancock 2014). Which of these proposed models is closer to true dynamics is under investigation (Donaldson J, Segev N, 2009).

The first model termed microtubule tethering suggests that both motor proteins will bind to the cargo, but with differing affinities depending on the location of the complex along the microtubule. As movement occurs in one direction the affinities change, allowing the transport to a particular cellular location. However, when only one motor protein is bound to the organelle the interaction with the microtubule is not strong enough to keep the resulting complex on the track.

The second model termed mechanical activation suggests that weak pulling forces exerted by a motor protein, opposing a stronger force exerted by the oppositely directing motor protein; triggers organelle transport in the direction of the stronger force.

The third model termed steric disinhibition suggests that motor proteins undergo auto-inhibition- whereby each inactivates its walking function when not bound either to the opposing motor protein or to a regulatory protein. However, when both motor proteins are present auto-inhibition is diminished enabling cargo transport.

At the end of the anterograde transport, cargo is passed from the microtubule to actin filaments. Thus, there is a segregation and interconnectedness of transport between the majority of the cell and the region adjacent to the cell membrane, as indicated in figure 1.10.

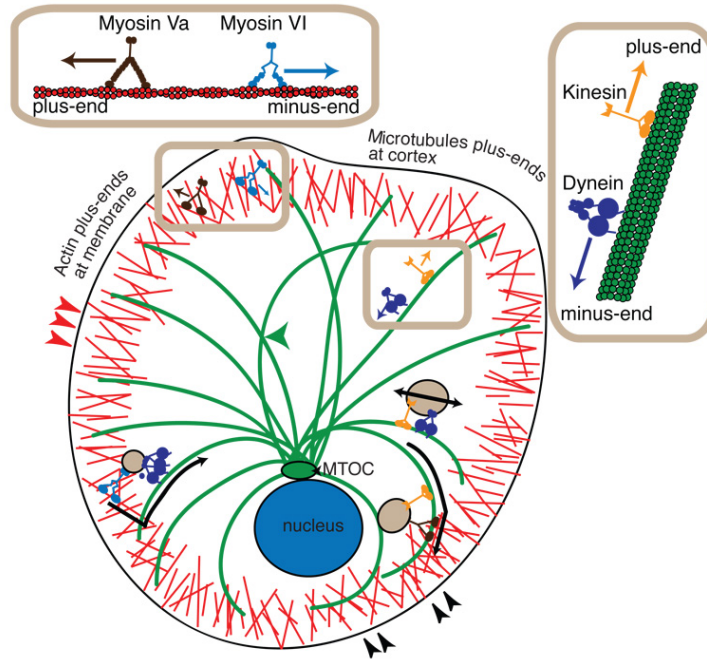


Figure 1.10. Representation of how myosin, kinesin, and dynein are involved in the transport of vesicles/ organelles in the cell. Microtubules (green) originate at the MTOC where the minus (-) end of the microtubule is located. From the nucleus to the peripheral cell region- dynein (dark blue) moves cargo retrograde to the minus (-) end of the microtubule, while kinesin (yellow) moves cargo anterograde to the plus (+) end. Two myosin family motor proteins myosin Va (dark brown) and myosin VI (light blue) transport cargo along actin filaments (red) within the peripheral-to-plasma membrane region of the cell, also called the cell cortex. Reprinted from Ross, Ali & Warshaw (2008).

Myosin Va proceeds towards (+) plus end of actin filaments- these are directed towards the membrane. Myosin VI walks proceeds towards the (-) end of the actin filament – this is away from the membrane. Actin filaments and microtubules meet within the cell’s cortical region as indicated by arrowheads. Also, actin filaments meet other actin filaments in this region, as indicated by the red arrowheads. Microtubules also have junctions as indicated by the green arrowhead. The actin and microtubule transport systems interact such that cargo (light brown) is able to bind to both myosin Va and microtubules which enable switching as the vesicle or organelle moves towards the cell membrane. Furthermore, cargo is able to bind to both myosin VI and dynein enabling switching of cargo in the movement towards the cell’s interior or nucleus. Reprinted from Ross, Ali & Warshaw (2008).

1.1.7 Dynamics of organelle trafficking involving actin filaments

Myosins are proteins that have ATPase activity and this activity functions to enable long-range motility of organelles in cells via binding to, and dissociation from, actin in the cytoskeleton. Two myosin motor proteins carry cargo on actin filament tracks at the cortical region of the cell, namely myosin V and myosin VI. Here cargo is passed between microfilaments and actin filaments via two possible mechanisms (Ross, Ali & Warshaw, 2008). The first is tug-of-war model explained above so that there is competition for the cargo by means of the pulling force exerted by each of the motor proteins that are bound to the cargo. The second is involves dissociation of the myosin proteins in a coordinated manner, allowing binding by the other myosin proteins, ensuring that the cargo is not lost in the cell (Giampiero and Mauro 2012).

In melanosomes, the myosin Va is responsible for anterograde transport. It is a Y-shaped molecule consisting of 3 domains; the motor domain, also termed the head; of which there are two at the top ends of the Y; the neck extending down from the Y shape, and the tail; as shown in figure 1.11(a). The molecule forms a dimer through the association of the tail domain in a coiled-coil with breaks in the structure. The head and neck domains are flexible. Head domains can have a site for binding actin at one set of residues, and ATP at another. Each of the 'neck' is heavy chains composed of α -helices that are capable of binding to calmodulin by virtue of the presence of six contiguous IQ motifs.

The myosin is able to transport the cargo through the walking action of the molecule on the actin filaments. During motion of the myosin protein there is a cyclical series of events where the head of the myosin molecule binds actin with a high affinity when not attached to ATP; upon ATP binding myosin has reduced actin affinity. The ATP is then hydrolyzed by the myosin to ADP, with the release of inorganic phosphate (Pi) and the detachment of the head from the actin. The rate of ADP release limits the speed of walking of the molecule (Warshaw, 2005).

Current evidence suggests the walking action of myosin Va is coordinated as follows, as shown in figure 1.11(c):

1. Myosin Va is likely to have a resting state with the head domains bound to ADP (Odrionitz & Kollmar 2007), with intramolecular strain being exerted by confirmation of these domains (Lipatova 2008, Sakamoto *et al.*, 2000, Sakamoto *et al.*, 2010, Kogel 2010, Odrionitz & Kollmar 2007).
2. One head, termed the trailing head then releases its ADP, and exchanges it for ATP.
3. This causes a fast release of the head from the actin chain.
4. The power stroke follows as ATP is hydrolyzed to ADP and Pi, and the head moves along to a location 36 nm forward on the actin chain.
5. The head then attaches to the next actin monomer, while releasing Pi, and thus allowing adoption of the high-affinity state.

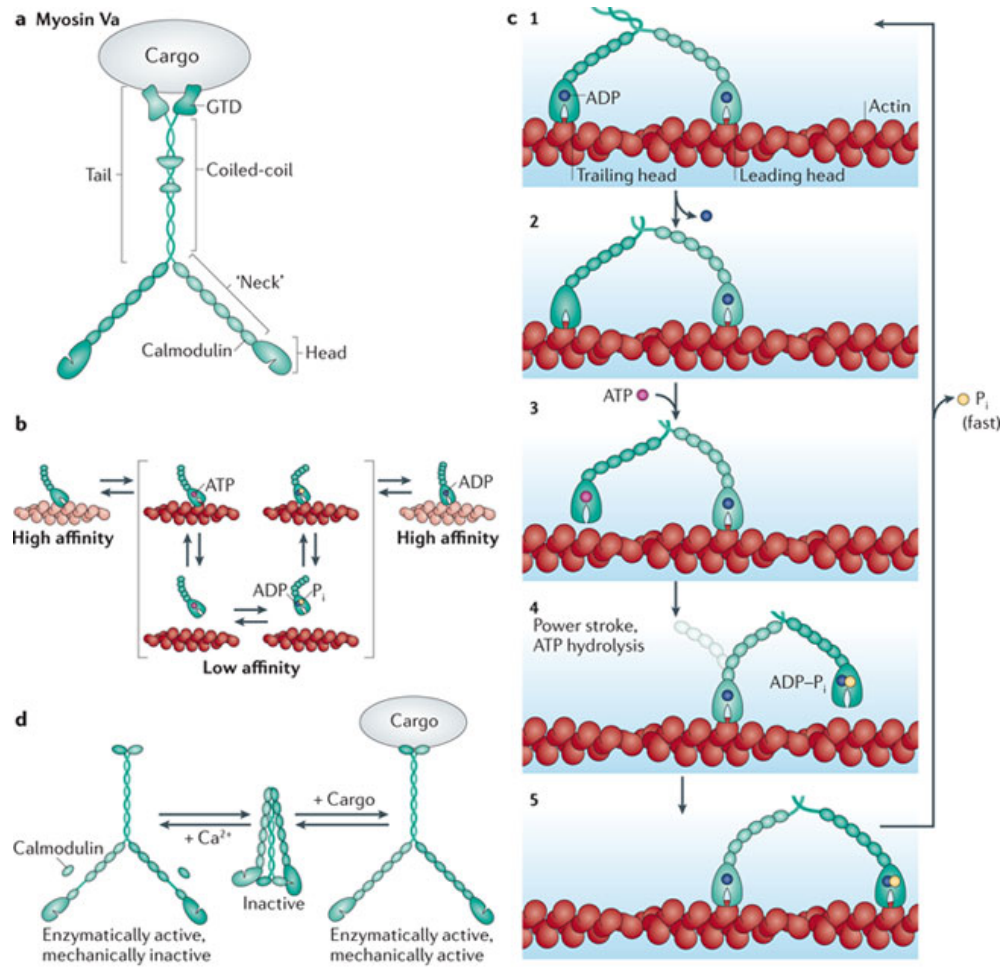


Figure 1.11. The structure and function of the myosin Va molecule. a. The structure of the myosin Va is a dimer, with a head, neck and tail region. The tail can attach to, and carry the cargo, i.e. the melanosome; while the flexible neck helps the head to move by walking along actin chains in the cytoskeleton, as seen in b (the kinetic cycle) and c. The molecule alternates between high and low affinity for actin in order to achieve attachment and detachment which enables movement of the cargo along the cytoskeleton. The binding of calcium alone leaves it unable to walk along the actin chains due to a weakened neck region. Without calcium or cargo, the myosin is completely inactive. However, when the cargo is present myosin has both enzymatic and mechanical activities as seen in d. Reprinted from John & James (2012).

The binding of myosin to the actin chain is regulated by the intracellular calcium concentration. Without the presence of either Ca^{2+} or the melanosome in the case of myosin Va; the molecular conformation is 'bent', and in this state it is unable to act as an ATPase or bind the actin. When just calcium is present the molecule can act as an ATPase, but cannot transport the melanosome as calmodulin is bound to calcium ion, and is thus, detached from the myosin. This makes the neck region too weak for the power stroke. When the melanosome binds myosin is restored to both ATPase and transport activity as determined by *in vitro* and enzymatic assay.

The speed of transport has been investigated using melanosomes. If the melanocyte cell loses myosin Va the rate of retrograde transport increases, lending credence to a tug-of-war mechanism. Alternatively, it has been suggested that migratory speed limits are due to overcrowding or the presence of other cargo units on microtubules.

Experimental studies have shown that the length of transport is increased when more motor proteins are available (Vershinin *et al.*, 2007) *in vitro*, while only one motor protein complex may transport a specific cargo at any given time (Kural *et al.*, 2007, Watanabe & Higuchi, 2007).

Experiments examining the movement of myosin Va at the interface between actin and microtubules in melanosomes found that the motor protein is able to leave the actin and bind to microtubules (Ali *et al.*, 2007). Here it diffuses along the microtubule surface by virtue of electrostatic attraction between a negatively charged E-hook region on tubulin and the positively-charged surface of myosin Va's Loop region. Furthermore, at actin-actin junctions, the myosin Va is able to move to the next filament enabled by its inherent flexibility (Ross, Ali & Warshaw, 2008), so that in *in-vivo*, the rate of 50% switching to another actin filament is observed (Snider *et al.*, 2004).

Anterograde transport can be followed by exocytosis, whereas endocytosis can be the step prior to exocytosis. To understand the overall mechanisms in cellular transport, general and specific characterization of these processes is essential.

1.2 Overview: Melanocytes and melanosomes

Melanocytes are a diverse group of cells, with a single point of origin – the neural crest in the embryo – and function to produce melanin pigments in specialised organelles, which are transferred to neighbouring cells. In the iris, hair and epidermis these pigments then provide colouration to these structures. In addition, these cells are also found in the nervous system, the heart and the inner ear; and therefore, pigment production must have a role in the normal functioning of these organs and tissues. Evidence suggests that more such cells will be present elsewhere in mammals (Brito & Kos, 2008). Yet there are other cells which are also able to generate pigment (Hu, Simon & Sarna, 2008, Randhawa *et al.*, 2008) such as the retinal pigment epithelial cells; but these do not transfer their pigment granules, but rather maintain these organelles (Wasmeier, *et al.*, 2008).

After originating as melanoblasts at the neural crest, the cells migrate, proliferate and differentiate into melanocytes, a type of dendritic cell which can be spindle or oval shaped (Cichorek *et al.*, 2013). After a process of maturation, the cell is able to produce melanin within specialised organelles called melanosomes. The end of the cell is its death, and it is replaced by another melanocyte in the tissue.

The ratio of melanocytes to keratinocytes varies between 10:1 in the basal layer of the epidermis to 40:1 above this; with the keratinocytes and the melanocytes forming an epidermal melanin unit (Cichorek *et al.*, 2013); as shown in figure 1.12. The dendritic processes of the melanosome adhere to keratinocytes via molecules including E-cadherins and P-cadherins, desmoglein and connexins (Haass, Smalley, & Herlyn, 2005). Communication via these, in tandem with paracrine signalling by keratinocytes, enables homeostatic control of the melanocyte proliferation, differentiation, quiescence and apoptosis (Haass, Smalley, & Herlyn, 2005). Additionally, autocrine signalling is also involved in melanocyte homeostasis (Yamaguchi & Hearing, 2009) Melanosomes are lysosome-related organelles (Natarajan *et al.*, 2014), as they contain lysosomal-associated membrane proteins and hydrolases which depend on an acidic pH to function. They are tasked with the synthesis of melanin in the

melanocytes, and transport to the keratinocytes which exist above the skin's basal epidermal layer.

Melanosomes protect DNA from damage in keratinocytes as they relocate to the circumnuclear area, where melanins are proposed to act absorbers of UV radiation. UV-B radiation with a wavelength of 290–320 nm can cause crossing linkages in DNA by base-pair dimerization. Whereas UV-A, radiation with a wavelength of 320–400 nm, can cause the production of reactive oxygen species (Ando, Ichihashi & Hearing, 2009). In fact, exposure to UV upregulates melanin synthesis (Wasmeier *et al.*, 2008). Furthermore, recent studies suggest that keratinocytes are stimulated to release exosomes containing microRNAs which stimulate melanin synthesis in melanocytes (Waster *et al.*, 2016).

A number of proteins have been identified as participating in melanosome transport in the studies of melanocytes. These include the Rab protein Rab27a, its effectors slac-2a and slp-2a, as well as the motor protein myosin Va.

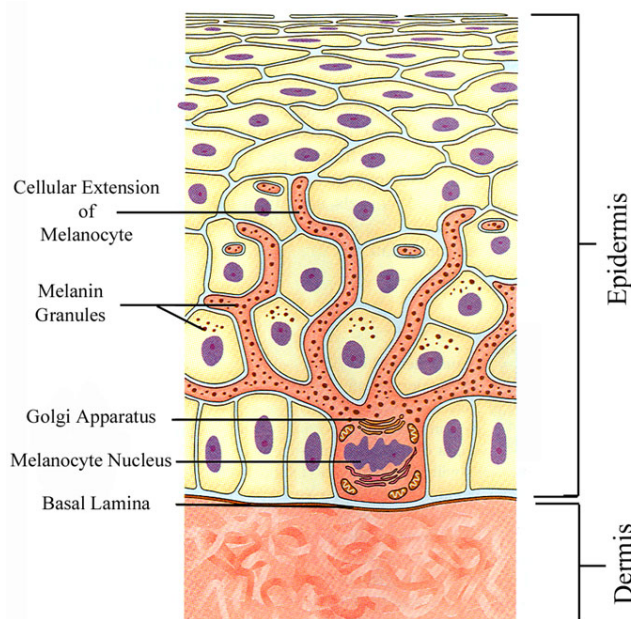


Figure 1.12. The melanocyte. The melanocyte sits on the basal lamina of the epidermis. Dendrites project upwards and interface with several keratinocytes. A single melanocyte is capable of delivering melanin to several cells through a process of melanocyte exocytosis coupled to keratinocyte endocytosis. This is aided by the presence of numerous dendrites which project from the body of the cell into the epidermal layer. (Reprinted from “Melanocytes” at healthfavo.com; Copyright © 2013 Health, Medicine and Anatomy Reference Pictures).

1.3 Melanosome transport

The experimental study of melanosome transport is an ideal system for studying membrane trafficking. As melanosomes contain melanin they appear darkly pigmented against a background in mammalian cell culture and in melanophores from lower organisms. The organelles are easily visualised due to their large size, flat morphology; and are can be discerned microscopically using phase contrast or bright field methods (Wasmeier *et al.*, 2008).

The melanosome story, from its beginning until it reaches its ultimate destination of the keratinocyte can be split into part as follows:

- a) Melanosome biogenesis
- b) Melanosome maturation
- c) Microtubule-dependent anterograde transport from MTOC along tubulin
- d) Transfer to actin at cell periphery ready for exocytosis, and actin-dependent anterograde melanosome transport
- e) Transfer of melanosome to keratinocyte

1.3.1 Melanosome biogenesis and maturation

Melanosomes develop in 4 stages. Firstly, in stage I, a pre-melanosome is produced by the fusion of membranes that bud off from the plasma membrane via endocytosis, with membranes from the melanocyte's secretory pathway. These pre-melanosomes contain both tubular and vacuolar regions. The internal bilayered vesicles rich in clathrin and the vacuolar sorting protein Hrs (hepatocyte growth factor-regulated tyrosine kinase substrate) form from vacuolar regions (Sitaram & Marks, 2012). The tubular region exchanges material with other organelles enabling maturation into a late endosomal multivesicular body (MVB). Fusion of the lysosomes digests any material in the lumen of the premelanosome. Stage I melanosomes contain irregular structures of amyloid fibrils. This is followed by stage II during which the melanosome generates regular internal fibrils from the amyloid. These lengthen and form sheet-like internal structures, also termed the 'melanosome matrix' (Sitaram & Marks, 2012).

During stage III melanin pigments are embedded onto the fibrils, after transfer of melanin synthesising enzymes including tyrosinase (TYR) and TYRP1 (tyrosine-related protein 1), and transporter proteins such as ATP7A, and the proposed transporter OCA2, from either early endosome to melanosomes (Sitaram & Marks, 2012). During stage IV increased concentration of melanin on the fibrils increases pigment density with the effect of obscuring the internal melanosome structure (Sitaram & Marks, 2012). The enzymes TRYP1, tyrosinase, and DCT, and the molecule glutathione are involved in melanin biosynthesis as shown in figure 1.14.

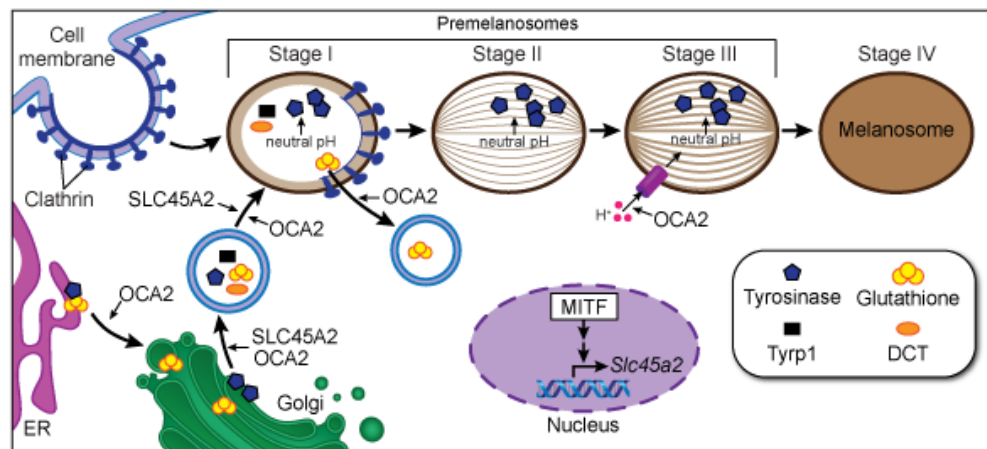


Figure 1.13. Melanosome maturation. Pre-melanosomes are formed from endocytotic vesicles fusing with secretory vesicles. Stage I melanosomes have a high-density clathrin coat on one side. Tyrosinase, glutathione, TYRP1 and DCT are trafficked to the melanosome at this stage. At stage II melanin striations can be seen via electron microscopy in the melanosome due to the formation of the melanosome matrix. At Stage III darker pigmentation appears due to deposition of eumelanin on the matrix. At stage IV striations are no longer observed as melanin density increases. The protein SLC54A2 (solute carrier family 45 members 2) is a transporter protein. SLC54A2 and the OCA2 gene product are thought to be required for the enzyme tyrosinase being trafficked and/or processed to the melanosome at stage I, possibly via maintenance of the neutral pH at stage I. In this way tyrosinase activity is minimised at stage I. The OCA2 gene product, protein P, is a transmembrane transporter that allows glutathione to accumulate in the melanosome (Staleva, Manga & Orlow, 2002) and also reduces tyrosinase activity (del Marmol *et al.*, 1993) as well as enabling tyrosinase maturation. The enzymes tyrosine-related protein 1 (TYRP1) and dopachrome tautomerase (DCT) are involved in the synthesis of melanin in melanosomes. SLC45A2 may be required for DCT and TYRP1 being transported to melanosomes. Reprinted from Labarchives.com (2012).

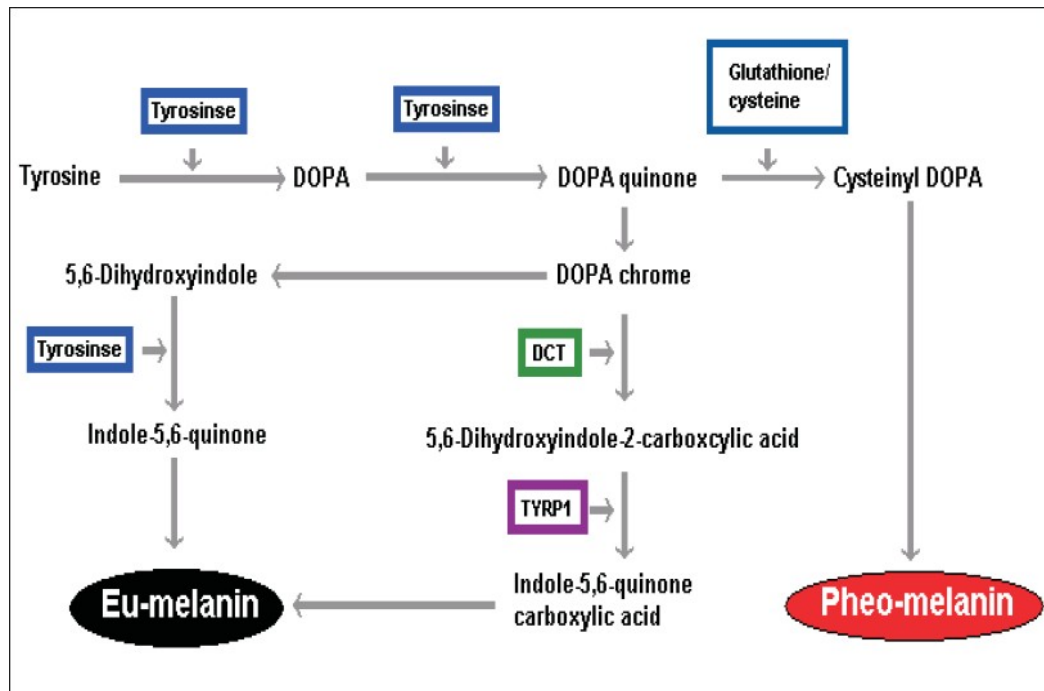


Figure 1.14. Synthesis of eumelanin and pheomelanin (Reprinted from Ranganathan, Vijayachandra & Radhakrishnan, 2007). Tyrosine is oxidised by tyrosinase (shown as tyrosinase) to dopa-quinone. Glutathione or cysteine is needed to biosynthesise pheomelanin. In the metabolic pathway eumelanin can be generated via the action of DCT and TRYPI.

1.3.2 Microtubule-dependent anterograde transport from MTOC along tubulin

While many studies have been undertaken on melanosome transport, the mechanism of anterograde transport in the cells of mammals-specifically the proteins involved, and the motor complex have not been characterised (Ishida, Ohbayashi, & Fukuda, 2015). However, recently fluorescent studies using mouse melanocyte culture have determined that the Rab1A protein controls this process. This involves Rab1A interacting with RUN domain located in the N-terminal of the protein SKIP. The SKIP protein then interacts with the kinesin light chain 2 protein (KLC2). Thereafter KLC2 itself interacts with the kinesin heavy chain (Kif5b). As a result, the 3-protein complex comes together, comprised of kinesin, SKIP, and Rab1A (Ishida, Ohbayashi, & Fukuda, 2015). Furthermore, the authors of the report also found a comparable complex in lysosome transport, but this contains Arl8b in place of Rab1A.

1.3.3 Transfer to actin at cell periphery ready for exocytosis, and actin-dependent anterograde melanosome transport

The melanosome can be transferred to actin filaments from microtubules at junctions where these two cytoskeletal tracks meet. This has often been termed as melanosome capture (Beaumont *et al.*, 2011) by the actin filaments. This transfer step has also not been fully characterised, however there have been suggestions that either Rab1A or/and Rab27a are involved in this process, as mutation of their respective genes results in accumulation of the melanosomes in the melanocyte perinuclear region (Chabrilat *et al.*, 2005, Bahadoran *et al.*, 2003, Ishida *et al.*, 2012).

The Rab27a GTPase protein and its effectors act to transport melanosomes along actin filaments towards the periphery of the cell. Rab27a recruits the effector named melanophilin (MP), which is also called Slac2-a. This functions to partner Rab27a with myosin Va (Bahadoran *et al.*, 2001, Hume *et al.*, 2001, Matesic *et al.*, 2001, Strom *et al.*, 2002, Wu *et al.*, 1996, Wu *et al.*, 2002). In the process, a three-membered complex, also termed a “tripartite complex” is formed as shown in figure 1.15.

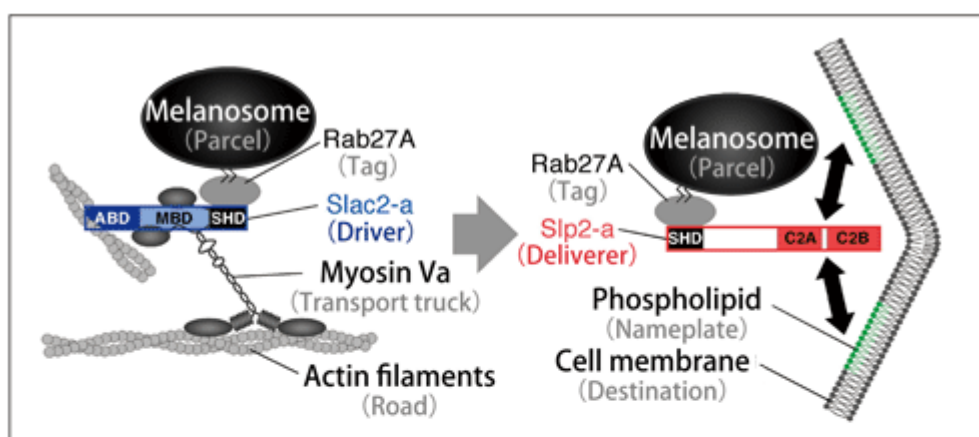


Figure 1.15. The proposed structure of the tripartite Rab27a, Slac-2a and myosin Va complex. The melanosome is thought to be driven by MP using the myosin Va motor on the actin filament track. Rab27a binds to both the MP at the SHD domain of the protein and the melanosome, bringing the complex together. Rab27a may also serve as a tag for the cellular export process. (Reprinted from Spring8.or.JP, 2016).

However, the association is reliant on the tertiary structure of each member of the complex. This means that any significant mutations which alter relevant regions of tertiary structure can lead to autosomal genetic diseases. One such example is Griscelli syndrome, which requires the inheritance of two recessive mutant alleles for the disease to be expressed. Three mutant mouse models, named “ashen”, “dilute” and “leaden” were used to identify the effects of the mutations. MP mutations, seen in the ashen mouse resulted in the loss of pigmentation. Myosin Va mutations, seen in the dilute mouse resulted in impaired neurological functioning. Rab27a mutations, seen in the leaden mouse resulted in immunological problems (Van Gele, Dynoodt, & Lambert, 2009). This also indicated that melanin has a role in skin pigmentations, the normal functioning of the brain, as well as the immune system. Research to clarify all the functions of melanin remains ongoing.

Dilute is so called as it reduces the concentration of the pigments eumelanin and melanin in pigmented cells, which is most obvious by a change in the coat colour.

More recent studies in rabbits have found that mutations in the MP gene *MLPH*, and were considered to be a suitable animal model for Griscelli syndrome type 3 (Fontanesi *et al.*, 2013).

Furthermore, Zhang and colleagues (2016) determined that the N-terminal end of the myosin Va globular tail domain binds to MP. They proposed that the binding of MP to myosin Va in a “pre-activated state” starts the movement of myosin Va on the actin filament track.

Also, *rab1A* is involved in regulating microtubule track transport, and *rab27a* is involved in actin filament transport; it may be that these two interact in some way during the microtubule to actin track transfer process.

1.3.4 Rab proteins and their roles

Rab proteins are GTPases, which are inserted into membranes via the tail region which is chemically modified by bonding to geranylgeranyl moieties. The role of Rabs is to control membrane transport by recruiting other proteins, which are termed effectors, to carry out the tasks involved as shown in figure 1.15 (Hutagalung & Novick, 2011). This includes an assortment of the transported molecules to the bud (cargo selection/budding/coat), movement of the vesicle (transport), docking and uncoating of the vesicle (tethering) and fusion of the vesicle. Each task of membrane transport is thought to involve a different Rab protein (Hutagalung & Novick, 2011). Rab proteins are involved in the formation of the SNARE complex as outlined in figure 1.16 below.

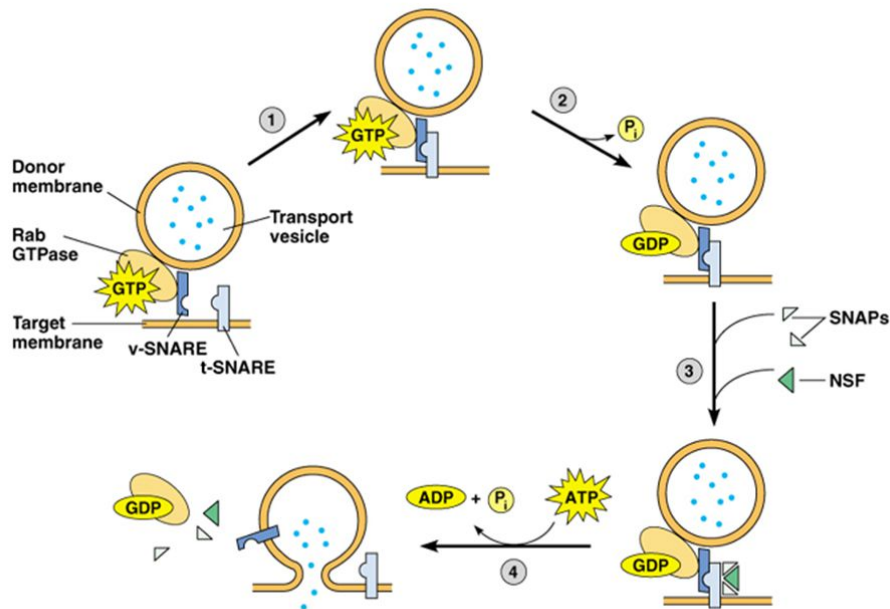


Figure 1.16. The SNARE protein hypothesis in relation to Rab GTPases. 1. The vesicular SNARE (v-SNARE), associated with the Rab GTPase seeks the target membrane SNARE (t-SNARE). 2. Upon complex formation, the Rab GTPase hydrolyses GTP to GDP, release inorganic phosphate (P_i). 3. SNAP and NSF then bind the complex. This process is called “zipping” and its initiation requires calcium ions (Chen & Scheller, 2001). Members of the synaptotagmin family detect calcium influx (Rizo and Xu, 2015). 4. NSF hydrolyses ATP and the active process of vesicular and target membrane fusion occurs. This causes dissociation of the protein complex and the components are recycled. Reprinted from Hardin & Bertoni (2016).

Rab proteins have two states- active and inactive, and their role is enabled through a cycling of the protein as follows (Hutagalung & Novick, 2011): In the inactive form, the protein is bound to GDP. The guanine nucleotide exchange factor then activates the Rab protein by exchanging GDP for GTP. The functioning of Rab protein depends on the binding of the protein to the γ -phosphate of the GTP molecule. Once active the Rab protein is able to engage its specific effectors. Following this engagement, the Rab protein is acted upon by a GTPase accelerating protein which hydrolyses GTP to GDP. The inactive Rab obtained in this way is then acted upon by a GDP dissociation inhibitor (GDI), and it functions to remove Rab from the membrane. In the last step, the Rab now attached to the is available for re-entry into the membrane for the vesicular transport to begin again. Rab effectors tend to preferentially associate to the GTP-bound / activated Rab (Rink J, Ghigo E, Kalaidzidis Y, 2005).

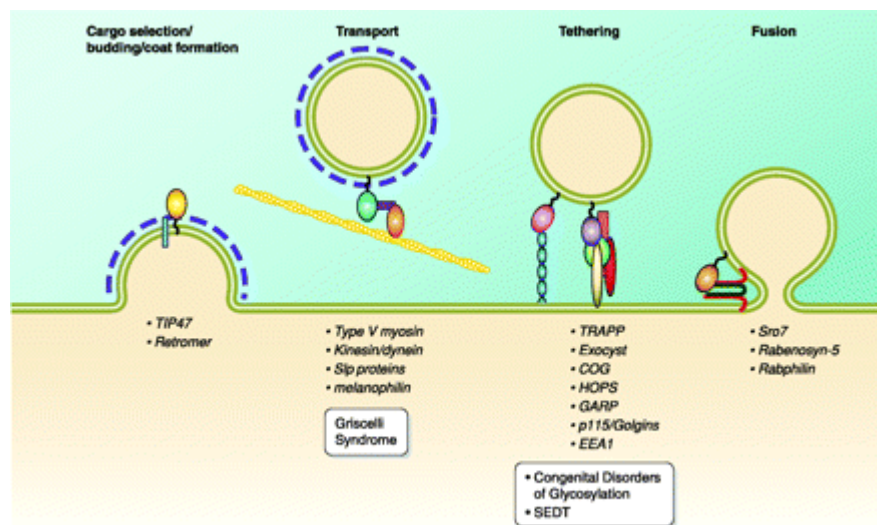


Figure 1.17. Examples of proteins recruited by Rab GTPases in the four general stages of membrane trafficking; cargo selection, transport, tethering, and fusion. Named proteins are provided below each stage. Genetic diseases have been linked to specific mutations in the effectors or the Rab proteins. In the case of faulty vesicular transport, Rab27A mutations or mutations in its effectors melanophilin/myosin Va can result in Griscelli Syndrome. Tethering can be disrupted by mutations in COG or its subunits COG1, COG7, and COG8; as well as TRAPP and its subunit Trs20. This resulting in dysfunction of vesicular coating found in inherited glycosylation disorders or spondylo-epiphyseal dysplasia tarda (SEDT). Reprinted from Hutagalung & Novick, 2011.

1.3.5 Roles of Slp2-a

Slp2-a is a member of the SLP family- the synaptotagmin-like proteins. These proteins sit on the inner face of the plasma membrane. Slp2-a appears to have a regulatory role in the trafficking of vesicles, for example in studies of Madin–Darby canine kidney (MDCK) cell culture, Slp2-a was found to tether vesicles to the membrane by binding to Rab27a (Yasuda *et al.*, 2012).

Kuroda, Ariga, and Fukuda (2003) found that Slp2-a binds actin and that this was required for the transport of melanosomes from the perinuclear region of the cell to the cell periphery. As a result, they proposed 3 possible roles of Slp2-a, as shown in figure 1.18, with the possibility of the protein being involved in a combination of 2 or all 3 roles (Taruho, Hiriyoshi & Fukuda (2003)).

Another role for Slp2-a is thought to be in providing polarity to cells. Cells with polarity have a basal face and an apical face via which exocytosis is performed in secretory cells. In the study published by Yasuda, Mrozowska and Fukuda in 2015 the Slp2-a associated itself with the apical face of the MDCK cells, and the authors suggested that this directs transport of vesicles towards only the apical face and that the level of Slp2-a protein expressed was related to the degree of cell polarisation.

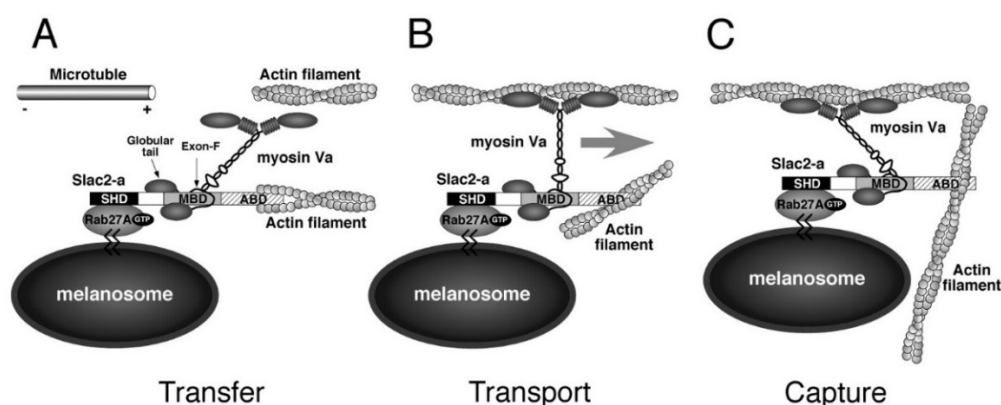


Figure 1.18. Melanosome transfer from the microtubules. Slac-2a binding to actin may allow transfer from the microtubules track to the actin filaments track of melanosomes (A). It may enable processivity of the cargo/motor protein complex on actin filaments (B). At the cell periphery, it may enable the capture of melanosomes by actin filaments (C). Reprinted from Taruho, Hiriyoshi & Fukuda (2003).

A summary of the overall process was provided by Hume and Seabra (2011), as shown in figure 1.19.

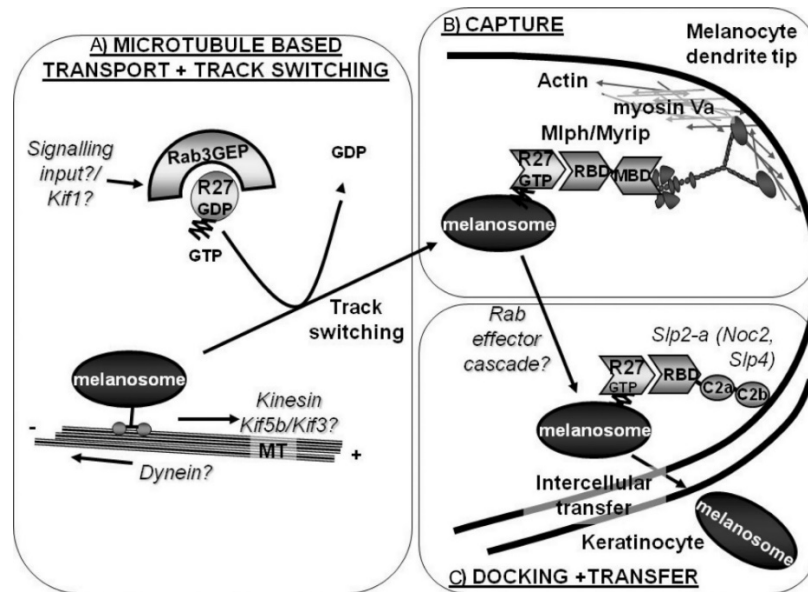


Figure 1.19. Microtubule-based transport. (A) Novel melanosomes are moved to the tip of dendrites in melanosomes possibly by kinesin motors in the anterograde direction and dynein in the retrograde direction on microtubules. (B) The formation of Rab27a-Slp2-a-myosin Va complex facilitates capture/transfer of the melanosome to the actin track close to the cell membrane. Rab3GEP regulates the activation of Rab27 activation and the formation of the tripartite complex, as shown in (A). (C) An effector cascade may be activated which enables Slp2-a in the complex to dock the membrane prior to transfer of the melanosome to keratinocytes. (Reprinted from Hume & Seabra, 2011)

1.3.6 Transfer of melanosome to keratinocyte

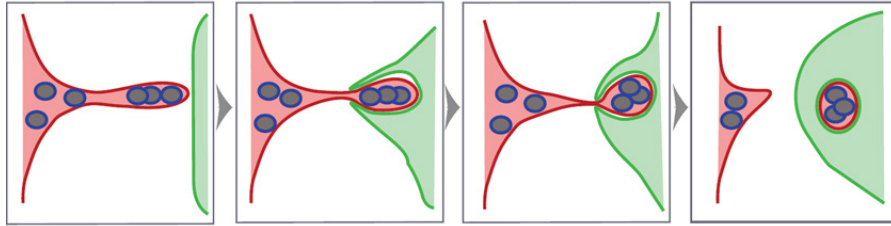
It is already established that keratinocytes stimulate melanocyte expression of melanin as mentioned above. Furthermore, paracrine signalling enables communication within the melanin epidermal unit. However, the exact nature of the transfer between the two cells is yet to be fully understood. Experts (Wu & Hammer, 2014) have proposed four different mechanisms by which this occurs; namely cytophagocytosis, membrane fusion, shedding phagocytosis and exocytosis-endocytosis, as shown in figure 1.20. Of these evidences suggests that the process is likely to be a mixture of shedding phagocytosis and exocytosis-endocytosis (Wu & Hammer, 2014).

Shedding phagocytosis involves the melanocyte losing membrane-enclosed sections of the cell at its peripheries that are rich in melanosomes. Thereafter keratinocyte perform phagocytosis on the shed bodies in order to internalise the melanosomes. This was supported by images presented

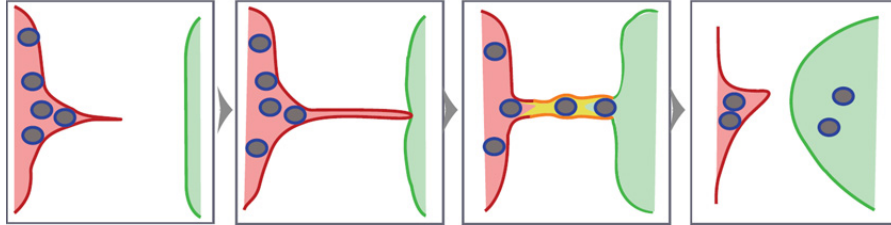
in studies by Ando *et al.*, (2012), and the phenomenon of filopodia formation observed in the laboratory (Scott *et al.*, 2002, Singh *et al.*, 2008, Singh *et al.*, 2010). Further, dynamic images were obtained using where membrane enclosed cell sections were observed by Wu *et al.*, (2012) at the keratinocyte cell surface; however, as the images were not from living tissue, this may be open to interpretation as an artefact. Also, Rab17 may regulate the formation of filopodia, supporting this mechanism (Beaumont *et al.*, 2011).

In the exocytosis-endocytosis model the core of the melanosome, termed the “melanocore”, which contains the melanin, is exocytosed by the melanocytes. This is subsequently phagocytosed by the keratinocyte. This is supported by electron-microscopy studies which noted that the melanin structure in keratinocytes only has a single membrane, as opposed to multiple membranes which would be observed under the membrane fusion mechanism (Van den Bosche, Naeyaert & Lambert, Tarafder *et al.*, 2014). However, as the images provided by Tarafder and colleagues) were still, this finding could be interpreted as needed further confirmation.

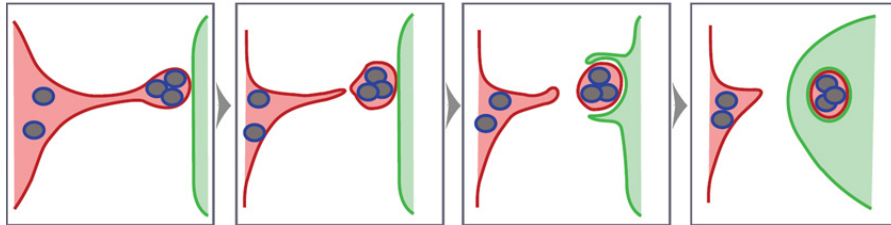
(1) Cytophagocytosis



(2) Membrane Fusion



(3) Shedding-Phagocytosis



(4) Exocytosis-Endocytosis

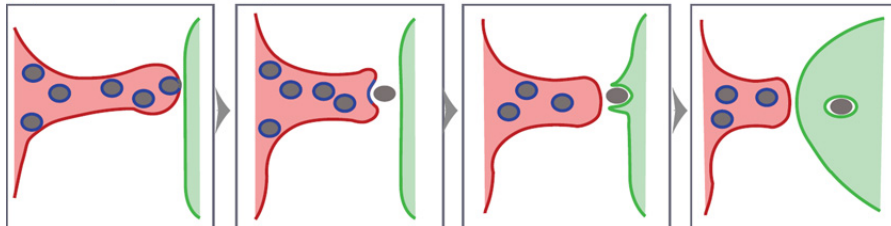


Figure 1.20. The four proposed mechanisms of melanosome transfer from melanocytes to keratinocytes. Phagocytosis is necessary for all but the membrane fusion mechanism. The blue borders represent the membranes of the melanosome, the red represents the melanocyte cell membrane and green the keratinocyte membrane. In the membrane fusion mechanism, the melanocyte and keratinocyte membrane fuse forming the hybrid yellow membrane. The connecting bridge may be formed by the extension of filopodia from the melanocyte. Reprinted from Xufeng & John (2014).

1.3.7 Comparison of melanosome transport to secretion

Melanosome transport has a similar feature to exocytosis by secretory cells. When comparing the two similarities include a sampling of the external environment via early endosomes, the coating of both the immature secretory granule and the stage I melanosome with clathrin, which binds to clathrin receptors on the target organelle/vesicle via adaptor protein complexes. Thus there has been some suggestion by researchers that hereditary pigmentation disorders including Chediaki Higashi syndrome and Hermansky–Pudlak syndrome could be due to mutations in the genes for particular adaptors, namely AP-1 and AP-3. This limits transport from the trans-Golgi network to the melanosome. This is summarised in figure 1.21.

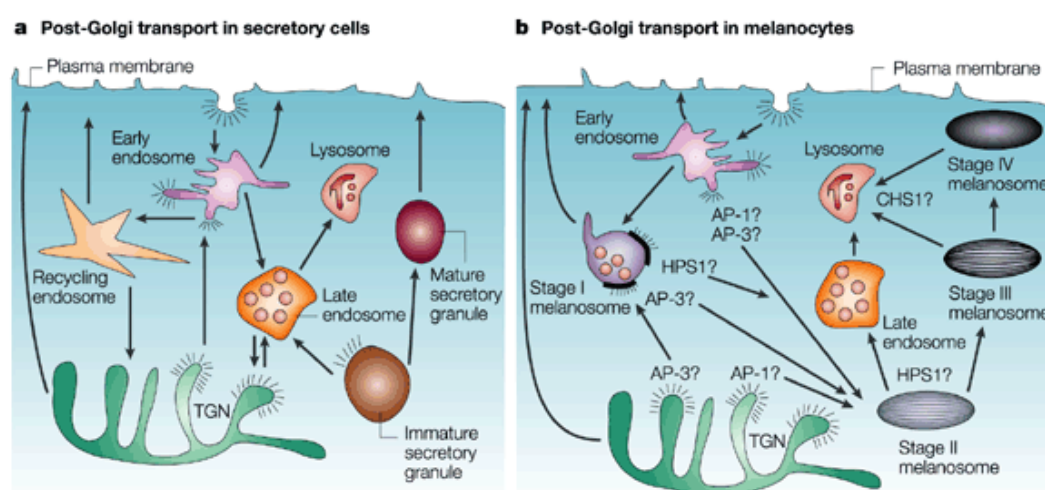


Figure 1.21. Representation of a. late endosomal transport in secretory cells, b. melanosome transport in melanocytes. Lipid and proteins from the different organelles in order to transport vesicles in the directions shown by the arrow. The presence of the clathrin coats on specific organelles is shown by the 'Spikes'. A higher clathrin density is shown as black shading in melanocytes. Vesicles present within organelles are shown as small circles. Lysosomes have non-uniform membranes. Stage II and III melanosomes have striations. Marks and Seabra (2001) suggest that the AP-1/AP-3 adaptor complexes have a role to play in Chediaki Higashi syndrome (CHS) and Hermansky–Pudlak syndrome (HPS) at the trans-Golgi network (TGN) and within the cell that relate to melanosome biogenesis and transport (Reprinted from Marks and Seabra 2001).

1.4 Fluorescence Microscopy

1.4.1 Introduction

The use of fluorescent-probe and modern optical microscope jointly helps researchers to observe and record the constant activity change in living cells with delicate fine resolution into time and space related. For instance, Fluorescence recovery after photo bleaching (FRAP) has been used for years in observing and recording molecular-dynamics both with cells and the surface of cells (Carla, Ching-Wei Chang, Mary-Ann and Richard, 2015).

Optical microscopes were originally devised to image things that cannot be observed with naked human eyes. The usefulness of microscopes was widened with the initiation of histological stains with particular physicochemical properties together with innovatory lenses, polarizers, and prisms that raised the most effective resolution near to boundaries that are theoretically possible (Elson, Munro, 2004). Certain molecular events, for example, the mechanism by which vesicles are transported across cytoskeletal components in cells, could not be observed and recorded as they were outside hypothetical diffraction determination confine limit of 200nm, but could be detected by further optimizing the contrast and by making use of improved image-capture technologies such as the use of histological stains with particular physicochemical properties mentioned above. (Sprague, Pego, Stavreva, and McNally, 2004).

To optical microscopy another aspect was added with the development and use of fluorescent probes. Fluorochromes are principally spectroscopic tests with positive attributes that permit them to react to natural surroundings at sub-atomic order (Wachsmuth, Weidemann, Muller, 2003) This natural quality help ascertain additional data about particular fluorescent probes by observation and recording; for example, average ensemble alterations in fluorescence intensities at particular wavelengths or the lifespan of the fluorophores resulting after an excitation pulse (Carla, Ching-Wei Chang, Mary-Ann and Richard, 2015)..

Molecular Biologists make use of the spectral characteristics of fluorescent probes to provide data at molecular scales. Non-radiative fluorescence

resonance energy transfer (FRET), Fluorescence recovery after photo-bleaching (FRAP), and Fluorescence lifetime imaging microscopy (FLIM) are the three distinct methodologies that exploit these properties. Significant details about the movement of molecules on the exterior and interior of the cells is provided by FRAP which is useful in observing and recording molecular construction and the dynamics of composite domain with time (Hess, Huang, Heikal and Webb 2002).

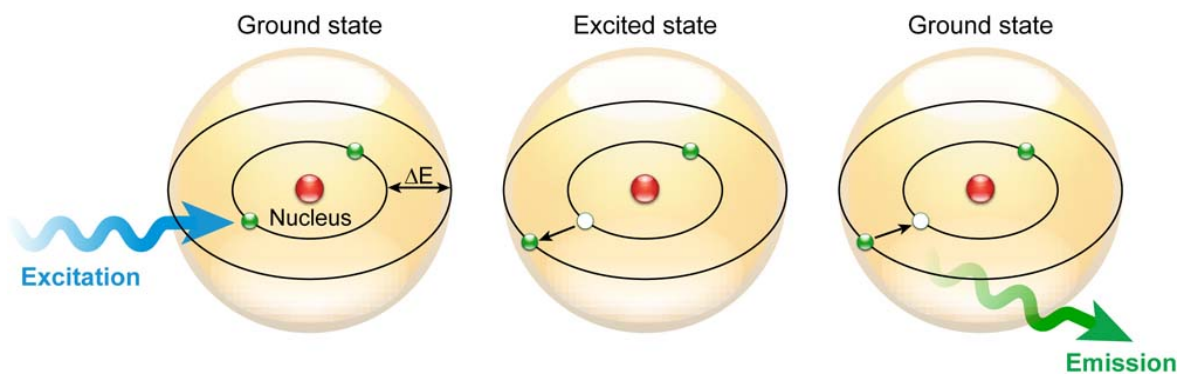


Figure 1.22: Bohr Model. Retention of a light quantum (blue) makes an electron move to a higher vitality circle. In the wake of dwelling in this "energized state" for a specific time, the fluorescence lifetime, the electron falls back to its unique circle and the fluorochrome disseminates the abundance vitality by transmitting a photon (green) (Hellen, Richard and Gregor, 2012).

1.4.2 Fluorescence Recovery After Photo-bleaching (FRAP)

FRAP generally operated for examining the activity of fluorescent molecules in living cells was introduced as “fluorescence photobleaching recovery” at the beginning. (Cardullo et al.,1991; Mullineaux and Kirchoff,2007; Carisey et al,2011). In order to observe and record subjectively and quantitatively molecular activity on the exterior and the interior part of the cell, the technique is now routinely used. The fluorescence recovery after photobleaching (FRAP) technique is used to visualise the dynamic characteristics in real time of selected molecules within living cells, and cell surface membranes. This is particularly useful

when examining how complex structures as such proteins come together and function (De Los Santos et al., 2015).

The fluorescence recovery after photobleaching (FRAP) technique is used to visualise the dynamic characteristics in real time of selected molecules within living cells, and cell surface membranes. This is particularly useful when examining how complex structures as such proteins come together and function (De Los Santos et al., 2015).

This technique makes use of fluorescence emission. Fluorophores are selected as probes or markers for the molecule of interest. These are capable of absorbing and emitting wavelengths of visible or ultraviolet light, of a particular frequency. Absorption of photons of a higher frequency causes promotion of electrons in the structure to an excited state. On return to the ground state, these electrons emit photons of a lower frequency, known as the Stokes shift is a characteristic of the fluorophores used (De Los Santos et al., 2015). However, the process can generate free radicals. A fluorophore can become chemically modified in this way due to the formation of new covalent bonds, and so is unable to emit the photon. This loss of fluorophore activity is termed photobleaching. A photobleached molecule will be replaced by nearby molecules, and this is termed recovery after photobleaching. This is exploited in the FRAP technique.

In order to visualise the fluorescence phenomenon, researchers use filters to identify the movements of a particular molecule.

1.4.3 Application of FRAP

High intensity light sources such as lasers ensure that photobleaching is achieved. A particular region of a cell is selected for examination, and a short burst of the laser light is shone on the area. Then, using a weak light source the dynamics of molecules with respect to time is observed and recorded. Two measurements are attainable by this method; the recovery rate constant and the percentage recovery. The first of these provides an indication of the speed of flow of molecules into and out of the region and can be used to examine the binding or interaction of different groups of molecules. The second measures the proportion of mobile molecules in the region (De Los Santos et al., 2015).

In the study of molecules in cells green fluorescent protein (GFP), which occurs naturally in *Aequorea Victoria*, is commonly used as a tag. This particular tag can be genetically engineered into a selected cell line such as it is inherited by daughter cells. In this way, the protein of interest can have the GFP tag attached, via a linker region. This allows monitoring of the protein when GFP is excited by light with a wavelength of 498 nm (De Los Santos et al., 2015).

Fluorescence Recovery After Photobleaching

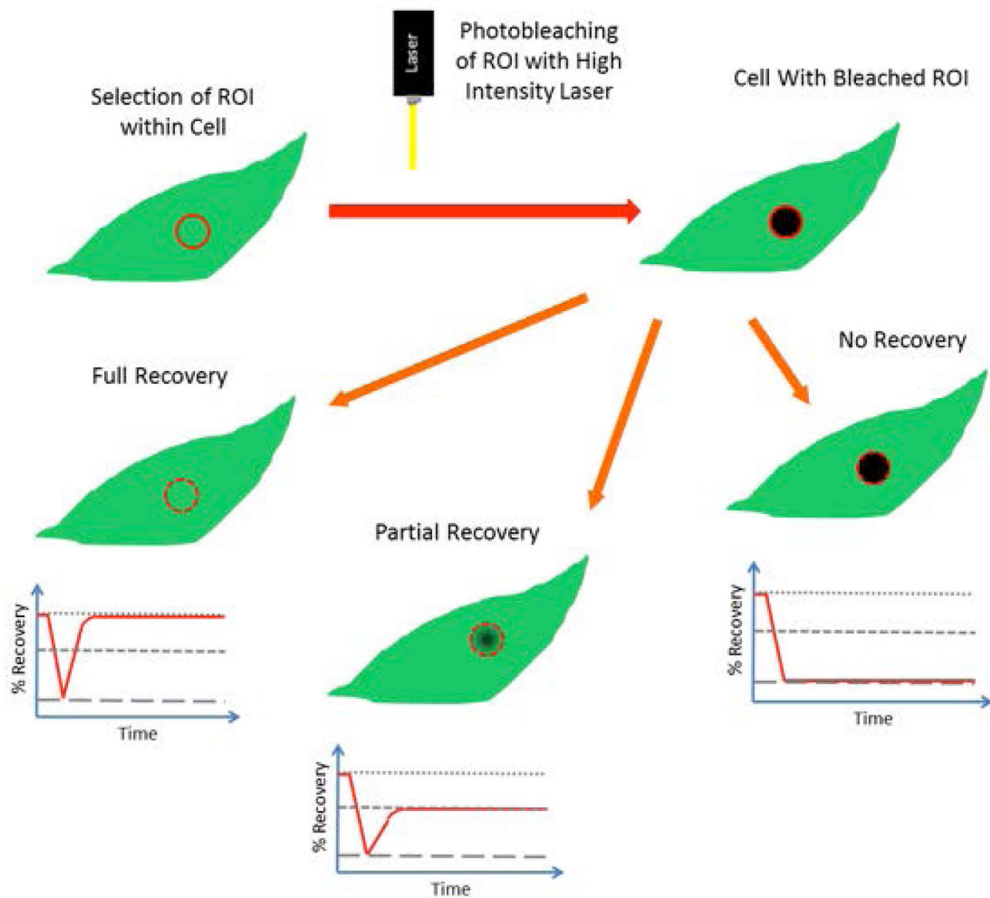


Figure 1.23: Principles of FRAP. The three stages of FRAP are Pre-bleach, bleach and post-bleach. A low intensity light source is used for the whole sample in the pre-bleach step to acquire the background signal. The molecules in the region of interest are photo bleached in the bleached step with a high intensity light source. In the post-bleach step, a low-intensity light is used to observe the movement of molecules in and out of the bleached region. The last step helps to see the recovery of the fluorescent molecules. (Reprinted from De Los Santos et al., 2015)

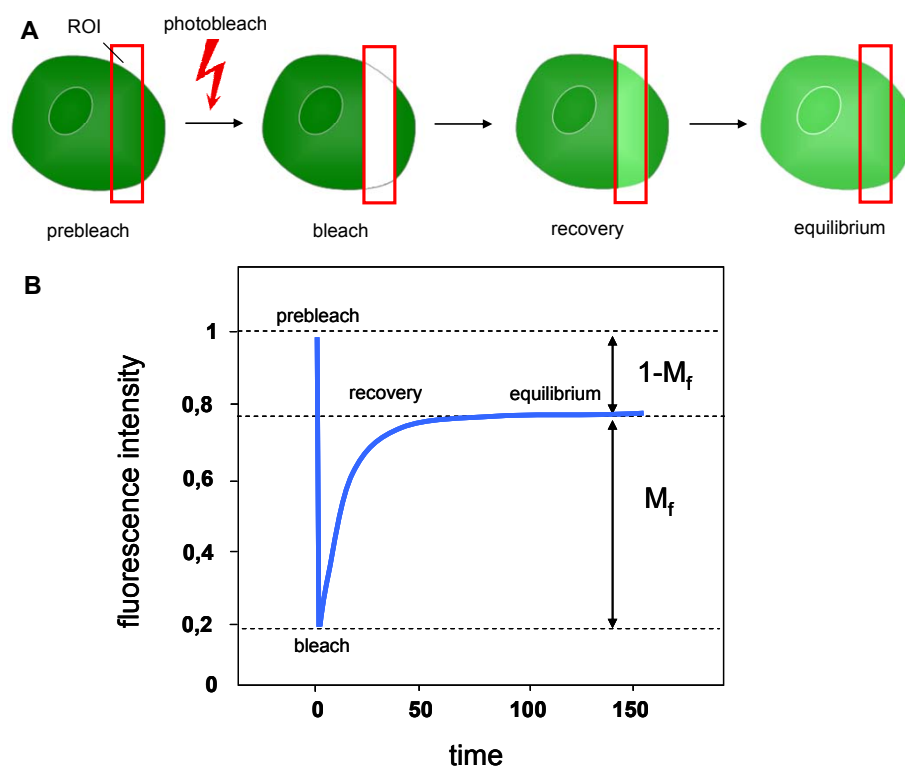


Figure 1.24: Detail of Fluorescence recovery curve. A. The GFP tagged proteins inside the region of interest are bleached by a high intensity light pulse. This destroys the GFP on the protein of interest. The bleached proteins are replaced by other GFP tagged proteins from the neighbouring regions. B. The recovery curve showing the different levels of fluorescent levels at different points of time. Prior to bleaching the intensity is 1 at t_0 and it reaches a very low intensity at t_1 when the region of interest is bleached. Until it reaches an equilibrium state, recovery takes place. The final recovery is not same as the pre-bleach intensity due to the immobile fraction of proteins that are on the immobile structures. (Reprinted from Markus Ulrich, 2008)

1.4.4 Limitations of FRAP

It is possible that the photobleaching performed is not permanent, rather temporary photobleaching, whereby the recovery observed is not due to the dynamics of the protein of interest, can occur. This is termed photoswitching. When photo switching happens, the measure of recovery is erroneous (De Los Santos et al., 2015).

Another limitation which can result in artefacts is the heating effect caused by the laser light source. Often large areas of the cytoplasm are exposed, and the heat absorbed by this can damage a molecule, so that effects not found in the native cell will be observed experimentally.

However, this can be reduced by having a shallow depth of exposure enabling absorption of energy by water in the cell rather than the protein or molecule of interest (De Los Santos et al., 2015).

1.5 Scope of study

This study aims to elucidate the involvement of Rab27a, and its effectors Slp2-a and Slac-2a, in the transport of melanosomes in mouse melanocytes.

1.5.1 Use of mutant cell lines

Three mutant mouse melanocyte cell lines, “ashen”, “dilute” and “leaden” were used in the study outlined in this paper. Ashen cells lack (melan-a cells) functional MP, dilute cells (melan-d cells) lack functional myosin Va, while leaden cells (melan-ln cells) lack Rab27a.

1.5.2 Aim of study

The aim of the study was to determine the nature of the interaction, in terms of length of time, between Rab27a and Slp-2a, and Rab27a and Slac-2a. If the interaction between the two was stabilising after recovery fluorescence recovery would be low compared to if the interaction was for a shorter time, i.e. more dynamic.

1.5.3 Hypotheses

It is expected that both proteins interact with Rab27a. This will confirm the role of Slac-2a and Slp-2a as effectors of Rab27a. Furthermore, it is expected that the interaction Rab27a with Slp-2a will be stabilising, as this is supported by the literature. However, the nature of the interaction of Slac-2a with Rab27a will be clarified.

Chapter 2

Materials and Methods

2.1 Analysis of the interaction of the proteins

2.1.1 Cell culture

The melanocyte cell lines derived from a C57BL/6 mouse and with different mutations such as melan-a (Wild Type), melan-d (myosin Va null), ashen (Rab27A null) and leaden (Mlph null) were maintained in RPMI-1640 culture medium, supplemented with 10% (V/V) fetal bovine serum (FBS), 100 units/ml, 1% (V/V) 100 x penicillin/streptomycin (P/S) and 200nmol PMA (phorbol 12-myristate 13-acetate) growth factor. Cells were incubated at 37°C in the presence of 10% CO₂.

When the confluency of the melanocytes reached 80-90%, the cells were passaged by incubating in 0.05% trypsin and 0.02% EDTA (sigma) in 1x PBS (Lonza) for 2-3 minutes at 37°C. Cells were then removed from the flask by gentle tapping and complete RPMI-1640 medium was added. For T-25 flasks containing 2ml of 1 x Trypsin/EDTA, 3ml of RPMI and for T-75 flask containing 7ml of Trypsin/EDTA, 8ml of RPMI was added. The cell culture mixture was pipetted to a sterile 25ml sterilin tube and centrifuged at 1500 g for 5 minutes. The pellet was re-suspended in 5ml complete RPMI-1640 medium followed by the splitting 1 in 5 into either T25 or T-75 flasks with 4ml or 20ml complete RPMI-1640 medium individually.

2.1.2 Transfection

Cells were plated onto 35mm glass-bottomed dishes (MaTek) at a density of 3-4 x 10⁴ cells per dish. Each of these glass bottom dishes contained 2ml of melanocyte growth medium. Cells were grown for 24 hours at 37°C prior to transfection.

1ml of Optimem was added to 7.5µl of FuGENE 6 and incubated for 5 min at room temperature to enable the formation of lipid vesicles before 1.5µg plasmid DNA (plasmid constructs used: pEGFP-Rab27A, pEGFP-Mlph, pEGFP-Myosin Va and pEGFP-Slp2) was added and incubated for an additional 15 min (Ramalho, J.S., et al. 2001). This transfection mixture

was then used to replace the spent original growth medium of the 24 hour old cell culture. Cells were allowed to incubate for either 3h or overnight, at which point the medium was replaced with full growth medium. Cells were then incubated for 24-48 hours in order to express transfected plasmid DNA encoding the GFP-tagged proteins of interest.

2.1.3 Fluorescence Recovery After Photo Bleaching (FRAP)

Expression of transfected plasmid-encoded GFP-tagged proteins should occur after 48 hours, at which point the growth medium was replaced with L15 medium containing 10% FBS and 1% penicillin/streptomycin to culture cell in the absence of bicarbonate buffer (and carbon dioxide). Cells were then incubated at 37°C in the absence of CO₂ for imaging on a preheated Zeiss LSM710 confocal microscope. The confocal microscope was equipped with a 63x/1.4 NA phase contrast oil immersion lens.

FRAP Protocol

FRAP was performed on four different cell types: melan-a, melan-ln, melan-ashen and melan-d. In these four cell types the recovery of up to five wild type or chimeric proteins was examined including Rab27-a, rab27-a missing the Rab binding domain (RBD), wild type melanophilin, slp2 and the chimeric protein produced in this study: slp2-mlph.

The glass bottomed dishes with the transfected GFP-expressing cells were placed on the confocal microscope stage and the region of interest was focussed on and bleached. Individual organelles were searched for with clustered regions being deliberately avoided.

The Zen Black software was used to choose, three small (6µm²) regions of interest (ROI). The chosen regions were bleached with a 100% illumination power beam using 30 iterations of a 5mW 488nm laser. Images were taken every 1.57 seconds for a total of 100 seconds. The first series of images shows the amount of fluorescence before bleaching, the next series displays at the time of bleaching, the selected regions were

bleached after every fifth image and the following images showing the recovery progress after bleaching.

2.1.4 Image processing in ImageJ

The recorded image series were then exported to ImageJ as a sequence of images and converted into a single stack of images. The channels were splitted under color in image option, the images were inverted, the brightness levels were adjusted, one of the Gaussian blur or median filters were used to reduce image noise. The melanosomes were filtered from the background fluorescence using “Enhance Contrast” and “Adjust/Threshold”, transforming them into a binary. The contrast enhancement was carried out such that the brightest 0.1% of pixels was set to saturation and others were scaled according to this. Image montages (Figure 3.2) were made to compare the fluorescent levels for each series of images by converting the image sequences into RGB color models to allow correlation of fluorescence intensity over time with the position of the melanosomes.

2.1.5 Volocity and prism image analysis

Volocity is a 3D imaging software that allows to visualization, exploration and analysis of multi-channel 3D volumes over time (Costes S.V., Daelemans D., Cho E.H., Dobbin Z., Pavlakis G., Lockett S. 2004). In this thesis, Volocity was used to track individual bleached granules within the region of interest (ROI) over a time period. This software was used to visualize data for proteins Rab27, Slac2-A, SLP2, and Rab27Asf1f4 (a chimeric molecule - Rab27A mutant lacking effector binding) in 4 different cell lines; melan-ln, melan-Ashen, melan-a, and melan-d (Tarafder AK et al., 2011). Light intensity readings were taken at a 1.57s time interval and fluorescence intensity at each time point was obtained for a time period of 100s. For every sample, the intensity level of a number of bleached GFP-tagged granules was monitored within ROI.

Volocity analysis of granules (each sample) of the protein against the 4 different cell lines was performed at least 3 times to obtain reliable data. Multiple image stacks derived from multiple cell lines and proteins were used in the analysis. The total mean intensity of the granules in a sample within the ROI was determined as follows. The ‘brightest point’ option was used to project image stacks into a single image which was then exported as a TIFF file which could subsequently be opened with ImageJ for further analysis (ImageJ. 2016).

Objects (granules) with fixed thresholds ranging more than 45 were selected using the ‘analyse parameter’ function. Measurement of the mean fluorescent intensity of the granules in cells expressing GFP-tagged proteins in individual cell boundary areas was calculated using the box tool in order to perform normalization. The image was then cropped and fluorescent objects with fixed threshold values >45 were applied. Followed by selecting the ‘measure object’ command to obtain the mean fluorescent intensity of the threshold objects in the selected box. Objects total mean fluorescent intensity of the selected box was obtained and the individual values were exported to Microsoft Excel where the normalization calculation took place.

Normalization

The fluorescent intensity levels of the individual bleached granules present in the ROI from each sample were then normalized against the box value intensities. Normalization was done to ensure results obtained are comparable and enable estimation of the relaxation half time ($t_{1/2}$).

The following formula was used to normalize each granule:

$$\frac{\textit{Intensity level of individual granule}}{\textit{Fluorescent Intensity Mean value of granules in box region}}$$

Calculation of the bleached granule normalization was performed for a minimum of three granules per sample per time point (from 0 to 100s). This was repeated for all samples.

Subsequently, percentage recovery was calculated for each granule, as follows:

$$\frac{F(t)-F(0)}{F(\text{inf.})-F(0)} \times 100$$

P(Fn(t))...Percentage recovery of fluorescence intensity at time t

F(t)... Fluorescence intensity at time t inside bleach ROI

F(0)... Fluorescence intensity at time 0(immediately after bleaching)

F(inf)... Fluorescence intensity at equilibrium

This calculation method is called the “Axelrod method” which sets the plateau value to 100% (Constantin Kappel and Roland Eils, 2004). Consequently, using a normalized plot, the relaxation half time can be graphically figured out.

This method of calculating percentage recovery is explained further in detail below,

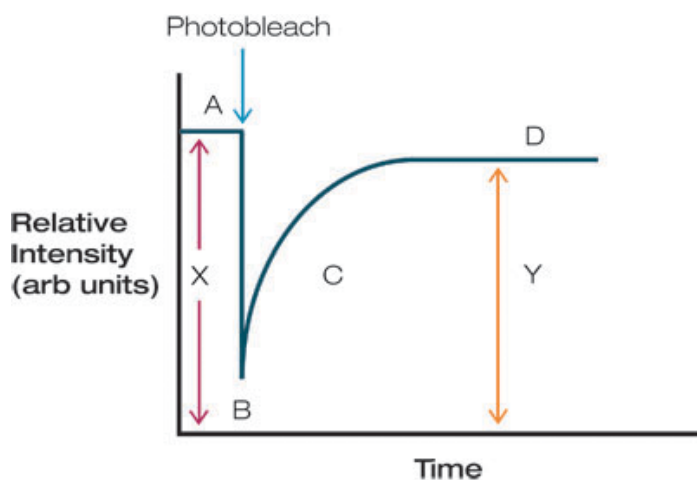


Figure 2.1. Percentage Recovery calculation. The percentage recovery uses the formula: $(Y/X) \times 100$. Where X is the percentage of fluorescence intensity immediately after bleaching (fluorescence loss) and Y is the level of fluorescence recovered to the area bleached. The slope of the curve gives the lateral mobility. The steeper the curve, the faster the recovery and therefore, the more mobile the molecules. Reprinted from Constantin Kappel and Roland Eils, 2004.

Next, the average percentage recovery of each protein in different cell lines is calculated for each region.

Average Percentage Recovery =

$$\frac{\text{Sum of the percentage intensities of the granules (for each bleaching)}}{\text{Number of granules used to calculate the percentage intensities}}$$

Using the outcome of the above calculation, plots were drawn and the fluorescence recovery of different proteins was compared. Standard deviation was calculated using the formula `standev()` in excel which was then displayed as error bars on graphs plotted using PRISM (GraphPad Prism, 2016).

2.2 Further investigation on the dynamic interaction of the Slac2-a with Rab27A. Generation of the chimeric molecule.

In order to investigate the interactive effects of the RBD of melanophilin and slp2, a chimeric molecule was generated in which the rab binding domain of melanophilin was replaced with that of Slp2. The following is an overview of the molecular cloning performed to achieve this.

The RBD of Slp2 was PCR amplified from mouse genomic DNA using primers S2hind5 and S2hind3 which add HindIII sites to the ends of the fragments. The melanophilin gene to be edited was encoded on pEGFP-Mlph sourced from Dr. Alistair Hume. pEGFP-Mlph encodes melanophilin with HindIII sites flanking the RBD allowing the PCR amplified RBD of Slp2 to be swapped in via restriction-ligation cloning. PCR product and vector backbone pEGFP-C2 were digested with HindIII, followed by dephosphorylation for the vector backbone. Agarose gel electrophoresis was employed to verify that DNA fragments were of the expected size. Fragments were gel purified before ligation proceeded. Ligation products were then transformed into *E. coli* DH5 α chemically competent cells.

2.2.1 PCR

The RBD of Slp2 was PCR amplified using primers S2hind5 and S2hind3 which were designed so as to add HindII sites to the ends of the PCR products were synthesized by Sigma. The reaction proceeded using the following recipe and conditions:

Components	Volume (μ l) (100 μ l reaction)
10 x NEB buffer	5
10mM DNTPs (Promega)	4
dH ₂ O	39 (to 100 μ l)
cDNA template (50 ng/uL) (slp2 RBD)	1
Pfu DNA polymerase (NEB)	1
Total	50ul
Primers (10 μ M)	2.5ul (made up to a final concentration of 0.5 μ M)

Table 2.1. PCR. The above table gives the quantity and condition of each component used in PCR.

Primer name	Primer sequence
Forward /S2hind 5	CTGAAGAAGCTTAATGTCAGGTC TATCCAAAAAC
Reverse /S2hind 3	TTTTTCAAGCTTGTATTATCCCA TCATTGTGT

Table 2.2. The primers used for the construction of the chimera slp2-mlph.

The above components were mixed by gently pipetting several times, centrifuged for few seconds and then the PCR mix is placed in the thermal cycler to undergo the below-PCR program.

Temperature (°C)	Time (min)	Number of Cycles
94	1	1
94	1	30
55	1	30
72	12	30
72	10	1

Table 2.3. PCR cycle conditions

2.2.2 Agarose Gel Electrophoresis

After each PCR, the DNA was analyzed in a solution of 6X DNA loading buffer (40% sucrose, 0.25% bromophenol blue in milli-Q water) and Milli-Q water which was diluted in the applicable ratio to obtain a final 1X concentration of DNA loading buffer.

A 1% agarose gel was prepared by adding 0.3g of Agarose powder and 30ml of 1 X TBE buffer (1.08% w/v Tris base, 0.55% w/v boric acid, 0.0585% EDTA w/v in dH₂O) into a conical flask in which it was mixed. The conical flask was then heated in a microwave until the agarose was fully dissolved solution. Melted agarose was allowed to cool to roughly 50°C after which ethidium bromide was added to a final concentration of 0.5µg/ml. The ethidium bromide was mixed thoroughly before the solution was poured into gel casting trays to set at room temperature with combs inserted to produce the lanes as appropriate.

After solidification the comb was removed and the casting tray was positioned in a gel tank filled with 1 x TBE buffer. DNA solutions diluted with 6x loading buffer were loaded to the wells and 80mA of current was passed across the gel for after around 45 minutes. Gels were visualized

using a Gel Doc system and the size of the DNA was compared with a 1kb DNA molecular weight ladder (NEB) (Robinson, Christopher L. (2016)).

2.2.3 Restriction Digest Protocol

For each restriction digest reaction, the following quantities were used: 2µg of plasmid DNA, 1µl of restriction endonuclease (10 units of enzyme), 2µl of suitable 10 X buffer obtained from Promega, this then was made up to a total volume of 20µl with MilliQ water (Table 2.4).

Components	Volume (20µl reaction)
DNA	1µg/2µg
Restriction endonuclease	1µl
10 x Buffer	2µl
MilliQ water	To 20µl

Table 2.4. Components of restriction digest protocol

The reaction mixture was then centrifuged for few seconds to mix everything thoroughly before incubation at 37°C for one hour. Digest products were examined using gel electrophoresis as described in 2.2.2.

2.2.4 De-phosphorylation

Dephosphorylation was employed on the vector backbone to prevent re-circularisation. Shrimp Alkaline Phosphatase (SAP) sourced from (NEB) was used following the manufacturer's instructions. Briefly, 1µl of enzyme was added per 1µg DNA and the reaction made up with buffer and ddH₂O before being incubated at 37° C for 30-60 minutes. SAP inactivation was achieved by heating at 65°C for 15 minutes.

2.2.5 DNA Purification and Ligation

The final procedure in the formation of the recombinant plasmid (chimera slp2-mlph) was ligation of the insert DNA (containing RBD of SLP2) into the HindIII digested vector backbone (pEGFP C2). T4 DNA ligase (Promega) was used as per the manufacturer's instructions. As explained above in the Restriction Digest Protocol (See 2.2.3), Hind III restriction endonuclease was used with both fragments of DNA to obtain the insert and the vector. After the de-phosphorylation (see 2.2.4) both digests were purified using a PCR clean-up kit (Machery Nagel) as per the manufacturer's guidance.

In the ligation protocol, the amount of each component used is given below in the table.

Components	Volume (20µl reaction)
10 X T4 DNA ligase buffer	2µl
Vector DNA (mass in ng)	volume in µl derived using the formulas given below
Insert DNA (mass in ng)	volume in µl derived using the formulas given below
dH ₂ O	to 20µl
T4 DNA Ligase	1µl

Table 2.5. Components used in DNA ligation

The volume of the insert and the vector needed was calculated in the ratio of 3:1 respectively. It is further explained by the equations given below,

$$\text{Insert DNA mass (ng)} = 3 \times \frac{\text{insert length in base pairs}}{\text{vector length in base pairs}} \times \text{vector mass (ng)}$$

$$\text{Volume } (\mu\text{l}) = \frac{\text{mass (ug)}}{\text{Concentration (ug/ul)}}$$

These components were added in a microcentrifuge tube on ice, gently mixed by pipetting up and down and followed by a brief centrifugation step. Ligations proceeded at 16°C for 18h.

The ligation mixture was then used to transform DH5 α *E. coli* cells and, after expansion of the cells overnight at 37°C, the plasmid DNA was extracted using miniprep as described in 2.2.8 and 2.2.9 below. The success of the ligation was evaluated through restriction digest (see 2.2.3) followed by gel electrophoresis (see 2.2.2).

2.2.6 Transformation

Chemically competent DH5 α *E. coli* cells were used for cloning steps. 50 μ l volumes of competent cells were defrosted on ice before the addition of the 3 μ l ligation mix or 1 μ l plasmid DNA. Microcentrifuge tubes containing the DNA-cell mixtures were then incubated on ice for 10 minutes before being added to a 42°C water bath for 1 minute. After heat-shock the cell-DNA mixture was placed on ice for a further two minutes before non-selective 250 μ l LB medium (1% tryptone (w/v), 0.5% yeast extract (w/v), 1% NaCl (w/v), pH adjusted to 7.5 with 1M NaOH) was added. The recovery cultures were incubated in a 37°C shaking incubator for around 1 hour. Recovered cells were centrifuged and the supernatant removed allowing the cells to resuspend in the residual supernatant. Re-suspended cells were spread onto selective LB agar plates and incubated statically at 37°C. Colonies representing successful transformants appeared after overnight incubation.

Contr ols	Liga se	Explanation s
Uncut Vector	-	To confirm the antibiotic resistance of the plasmid
Cut Vector	-	Background due to uncut vector
Cut Vector	+	To confirm the effectiveness of de- phosphorylat ion and the vector was fully digested
Insert	+	If any colonies were present, that implies any contaminatio n with the transformatio n reagents or with the whole plasmid in ligation

Table 2.6. Choice of vector, insert combination

2.2.7 Preparing agar plates

To prepare the agar plates, LB medium was prepared by adding 1% w/v tryptone, 0.5% w/v Yeast Extract and 1% w/v NaCl to 1L ddH₂O. Agar was added to a final concentration of 1.5% w/v. The mixture was swirled and the contents were well mixed before autoclaving. After autoclave, the agar solution was allowed to cool in a 55°C water bath, before addition of kanamycin to a final concentration of 50 µg/ml . The agar solution with kanamycin supplementation was poured into 10cm polystyrene petri dishes, allowed to set at room temperature before being inverted and stored at 4°C.

2.2.8 Inoculating Overnight Cultures

The components used in the propagation of bacteria and the method carried out is explained below.

Materials

1. Antibiotic
2. LB medium
3. LB agar plates (the transformation plates)

Method

10ml of LB medium supplemented with kanamycin solution (final concentration 50µg/ml) was added to a sterile tube and a single colony was picked from the LB agar plate using a sterile 200µl pipette tip and expelled into the tube under aseptic conditions. The tube was then left in the shaking incubator (200 rpm) at 37°C for roughly 18 hours for maximum aeration to permit the E. coli cells to multiply.

2.2.9 DNA Isolation (Mini Prep)

Using the Nucleospin plasmid purification kit (Machery Nagel) and according to the manufacturer's guidelines, the plasmid of interest was extracted from the *E. coli* cloning strain DH5 α

Chapter 3

Results

3.1 Rab27-a in different cell lines - Frap analysis of the dynamics of Rab 27A in the cell lines melan- a, melan-ln and melan-ash

3.1.1 Introduction

The proteins Rab27A, its effectors SLP2 and SLAC2-A and MYOVA have been suggested to play an important role in melanosome transport in a seminal video microscopic studies of melanosome transport in melanocytes (Wu et al., 1998). Defects in melanosome transport have been noticed with mutant (dilute) which is lacking the presence of MyoVa, in ashen in which the Rab27a is missing and in leaden mice in which the Mlph (also known as Slac2-a) which supports the previous suggestion of the involvement of these three proteins. Previous data through deletion analysis and site directed mutagenesis revealed that the N-terminal Slp(synaptotagmin-like protein) domain of Slac2-a binds to Rab27A and the C-terminal binds to the globular tail of myosin Va which give raise to the idea of a tripartite complex consists of these three proteins(Fukuda et al., 2002; Hume et al., 2002). In another analysis, when the Rab27a in detergent lysates of melanocytes were seen with beads coated with full-length melanocyte myosin Va and melanocyte myosin Va lacking exon D, the Rab27a interacted with both forms of myosin Va whereas when the Rab27a were seen in the beads coated with melanocyte myosin Va lacking exon F, an absence of interaction between the Rab27a and myosin Va was noticed. These findings support the idea of tri partite complex where the Rab27a is an important constitute of the complex that acts as a melanosome receptor for myosin Va and it also suggests that there is an additional protein involved in bridging the interaction between Rab27a and myosin Va (wu et al 2002).

This tripartite complex is found to be involved in the transfer of melanosomes from melanocytes to keratinocytes, by transporting the melanosomes from the perinuclear region to the peripheral region of the melanocytes (Fukuda et al., 2002, Hume, A.N., et al., 2006). To study the movement of these proteins, we have used Fluorescence Recovery After

Photobleaching (FRAP). In photobleaching, the desired region is selectively photobleached with a high-intensity laser and the recovery of the region as the GFP-tagged proteins from the unbleached regions move into the bleached region is observed over time with low-intensity laser light using a confocal microscope (Lippincott-Schwartz JI, Snapp E, Kenworthy A, 2001). Protein recovery can be the consequence of the distribution, coherence, uncoupling, and transmission process.

To further investigate the involvement of these proteins in the melanosome transport and to understand the nature of the interactions between these proteins as well as with the melanosome, FRAP technique was done. We first transfected mouse skin melanocytes with GFP-tagged Rab27A plasmid. The region of interest with a single melanosome attached to the GFP-tagged protein and with a reduced background signal (background fluorescence) was chosen and photo-bleached using high intensity laser using a confocal laser scanning microscope and their fluorescence recovery after photobleaching from the surrounding area into the photobleached area was monitored to understand the dynamic or stable nature of interaction of the Rab27A with the melanosomes. Different regions were photo-bleached in the same way and the fluorescence recovery was measured. The average intensity value of the region of interest at each time point were then normalised against the non-bleached region to minimise the background signal (background fluorescence) that arises to the instrument set up, imaging parameters, auto-fluorescence of samples and imaging media . The fluorescence in the bleached area was plotted against time to analyse the kinetics and extent of recovery.

It was seen that Rab27A recovers to $15.4\% \pm 4.66$ in wild-type cells as shown in figure 3.1. The percentage recovery was seen as quite low when compared with the data of Rab27a and the other components of tripartite complex in other cell lines which indicates that the Rab27A bound to the melanosomes in the bleached region doesn't get replaced with another GFP-tagged Rab27A from the non-bleached region after the photo bleaching. This suggests that it has a stable interaction with the melanosome which is preventing the swapping of the bleached GFP-

tagged Rab27A with a non-bleached GFP-tagged Rab27A from the surrounding region (figure 3.1).

To further understand the involvement of the endogenous Rab27A in the recovery, GFP-tagged Rab27A was seen in melan-ashen. This would only have the GFP-tagged Rab27a so would enable to see the interaction of these exogenous Rab27a with the melanosome. It was seen that the recovery was $25.3\% \pm 9.13$ as shown in figure 3.2, higher than the GFP-tagged Rab27A in wild type cell as the endogenous Rab27A are absent in melan-ashen and not competing with the GFP-tagged Rab27A.

To investigate the role of the other constituents of the tripartite complex in the stable nature of Rab27A with the melanosome, the above mentioned procedure was repeated in different cell lines where the proteins MyoVa and the Rab27A effectors slac2-a and slp2a were lacking. GFP-tagged Rab27A in the melan-In cell line, which lacks slac2-a recovered to $14.8\% \pm 6.78$ as shown in figure 3.3. In the absence of Slac2-a, the recovery hasn't much affected and only reduced from 15.4% to 14.8% which indicates that Slac2-a doesn't control the interaction of Rab27A with the melanosome.

Although the interaction of Rab27a with the pigment granules was seen in the absence of slac2-a proteins, we were unable to test whether the interaction depends on slp2 as there are no cell lines available which lack slp2. So to confirm the possible effect of slp2 on Rab 27A and to re-confirm the involvement of Slac2-a proteins in the stabilization of Rab27a with the melanosome, mutations were introduced into Rab27a (the chimeric mutant 222) to interrupt its potential to interact with the effector molecules slac2-a and slp2.

Frap was carried out in the wild type cell line, expressing Rab27a and Slac2-a, but not Slp2, and very low recovery of $22.5\% \pm 9.46$ in the bleached regions was observed as shown in figure 3.4, which assured us that both Slac2-a and Slp2 do not regulate this function of Rab27a.

Below given are the time point images of the results from the confocal microscope which were obtained using the software Image J and prism.

Images were taken every 1.57 seconds for a total of 100 seconds. The first series of images shows the amount of fluorescence before bleaching, the next series displays at the time of bleaching, the selected regions were bleached after every fifth image and the following images showing the recovery progress after bleaching.

3.1.2 Rab27-a in melan-a

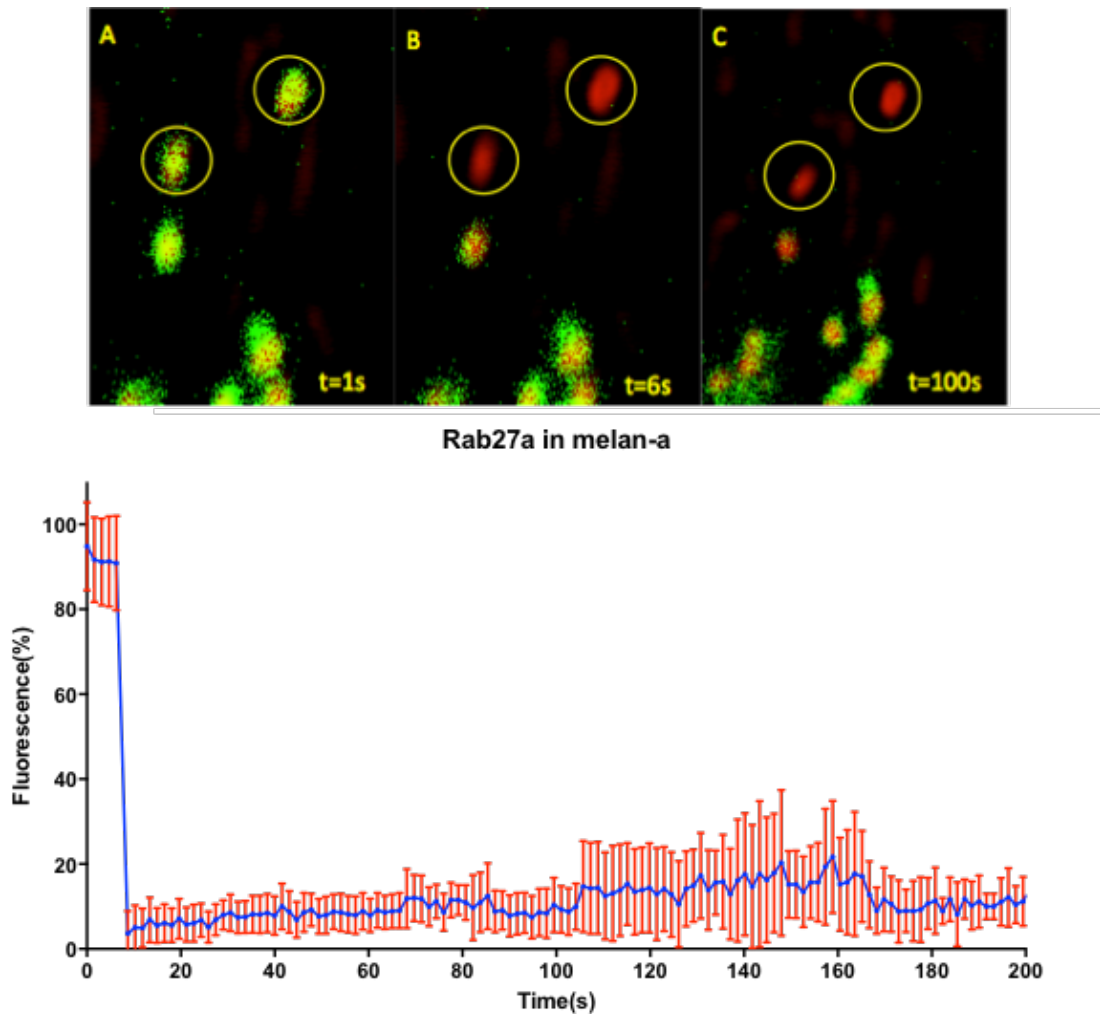


Figure 3.1. FRAP analysis of the dynamics of melanosomal GFP-rab27a in melan-a cells. FRAP micrographs showing time frames (A, B, C) of GFP-rab27 associated with melanosome in melan-a at t=1s ,6s,100s respectively. A shows the initial fluorescence set at 100% (t=1s), Fig B shows the fluorescence at the time of bleaching (t=6s) and Fig C represents the recovery of fluorescence after 100s. In this case, there was minimal recovery ($15.4\% \pm 4.66$), which means that the rab27a is stably targeted as represented by the recovery curves of fluorescence intensity (D). Shown are the mean \pm SD of different experiments (n=6).

3.1.3 Rab27 in melan-ashen

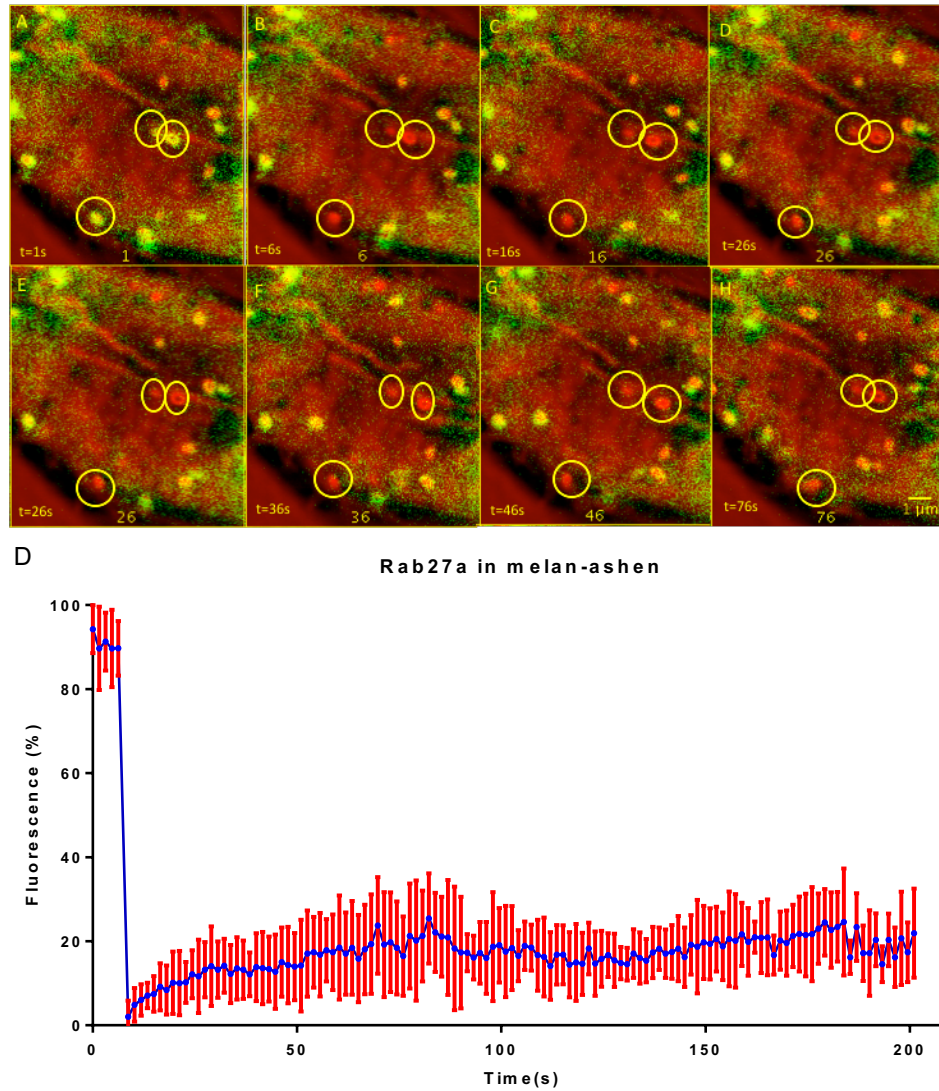


Figure 3.2 FRAP analysis of the dynamics of melanosomal GFP-Rab27a in melan-ashen cells. FRAP micrographs showing time frames (A, B, C) of GFP-Rab27 associated with melanosome in melan-ashen at $t=1s$ (initial fluorescence set at 100%), $6s$ (the fluorescence at the time of bleaching), $100s$ (the recovery of fluorescence after 100s) respectively. The amount of recovery ($25.3\% \pm 9.13$) was slightly higher in melan-ashen than in melan-a and melan-ln as there weren't any endogenous rab27a competing with the exogenous GFP-Rab27a. The stable interaction of Rab27a was seen again as represented by the recovery curves of fluorescence intensity(D). Shown are the mean \pm SD of different experiments ($n=20$).

3.1.4 Rab27a in melan-In

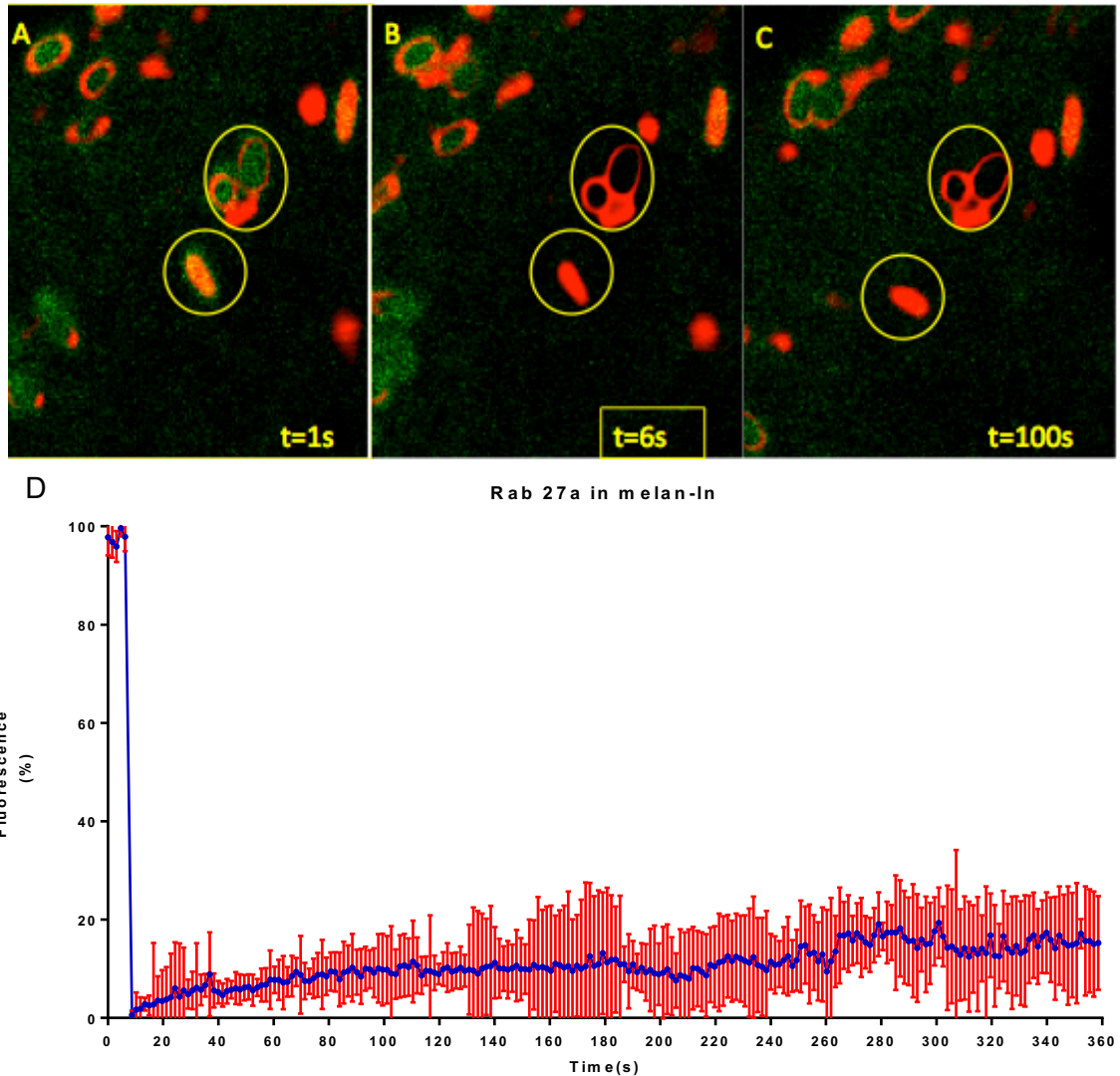


Figure 3.3 FRAP analysis of the dynamics of melanosomal GFP-Rab27a in melan-In cells. FRAP micrographs showing time frames (A, B, C) of GFP-Rab27 associated with melanosome in melan-In at t=1s (initial fluorescence set at 100%) ,6s (the fluorescence at the time of bleaching),100s (the recovery of fluorescence after 100s) respectively. The amount of recovery was the almost the same as in melan-a, $14.8\% \pm 6.78$, which means that slac2-a protein doesn't play any role in the stable interaction of Rab27a with the melanosome as represented by the recovery curves of fluorescence intensity(D). Shown are the mean \pm SD of different experiments(n=5).

3.1.5 Rab27-a Chimeric mutant in melan-a

The interaction of Rab27a in the cell lines melan-1n (absence of melanophilin) suggested that it has a stable interaction. To study the importance of SLP2-a in the dynamics of Rab27a, a chimeric molecule of Rab27a was constructed which highly reduces the binding of slp2 and melanophilin on to it. The image analysis of the chimeric molecule in wild-type cells had a fluorescence recovery of $22.5\% \pm 9.46$ which confirmed that both effector proteins, SLP2-a and melanophilin doesn't play a role in the dynamics of Rab27a with the melanosome.

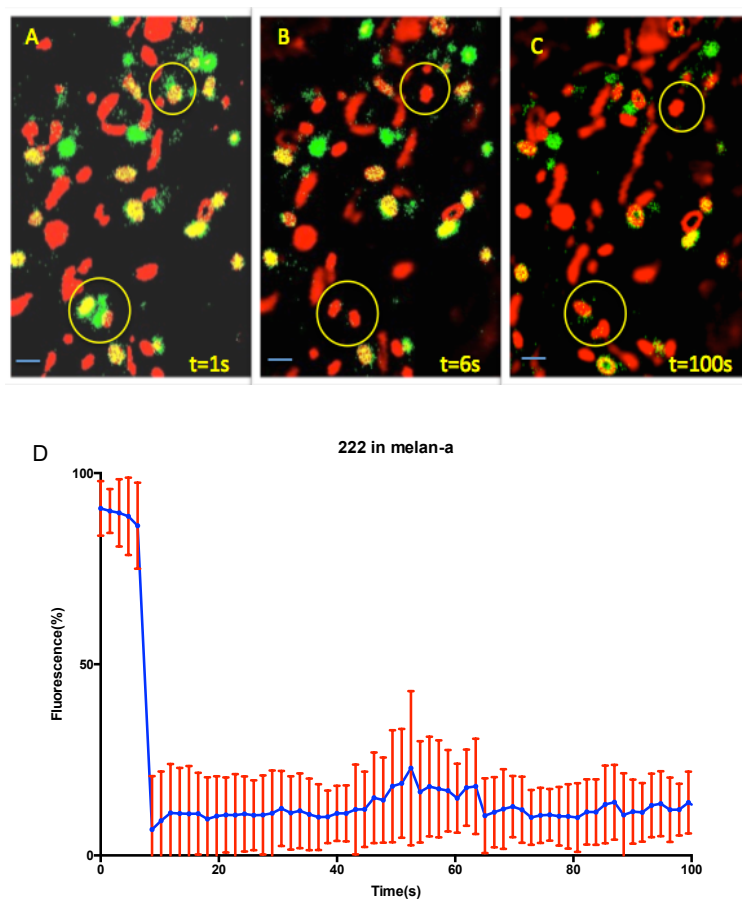


Figure 3.4. FRAP analysis of the dynamics of melanosomal GFP-mutated Rab27 chimeric molecule in melan-a cells. FRAP micrographs showing time frames (A, B, C) of GFP-Rab27 chimera in which the interaction of Rab27 with slp2 and slac2-a is highly reduced, associated with melanosome in melan-a at t=1s (initial fluorescence set at 100%), 6s (the fluorescence at the time of bleaching), 100s (the recovery of fluorescence after 100s) respectively. The amount of recovery ($22.5\% \pm 9.46$) confirms that the Rab27a effectors do not play any role in the stability of Rab27a with the melanosome. The stable interaction of Rab27a was seen again as represented by the recovery curves of

fluorescence intensity (D). Shown are the mean \pm SD of different experiments (n=29).
Scale bar = If the line is 0.7 it represents 2 μ m.

3.1.6 Rab27A comparison graph in different cell lines

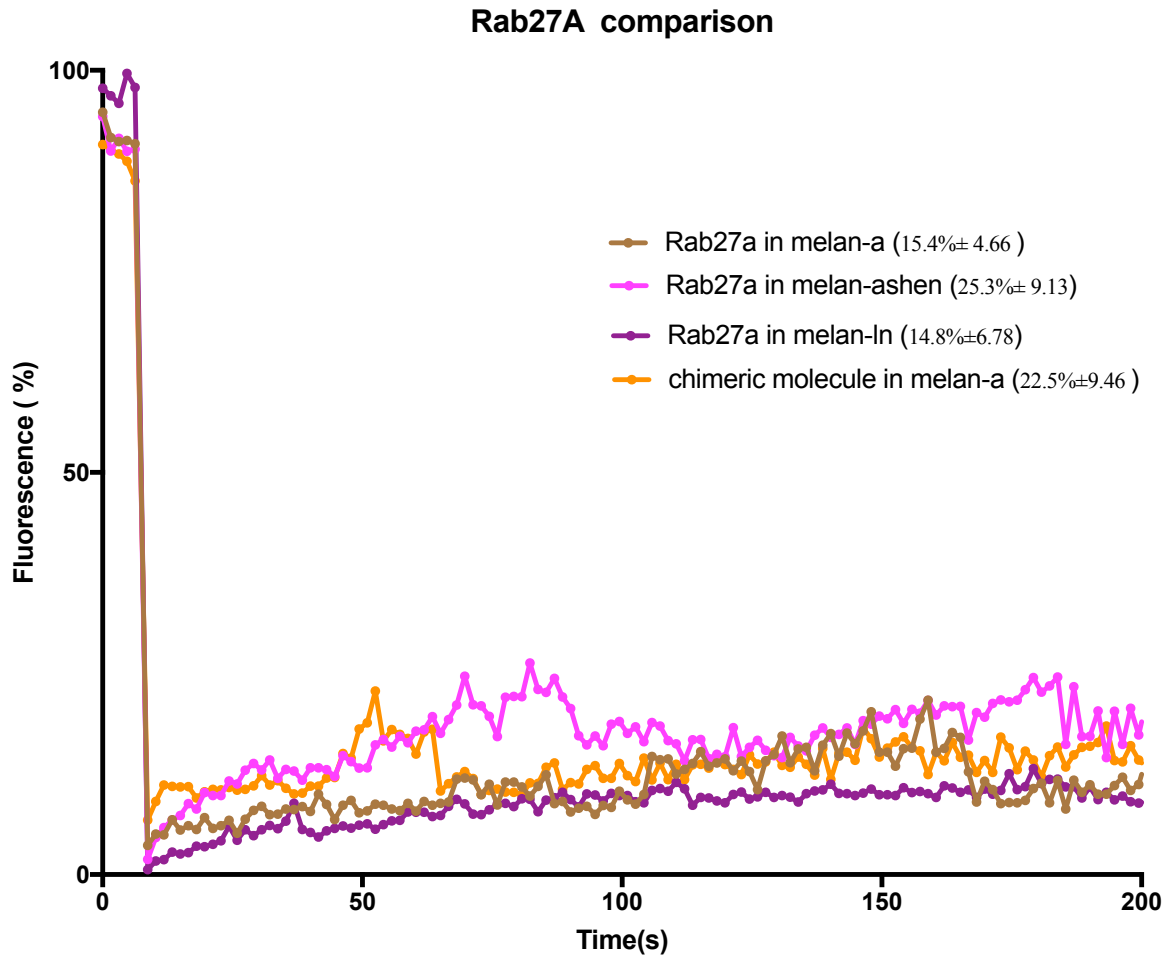


Figure 3.5. Rab27A recovery comparison graph This figure shows the recovery of the protein Rab27A in various combination of cell lines that were experimented and the recovery of Rab27A chimeric mutant in melan-a.

3.2 Rab27a effectors in different cell lines - Frap analysis of the dynamics of Slac2-a in the cell lines melan-a, melan-ln and melan-d suggesting that it has a dynamic interaction.

The next step was to test the behaviour of Rab27A effectors alone in different cell lines. We transfected wild type GFP-tagged Slac2-a plasmid into the different cell line.. When the experiments with FRAP were carried out on the Full melanophilin which consists the rab binding domain(RBD), myosin binding domain(MBD) in the wild type cells, the cells recovered to $60.4\% \pm 7.81$ as shown in figure 3.6 and melanophilin RBD in wild type cells recovered to 52.5 ± 29.1 as shown in figure 3.7. The greater recovery of full melanophilin in wild type than melanophilin RBD shows that ABD and MBD play a role in the dynamic nature of melanophilin with the Rab27a.

Slac2-a RBD in melan-ln recovered to $57.5\% \pm 9.30$ as shown in figure 3.8, which is greater than Slac2-a RBD in melan-a. This is because melan-a contains the endogenous melanophilin that would compete with the exogenous melanophilin reducing the chance of the replacement of the bleached melanophilin with the GFP-tagged melanophilin from the non-bleached region.

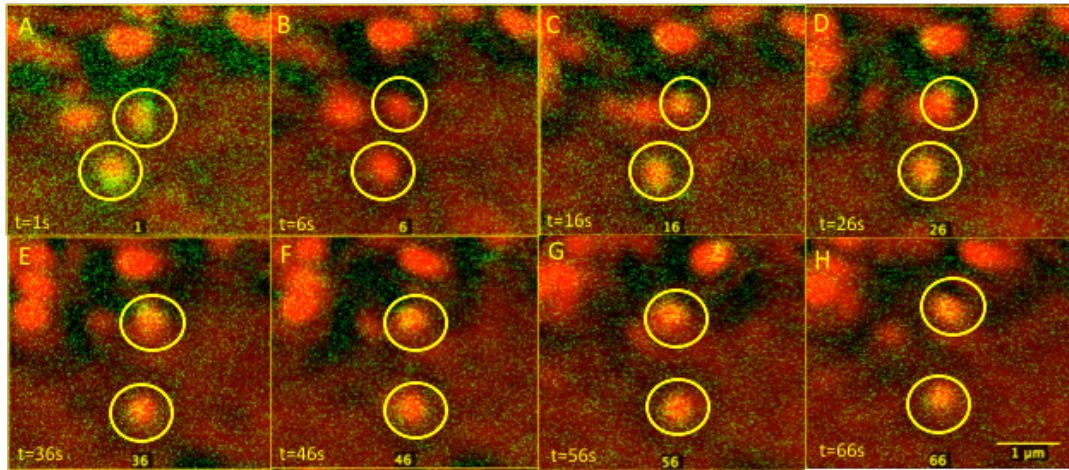
The mlph was also seen in melan-d, in the absence of Myosin Va to see its involvement in the degree of binding of the effectors with the Rab27-a. The amount of recovery of $43.72\% \pm 10.7$ as shown in figure 3.9 shows that there is not much difference in the absence of myosin Va. It also confirms mlph has a dynamic interaction with Rab27-a compared to slp2 interactions with melanosome

Slp2 RBD in melan-a recovered to $27.1\% \pm 8.51$ as shown in figure 3.10 which is lower than slac2-a RBD in melan-ln with the recovery of $57.5\% \pm 9.30$ as shown in figure 3.8 which suggests suggests slp2 has a stable

interaction with the Rab27a which makes them stay attached to Rab27a, preventing the replacement with a GFP-tagged Rab27a from the non-bleached region after bleaching and slac2-a has a dynamic interaction with the Rab27A so the slac2-a moves away from the Rab27a after bleaching which allows another GFP-tagged slac2-a to occupy.

This led to the idea of producing an artificial molecule to replace the rab Binding domain of the Slac2-a with the rab binding domain of slp2. RBD is the region where the Rab27-a binds on to the effectors. We hypothesized that this would enable Slac2-a to stably interact with Rab27a in a similar manner to Slp2. As predicted, the chimeric molecule highly reduced the percentage recovery of fluorescence from $57.5\% \pm 9.30$ (MLPH RBD in melan-ln) to $31.3\% \pm 8.07$ (slp2-mlph in melan-ln). We, therefore, conclude that...the interaction has been stabilized in the chimeric molecule and the difference in binding stability was observed between slp2-a and melanophilin.

3.2.1 slac2-a(full) in melan-a



MLph full in melan-a

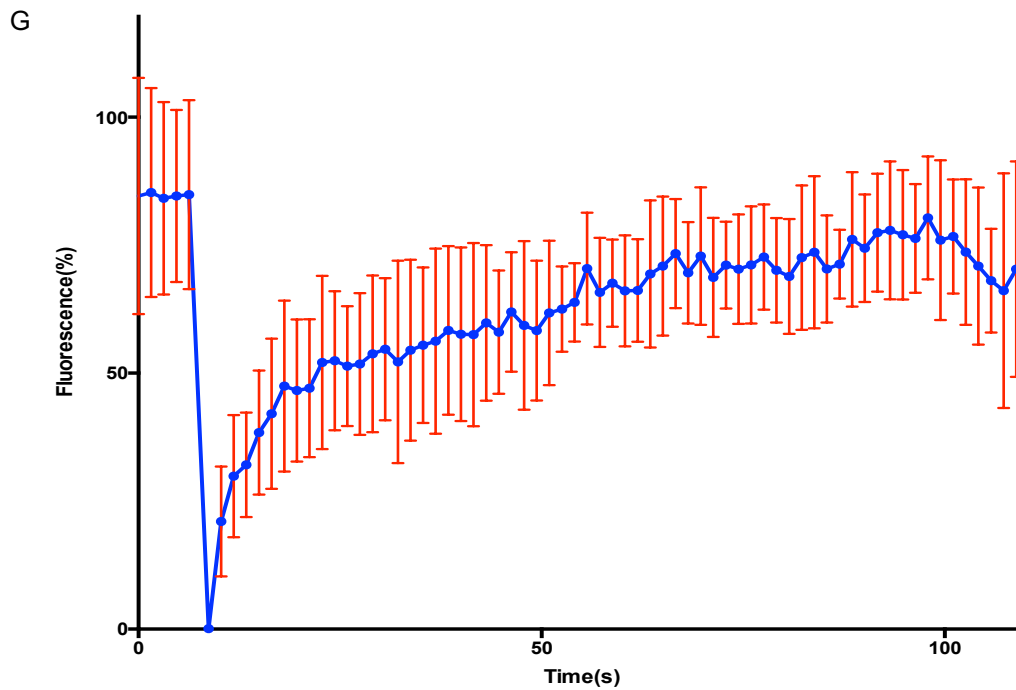


Figure 3.6. FRAP analysis of the dynamics of melanosomal GFP-MLPH in melan-a cells. FRAP micrographs showing time frames of GFP-MLPH associated with melanosome in melan-a at t=1s (initial fluorescence set at 100%), 6s (the fluorescence at the time of bleaching), 10, 20, 30, 75 (the gradual recovery of fluorescence) respectively. The amount of recovery ($60.4\% \pm 7.81$) shows that mlph has a dynamic interaction with Rab27-a as represented by the recovery curves of fluorescence intensity (G) allowing the new GFP-MLPH to bind to the melanosome after the bleaching. Shown are the mean \pm SD of different experiments (n=16)

3.2.2 Mlph- RBD in melan-a

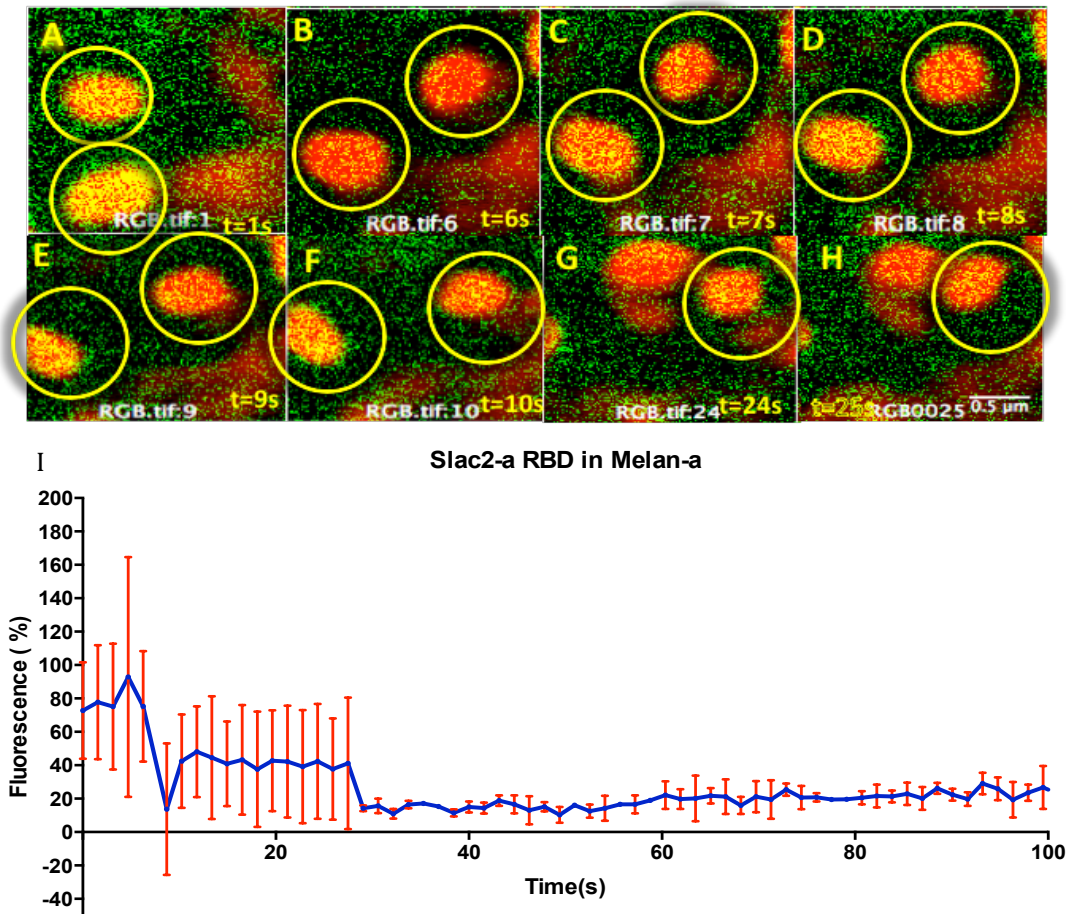


Figure 3.7. FRAP analysis of the dynamics of melanosomal GFP-MLPH RBD in melan-a cells. FRAP micrographs showing time frames (A, B, C, D, E, F, G, H) of GFP-MLPH associated with melanosome in melan-a at t=1s (initial fluorescence set at 100%), 6s (the fluorescence at the time of bleaching), 7s-10s, 24s and at 25s (the gradual recovery of fluorescence) respectively. The amount of recovery ($52.5\% \pm 29.1$) shows that the rest of the parts of melanophilin such as myosin binding domain (MBD) and actin binding domain (ABD) play a role in the dynamic nature of melanophilin with the melanosome as represented by the recovery curves of fluorescence intensity(I). Shown are the mean \pm SD of different experiments (n=7).

3.2.3 Mlph RBD in melan-In

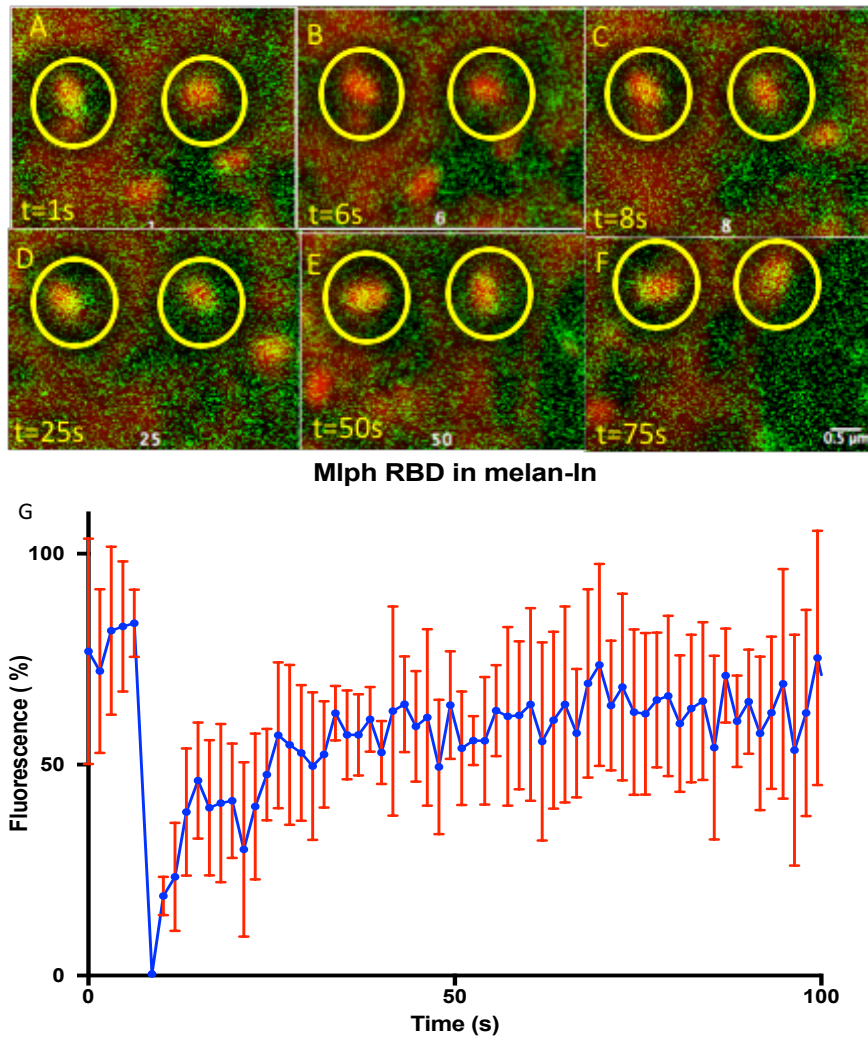


Figure 3.8. FRAP analysis of the dynamics of melanosomal GFP-MLPH RBD in melan-In cells. FRAP micrographs showing time frames (A, B, C, D, E, F) of GFP-MLPH associated with melanosome in melan-In (in the absence of endogenous melanophilin) at t=1s (initial fluorescence set at 100%), 6s (the fluorescence at the time of bleaching), 8s, 25s, 50s and at 75s (the gradual recovery of fluorescence) respectively. The amount of recovery ($57.5\% \pm 9.30$) shows it slightly has a greater recovery than the mlph full in melan-a due to the absence of endogenous melanophilin which will be competing with the GFP-MLPH. It also proves that mlph has a dynamic interaction with Rab27-a as represented by the recovery curves of fluorescence intensity (G). Shown are the mean \pm SD of different experiments (n=5).

3.2.4 Mlph in melan-d

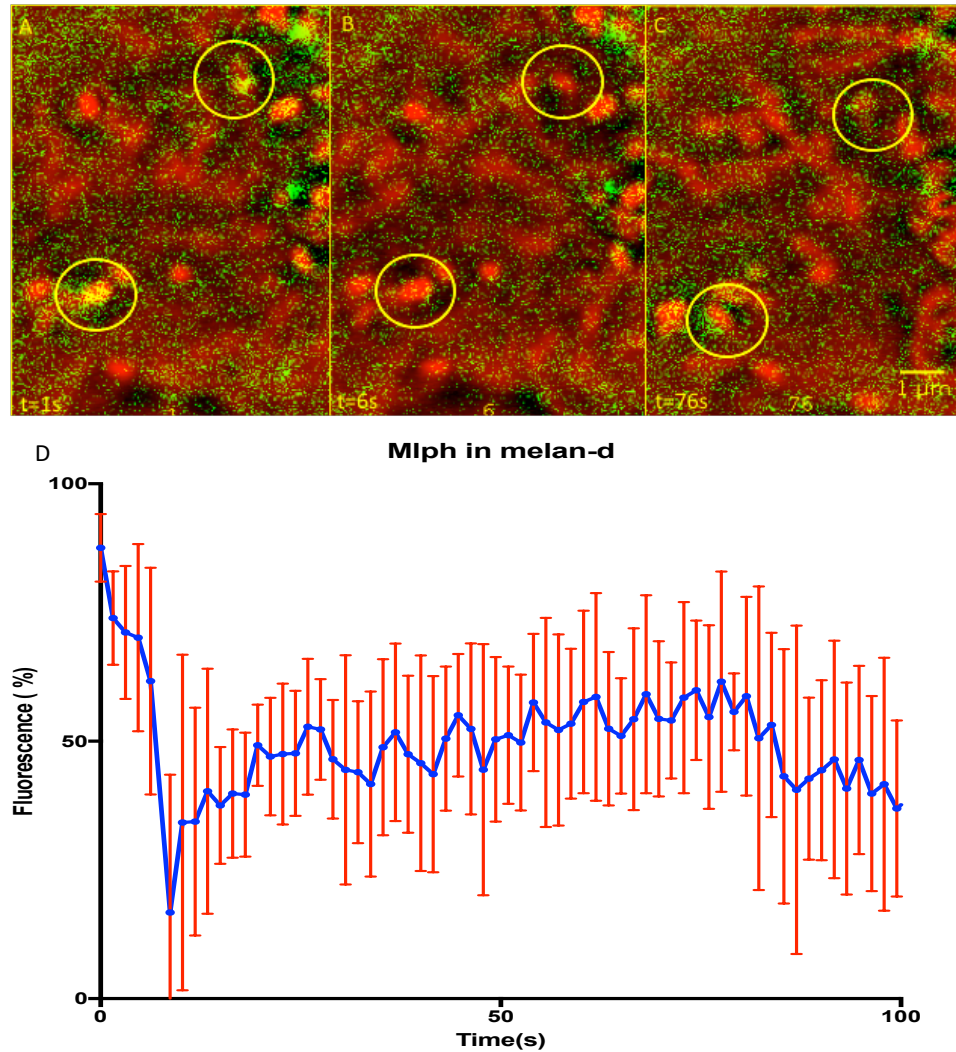


Figure 3.9. FRAP analysis of the dynamics of melanosomal GFP-MLPH RBD in melan-d cells. FRAP micrographs showing time frames (A, B, C) of GFP-MLPH associated with melanosome in melan-d (in the absence of myosin) at t=1s (initial fluorescence set at 100%) ,6s (the fluorescence at the time of bleaching) and at 76s (the gradual recovery of fluorescence) respectively. The amount of recovery ($43.72\% \pm 10.7$) shows that there is not much difference in the absence of myosin Va. It also confirms mlpH has a dynamic interaction with Rab27-a compared to slp2 interactions with melanosome as represented by the recovery curves of fluorescence intensity(D). Shown are the mean \pm SD of different experiments (n=7).

3.3 Frap analysis of the dynamics of Slp2 in the cell lines melan-a suggesting that it has a stable interaction.

To study the interaction of SLP2-a with Rab27a, frap was performed on GFP tagged SLP2-a in melan-a and the recovery rates indicated that it has a stable interaction with Rab27-a.

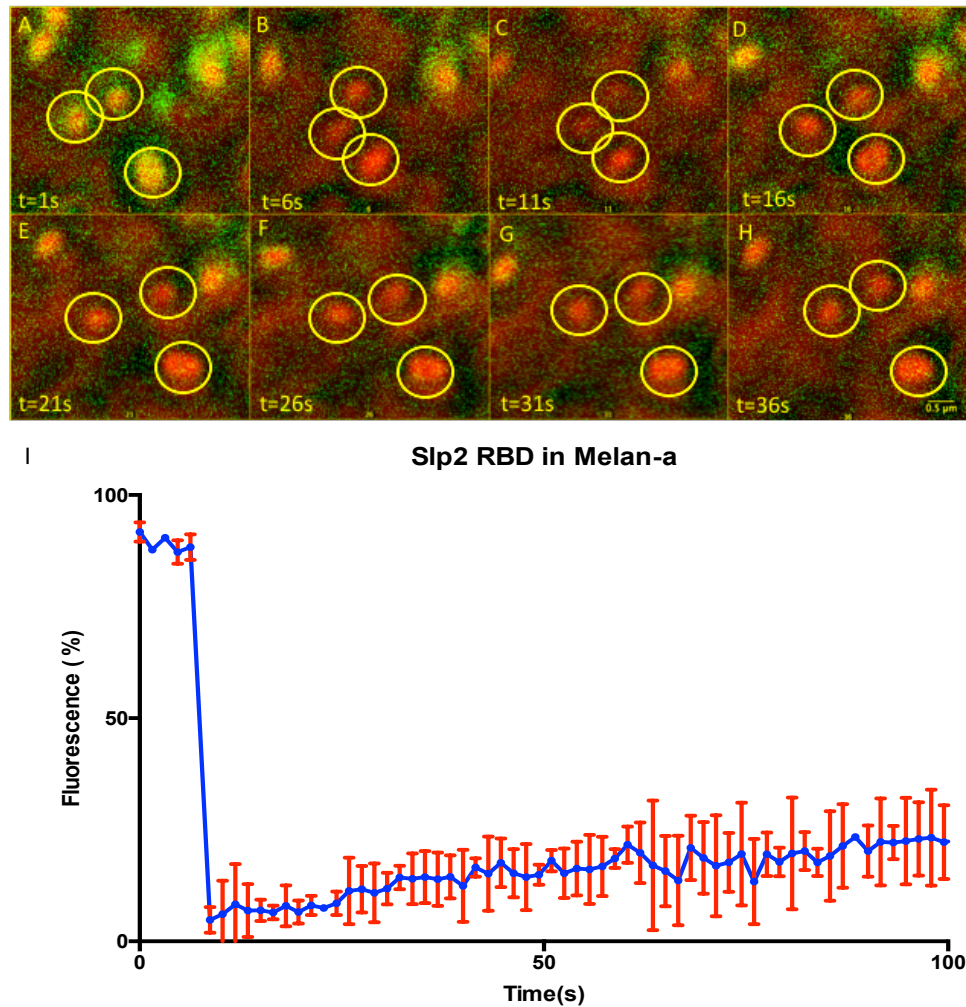


Figure 3.10 FRAP analysis of the dynamics of melanosomal GFP-SLP2 in melan-a cells. FRAP micrographs showing time frames (A, B, C, D, E, F, G, H) of GFP-SLP2 associated with melanosome in melan-a at t=1s (initial fluorescence set at 100%) ,6s (the fluorescence at the time of bleaching) and at 11s,16s, 21s, 26s, 31s and 36s (the gradual recovery of fluorescence) respectively. The amount of recovery ($27.1\% \pm 8.51$) shows that slp2 has a stable interaction with Rab27a as represented by the recovery curves of fluorescence intensity (I). Shown are the mean \pm SD of different experiments (n=20).

3.4 Chimeric Molecule (slp2-mlph Chimera) in Melan-In

The findings of the interaction of the Rab27a effectors slp2 and melanophilin, with Rab27a whereas mlph has a dynamic interaction and slp2 has a stable interaction lead to the idea of constructing a chimeric molecule to have a stable interaction when the gene encoding the RBD of mlph is replaced by the gene encoding the RBD of slp2-a. In the previous experiments, it was found out that RBD of mlph has a dynamic interaction and RBD SLP2-a has a stable interaction with Rab 27a. As expected, the fluorescence recovery of mlph-RBD in melan-In with the recovery of $57.5\% \pm 9.30$ was reduced to $31.3\% \pm 8.07$ in chimera slp2-mlph in melan-a as shown in figure 3.12 which confirms that the RBD of slp2 has reduced the dynamic nature of melanophilin and improved stability with Rab27-a. This supports the hypothesis that RBD region of effector protein slp2 gives a stable interaction with Rab27a and the RBD region of the effector protein mlph has a dynamic interaction. The diagrams given below show the structure of Slp2, mlph, and the chimeric molecule.

(A) Slp2



(B) Slac2-a



(C) Chimeric molecule

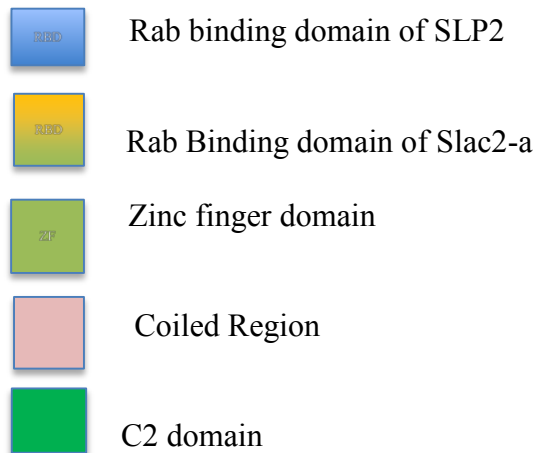


Figure 3.11. Construction of chimera. A and B shows the representation of the domain structure of Slp2 and Mlph showing the RBD regions clearly which believed to be involved in the dynamic and stable interaction of the effectors with the Rab27A. Then the representation of the chimeric molecule(C) is shown with the RBD region of Mlph is being replaced by the RBD region of SLP2 which is expected to have a stable interaction with Rab27A.

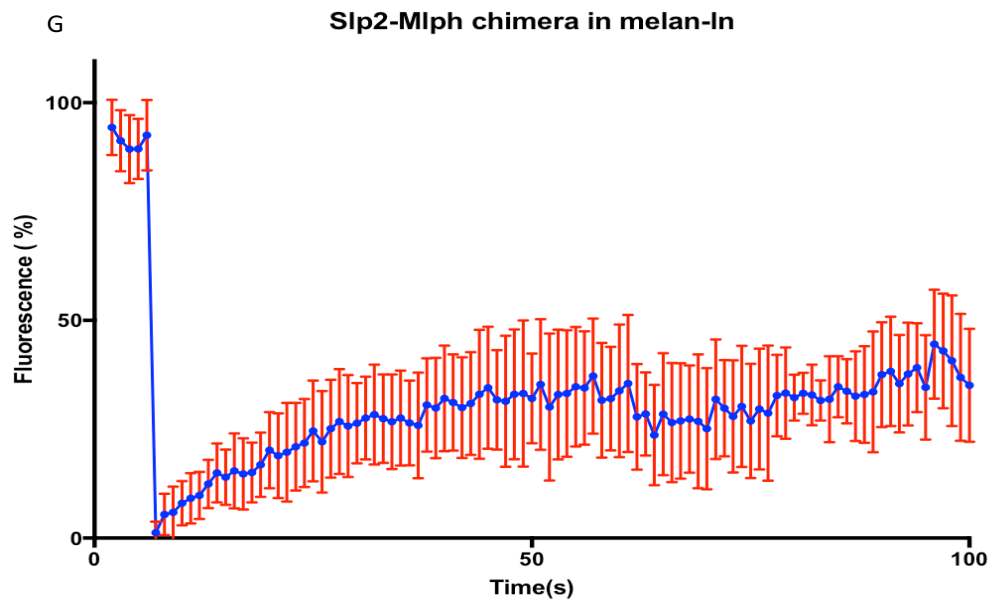
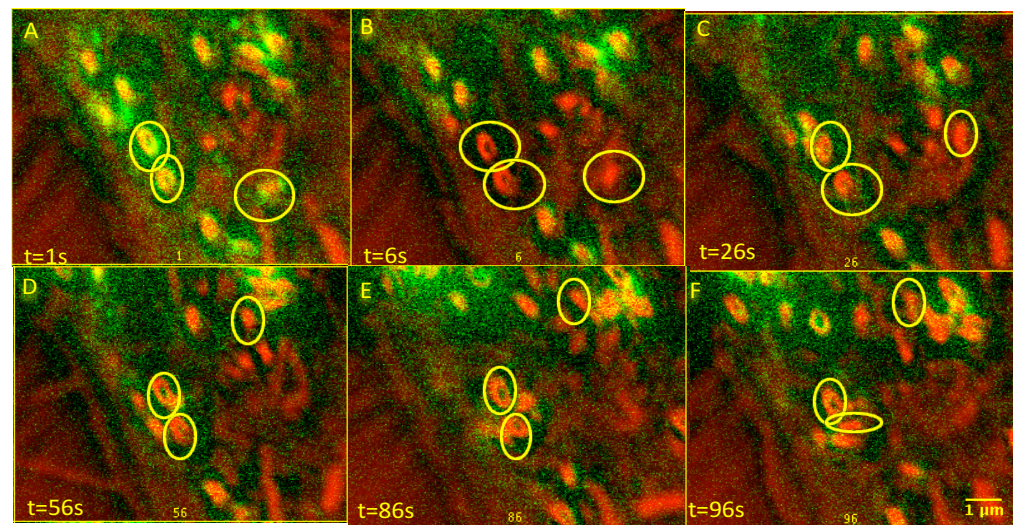


Figure 3.12. FRAP analysis of the dynamics of melanosomal GFP-Slp2-Mlph chimera in melan-In cells. FRAP micrographs showing time frames (A, B, C, D, E, F, G, H) of GFP-SLP2-Mlph chimera associated with melanosome in melan-In at t=1s (initial fluorescence set at 100%) ,6s (the fluorescence at the time of bleaching) and at 26s, 56s, 86s and 96s (the gradual recovery of fluorescence) respectively. The amount of recovery ($31.3\% \pm 8.07$) shows as represented by the recovery curves of fluorescence intensity(I), that the fluorescence level recovery is highly reduced with the help of RBD of Slp2 from 57.5 % (MLPH in melan-In) to 30.7%. Shown are the mean \pm SD of different experiments (n=16).

3.5 Summary

The table and the graph given below summarises the percentage recovery of different proteins in different cell lines. Rab27 in all cell lines doesn't recover much which indicate that it has a stable interaction with the melanosomes. By maintaining the low recovery even with the chimera which highly reduces the binding of the Rab27 effectors of slp2 and mlph, it proves that the effectors don't control the interaction of Rab27-a with the melanosome.

The Rab27-a effector mlph in cell lines recovers so it has a dynamic interaction with Rab27-a whereas slp2-a has a stable interaction with Rab27-a as it doesn't recover much. The slp2-mlph chimera recovers lesser as expected and it further supports the finding that slp2 has a stable interaction and RBD controls the interaction of the effectors with Rab27-a.

Cell type	% Fluorescence recovery of Rab27-a	% Fluorescence recovery of chimeric molecule (which reduces the binding of slp2 & mlph)	% Fluorescence recovery of melanophilin full	% Fluorescence Recovery melanophilin RBD	% Fluorescence Recovery of slp2	% Fluorescence Recovery of chimeric molecule slp2-mlph
Melan-a	15.4%±4.66 (n=6)	22.5%±9.46 (n=29)	60.4%±7.81 (n=16)	52.5%±29.1 (n=7)	27.1±8.51 (n=20)	Not performed
Melan-ln	14.8%±6.78 (n=5)	Not performed	Not performed	57.5%±9.30 (n=5)	Not performed	31.3%±8.07 (n=16)
Melan-ashen	25.3%±9.13 (n=20)	Not performed	Not performed	Not performed	Not performed	Not performed
Melan-d	Not performed	Not performed	Not performed	43.72%±10.7 (n=7)	Not performed	Not performed

Table 3.1 Average percentage recovery (mean \pm SD) The table shows the mean Intensity level of GFP for cell lines with different protein expression. n states the number of experiments done to obtain the mean value. Shown are the mean \pm SD of different experiments (n).



Figure 3.13. Average percentage recovery. The above graphs show the mean Intensity level of GFP of the experiments performed at each time point for cell lines with different protein expression. At the initial stage, the graph shows almost 100% fluorescent level and at the time of bleach, all of the lines almost reach zero and recovers differently according to various involvement of proteins in different cell lines.

Chapter 4

Conclusion & Discussion

The aim of this project was to understand the mechanism of the interaction between the melanosome and the tri-partite complex consisting of the proteins Rab27a and its effectors slp2-a and melanophilin. The mechanism of these proteins in transporting melanosome were analysed by performing the live cell imaging technique fluorescence recovery after photobleaching (FRAP) in different melanocyte lines, wild-type, melan-ln (lacking melanophilin), melan-ashen (lacking Rab27-a) and melan-d (lacking myosin Va).

Firstly, the role of Rab27-a in the formation of tri-partite complex to transport the melanosome was investigated. The importance of Rab27-a in the transport of melanosome was experimented in previous studies and our findings are consistent with the previous data. One of the study was staining of Rab27A in wild type cells Mlph antibodies disclosed that the loss of Rab27-a highly affects the binding of Mlph to melanosome. (Alistair Hume, Dmitry, Abul 2007).

The fluorescence intensity of Rab27-a in the wild-type and mutant cell lines recovered to $15.4\% \pm 4.66$ suggesting that it has a stable interaction with the melanosome (figure 3.1.2). When this was repeated in mutant cell lines, GFP-tagged Rab27A in the melan-ln cell line, which lacks slac2-a, recovered to $14.8\% \pm 6.78$ (figure 3.1.4) and in Melan-ashen cells, which lacks the endogenous rab27A, recovered to about $25.3\% \pm 9.13$ (figure 3.1.3). This shows that Rab27-a doesn't constantly get replaced by an incoming GFP tagged Rab27 indicating that it has a stable interaction with melanosome.

We observed a faster recovery time with the Rab27A in the melan-ashen, which lack Rab27-a, compared to other cell lines. Rab27A has a better recovery in melan-ashen than in melan-a. Rab27A in melan-a, we expect the endogenous Rab27-a to play a role here in competing with the exogenous GFP-Rab-27a, which would reduce the fluorescence recovery

as the endogenous Rab27a occupies the complex preventing the exogenous from attaching in to the tri partite complex. Overall, the protein Rab27-a in the cell lines melan-a, melan-ln and melan-ashen shows a reduced percentage fluorescence intensity recovery, which suggests that it has a stable interaction with the melanosome. The percentage fluorescence intensity recovery ($14.8\% \pm 6.78$ (figure 3.1.4)) of Rab27A in melan-ln indicate that melanophilin doesn't control the interaction of Rab27-a with the melanosome as there is a lower percentage recovery even in the absence of melanophilin.

Then, the role of slp2 in the stable nature of Rab27A with the melanosome was examined. Although the interaction of Rab27a with the pigment granules was seen in the absence of Mlph, we were unable to test whether the interaction depends on slp2 due to the availability of cell line lacking slp2. So to confirm the effect of slp2 on Rab 27A and to re-confirm the involvement of Mlph in the stabilization of Rab27a with the melanosome, mutant Rab27 was made, which highly reduces the binding of slac2-a and slp2 on Rab27A.

FRAP was carried out with the Rab27-a chimeric protein in the wild type cell line which showed a recovery of $22.5\% \pm 9.46$ which assured us that both Slac2-a and Slp2 do not regulate the stable nature of Rab27a with the melanosome.

Next, the behavior of Rab27A effectors alone were tested in different cell lines. We transfected melanophilin(full) with the regions, Rab Binding Domain (RBD), Melanophilin Binding Domain (MBD) and Actin Binding Domain (ABD). The wild-type cells had a recovery of $60.4\% \pm 7.81$ and melanophilin RBD recovered to $52.5\% \pm 29.1$ which shows that ABD and MBD play an important role in the dynamic nature of melanophilin with the Rab27a. Mlph-RBD in melan-ln recovered to $57.5\% \pm 9.30$ showing that it recovers better in melan-ln than in melan-a as in melan-a the endogenous melanophilin will be competing with the GFP-

mlph. When GFP-slp2 was seen in melan-a, it only recovered to about 27.1%±8.51. These findings imply that slac2-a has a dynamic nature with rab27-a, as there is a higher recovery of the fluorescence intensity due to the constant replacement of the GFP-mlph once the bleaching of GFP is performed. Whereas slp2 is suspected to have a stable interaction with rab27-a as the fluorescence intensity doesn't recover much.

The above discoveries led to the idea of producing an artificial molecule to replace the rab Binding domain of the Slac2-a with the rab binding domain of slp2. RBD is the region where the Rab27-a binds on to the effectors. We hypothesized that this would enable Slac2-a to stably interact with Rab27a in a similar manner to Slp2. Figure 3.11 shows the structure of Slp2, Slac2-a, and the chimeric molecule. As predicted, the chimeric molecule highly reduced the percentage recovery of fluorescence from 57.5 % (mlph RBD in melan-In) to 31.3% (slp2-mlph in melan-In). stabilizing the interaction of the chimera slp2-mlph with the Rab27-a.

This study concludes that Rab27-a has a stable interaction with melanosome, the Rab27-a effectors slp2 and mlph don't control the interaction of Rab27-a with melanosome. It also provides evidence that slp2 has a stable interaction with Rab27-a, mlph has a dynamic interaction with Rab27-a and this nature depends on the rab binding domains of both effectors. And, it gives support to the idea that the interaction of mlph with Rab27-a can be stabilized if the RBD of mlph is altered with RBD of slp2.

Chapter 5

References

- Ali, M. Y., Krementsova, E. B., Kennedy, G. G., Mahaffy, R., Pollard, T. D., Trybus, K. M., & Warshaw, D. M. (2007). Myosin Va maneuvers through actin intersections and diffuses along microtubules. *Proceedings of the National Academy of Sciences*, *104*(11), 4332–4336.
<https://doi.org/10.1073/pnas.0611471104>
- Ando, H., Ichihashi, M., & Hearing, V. J. (2009). Role of the Ubiquitin Proteasome System in Regulating Skin Pigmentation. *International Journal of Molecular Sciences*, *10*(10), 4428–4434. <https://doi.org/10.3390/ijms10104428>
- Ando, H., Niki, Y., Ito, M., Akiyama, K., Matsui, M. S., Yarosh, D. B., & Ichihashi, M. (2012). Melanosomes are transferred from melanocytes to keratinocytes through the processes of packaging, release, uptake, and dispersion. *The Journal of Investigative Dermatology*, *132*(4), 1222–1229.
<https://doi.org/10.1038/jid.2011.413>
- Andrei A Tokarev, Aixa Alfonso, and Nava Segev. (2009). Overview of Intracellular Compartments and Trafficking Pathways.
- Bahadoran, P., Aberdam, E., Mantoux, F., Buscà, R., Bille, K., Yalman, N., ... Ballotti, R. (2001). Rab27a: A key to melanosome transport in human melanocytes. *The Journal of Cell Biology*, *152*(4), 843–850.
- Bahadoran, P., Busca, R., Chiaverini, C., Westbroek, W., Lambert, J., Bille, K., ... Ballotti, R. (2003). Characterization of the Molecular Defects in Rab27a, Caused by RAB27A Missense Mutations Found in Patients with Griscelli Syndrome. *Journal of Biological Chemistry*, *278*(13), 11386–11392.
<https://doi.org/10.1074/jbc.M211996200>
- Bastiaens, P. and Squire, A. (1999). "Fluorescence lifetime imaging microscopy: spatial resolution of biochemical processes in the cell." *Trends Cell Biol.* **9**: 48-52
- Beaumont, K. A., Hamilton, N. A., Moores, M. T., Brown, D. L., Ohbayashi, N., Cairncross, O., Stow, J. L. (2011). The Recycling Endosome Protein Rab17 Regulates Melanocytic Filopodia Formation and Melanosome Trafficking. *Traffic*, *12*(5), 627–643. <https://doi.org/10.1111/j.1600-0854.2011.01172.x>
- Bhattacharya, D., Mazumder, A., Miriam, S. A. and Shivashankar, G. V. (2006). "EGFP- Tagged Core and Linker Histones Diffuse via Distinct Mechanisms within Living Cells." *Biophysical Journal* **91**(6): 2326-2336.

- Brito, F. C., & Kos, L. (2008). Timeline and distribution of melanocyte precursors in the mouse heart. *Pigment Cell & Melanoma Research*, 21(4), 464–470.
<https://doi.org/10.1111/j.1755-148X.2008.00459.x>
- Cardullo, RA.; Mungovan, RM.; Wolf, DE. Imaging membrane organization and dynamics. In: Dewey, G., editor. *Biophysical and Biochemical Aspects of Fluorescence Spectroscopy*. Plenum Press; New York: 1991. p. 231-260.
- Carla De Los Santos, Ching-Wei Chang, Mary-Ann Mycek and Richard (2015). FRAP, FLIM and FRET: Detection and analysis of cellular dynamics on a molecular scale using fluorescence microscopy. 82(0):587-604.
- Chabrilat, M. L. (2005). Rab8 Regulates the Actin-based Movement of Melanosomes. *Molecular Biology of the Cell*, 16(4), 1640–1650.
<https://doi.org/10.1091/mbc.E04-09-0770>
- Chang, L., Barlan, K., Chou, Y.-H., Grin, B., Lakonishok, M., Serpinskaya, A. S., ... Goldman, R. D. (2009). The dynamic properties of intermediate filaments during organelle transport. *Journal of Cell Science*, 122(16), 2914–2923.
<https://doi.org/10.1242/jcs.046789>
- Chen, Y. A., & Scheller, R. H. (2001). SNARE-mediated membrane fusion. *Nature Reviews. Molecular Cell Biology*, 2(2), 98–106.
<https://doi.org/10.1038/35052017>
- Cichorek, M., Wachulska, M., Stasiewicz, A., & Tymińska, A. (2013). Skin melanocytes: biology and development. *Advances in Dermatology and Allergology*, 1, 30–41. <https://doi.org/10.5114/pdia.2013.33376>
- Conibear E, Tam Y. The endocytic pathway. In: Segev N, editor. *Trafficking Inside Cells: Pathways, Mechanisms and Regulation*. Austin/New York: Landes Bioscience/Springer Science+Business Media; 2009. pp. 67–83.
- Constantin Kappel and Roland Eils, 2004. resolution, Fluorescence recovery after photobleaching with the Leica TCS SP2, German Cancer Research Center.
<http://www.bio.brandeis.edu/edtest/Publish/Applications%20notes/Leica%20tutorials/FRAP.pdf> .
- Cooper, G. (2000). *The Cell: A Molecular Approach*. (2nd ed.). Sunderland (MA): Sinauer Associates.
- Cooper, G. M., & Hausman, R. E. (2007). *The cell: a molecular approach* (4th ed). Washington, D.C.: Sunderland, Mass: ASM Press; Sinauer Associates.

- Coquelle, F. M., Vitre, B., & Arnal, I. (2009). Structural basis of EB1 effects on microtubule dynamics. *Biochemical Society Transactions*, 37(5), 997–1001. <https://doi.org/10.1042/BST0370997>
- Costaguta G, Payne G. Overview of protein trafficking mechanisms. In: Segev N, editor. *Trafficking Inside Cells: Pathways, Mechanisms and Regulation*. Austin/New York: Landes Bioscience/Springer Science+Business Media; 2009. pp. 105–14.
- Costes S.V., Daelemans D., Cho E.H., Dobbin Z., Pavlakis G., Lockett S. 2004. Automatic and quantitative measurement of protein-protein colocalization in live cells. *Biophys. J.* 86:3993–4003.
- De Los Santos, C., Chang, C.-W., Mycek, M.-A., & Cardullo, R. A. (2015). FRAP, FLIM, and FRET: Detection and analysis of cellular dynamics on a molecular scale using fluorescence microscopy: FRAP, FLIM, AND FRET: DETECTION AND ANALYSIS. *Molecular Reproduction and Development*, 82(7–8), 587–604. <https://doi.org/10.1002/mrd.22501>
- Del Marmol, V., Solano, F., Sels, A., Huez, G., Libert, A., Lejeune, F., & Ghanem, G. (1993). Glutathione depletion increases tyrosinase activity in human melanoma cells. *The Journal of Investigative Dermatology*, 101(6), 871–874.
- Diplom-Biologe Markus Ulrich (2008) Tropical – Software for quantitative analysis of FRAP experiments. PhD thesis, Ruperto-Carola University of Heidelberg, Germany.
- Dominguez, R., & Holmes, K. C. (2011). Actin Structure and Function. *Annual Review of Biophysics*, 40(1), 169–186. <https://doi.org/10.1146/annurev-biophys-042910-155359>
- Donaldson J, Segev N. Regulation and coordination of intracellular trafficking: an overview. In: Segev N, editor. *Trafficking Inside Cells: Pathways, Mechanisms and Regulation*. Austin/New York: Landes Bioscience/Springer Science+Business Media; 2009. pp. 329–41.
- Elson EL. Fluorescence correlation spectroscopy: past, present, future. *Biophys J.* 101:2855–2870. [PubMed: 22208184]

- Elson DS, Munro I, Requejo-Isidro J, McGinty J, Dunsby C, Galletly N, Stamp GW, Neil MAA, Lever MJ, Kellett PA, Dymoke-Bradshaw A, Hares J, French PMW. Real-time time-domain fluorescence lifetime imaging including single-shot acquisition with a segmented optical image intensifier. *New J Phys.* 2004; 6:180–192.
- Esposito A, Gerritsen HC, Wouters FS. Optimizing frequency-domain fluorescence lifetime sensing for high-throughput applications: photon economy and acquisition speed. *J Opt Soc Am A Opt Image Sci Vis.* 2007; 24:3261–3273. [PubMed: 17912319]
- Fletcher, D. A., & Mullins, R. D. (2010). Cell mechanics and the cytoskeleton. *Nature*, 463(7280), 485–492. <https://doi.org/10.1038/nature08908>
- Fontanesi, L., Scotti, E., Allain, D., & Dall’Olio, S. (2014). A frameshift mutation in the *melanophilin* gene causes the dilute coat colour in rabbit (*Oryctolagus cuniculus*) breeds. *Animal Genetics*, 45(2), 248–255. <https://doi.org/10.1111/age.12104>
- Fukuda, M., T.S. Kuroda, and K. Mikoshiba, *Slac2-a/melanophilin, the missing link between Rab27 and myosin Va: implications of a tripartite protein complex for melanosome transport.* *J Biol Chem*, 2002. 277(14): p. 12432-6.
- Gennerich, A., & Vale, R. D. (2009). Walking the walk: how kinesin and dynein coordinate their steps. *Current Opinion in Cell Biology*, 21(1), 59–67. <https://doi.org/10.1016/j.ceb.2008.12.002>
- GraphPad Prism, 2016. <http://www.graphpad.com/scientific-software/prism/>
- Giampiero Cai and Mauro Cresti (2012). Are kinesins required for organelle trafficking in plant cells?. *Front Plant Sci.* 3:170
- Haass, N. K., Smalley, K. S. M., Li, L., & Herlyn, M. (2005). Adhesion, migration and communication in melanocytes and melanoma. *Pigment Cell Research / Sponsored by the European Society for Pigment Cell Research and the International Pigment Cell Society*, 18(3), 150–159. <https://doi.org/10.1111/j.1600-0749.2005.00235.x>
- Hammer, J. A., & Sellers, J. R. (2011). Walking to work: roles for class V myosins as cargo transporters. *Nature Reviews Molecular Cell Biology.* <https://doi.org/10.1038/nrm3248>

- Hancock, W. O. (2014). Bidirectional cargo transport: moving beyond tug of war. *Nature Reviews Molecular Cell Biology*, 15(9), 615–628.
<https://doi.org/10.1038/nrm3853>
- Hardin, J., & Bertoni, G. (2016). *Becker's World of the cell* (Nineth Edition). Boston: Pearson.
- Hellen C. Ishikawa-Ankerhold, Richard Ankerhold and Gregor P. C. Drummen. Advanced Fluorescence Microscopy Techniques – FRAP, FLIP, FLAP, FRET and FLIM. *Molecules* 2012, 17, 4047-4132
- Hess, S. T., Huang, S., Heikal, A. A. and Webb, W. W. (2002). "Biological and Chemical Applications of Fluorescence Correlation Spectroscopy: A Review." *Biochemistry* 41(3): 697-705.
- Hu, D.-N., Simon, J. D., & Sarna, T. (2008). The role of ocular melanin in ophthalmic physiology and pathology. *Photochemistry and Photobiology*, 84(3), 639–644. <https://doi.org/10.1111/j.1751-1097.2008.00316.x>
- Hua Z, Graham T. The Golgi apparatus. In: Segev N, editor. Trafficking Inside Cells: Pathways, Mechanisms and Regulation. Austin/New York: Landes Bioscience/Springer Science+Business Media; 2009. pp. 42–66.
- Hume, A. N., Collinson, L. M., Rapak, A., Gomes, A. Q., Hopkins, C. R., & Seabra, M. C. (2001). Rab27a regulates the peripheral distribution of melanosomes in melanocytes. *The Journal of Cell Biology*, 152(4), 795–808.
- Hume, A. N., & Seabra, M. C. (2011). Melanosomes on the move: a model to understand organelle dynamics. *Biochemical Society Transactions*, 39(5), 1191–1196. <https://doi.org/10.1042/BST0391191>
- Hume, A.N., et al., *A coiled-coil domain of melanophilin is essential for Myosin Va recruitment and melanosome transport in melanocytes*. *Mol Biol Cell*, 2006. 17(11): p. 4720-35.
- Hurst, J. H. (2013). Richard Scheller and Thomas Südhof receive the 2013 Albert Lasker Basic Medical Research Award. *Journal of Clinical Investigation*, 123(10), 4095–4101. <https://doi.org/10.1172/JCI72681>
- Hutagalung, A. H., & Novick, P. J. (2011). The role of Rab GTPases in Membrane Traffic and Cell Physiology. *Physiological Reviews*, 91(1), 119–149.
<https://doi.org/10.1152/physrev.00059.2009>

- Ikegami, K., & Setou, M. (2010). Unique post-translational modifications in specialized microtubule architecture. *Cell Structure and Function*, 35(1), 15–22. ImageJ, 2016. <http://rsbweb.nih.gov/ij>
- Ishida, M., Ohbayashi, N., & Fukuda, M. (2015). Rab1A regulates anterograde melanosome transport by recruiting kinesin-1 to melanosomes through interaction with SKIP. *Scientific Reports*, 5, 8238. <https://doi.org/10.1038/srep08238>
- Ishida, M., Ohbayashi, N., Maruta, Y., Ebata, Y., & Fukuda, M. (2012). Functional involvement of Rab1A in microtubule-dependent anterograde melanosome transport in melanocytes. *Journal of Cell Science*, 125(21), 5177–5187. <https://doi.org/10.1242/jcs.109314>
- Jennifer Lippincott-Schwartz, Nihal Altan-Bonnet and George H. Patterson. (2003). *Nature cell Biology* 5, S7-S14
- Jody P. Ebanks, R. Randall Wickett and Raymond E. Boissy, mechanisms regulating skin pigmentation: The rise and fall of complexation coloration. *Int J Mol Sci.* 2009 Sep;10(9): 4066-4087
- Jody P. Ebanks, R. Randall Wickett and Raymond E. Boissy, mechanisms regulating skin pigmentation: The rise and fall of complexation coloration. *Int J Mol Sci.* 2009 Sep;10(9): 4066-4087
- John A. Hammer III & James R. Sellers, Walking to work: roles for class V myosins as cargo transporters. *Nature Reviews Molecular Cell Biology* 13,13-2(2012)
- John A. Mercer, P.K.s., Marjorie C. Strobel, Neal G. Copeland & Nancy A. Jenkins, *Novel myosin heavy chain encoded by murine dilute coat colour locus.*
- Jordens, I., et al., Rab7 and Rab27a control two motor protein activities involved in melanosomal transport. *Pigment Cell Res*, 2006. **19**(5): p. 412-23.
- Kaufman, E. N. and Jain, R. K. (1990). "Quantification of transport and binding parameters using fluorescence recovery after photobleaching. Potential for in vivo applications." *Biophys. J.* **58**(4): 873-885.
- Kloc, M., Kubiak, J. Z., Li, X. C., & Ghobrial, R. M. (2014). The newly found functions of MTOC in immunological response. *Journal of Leukocyte Biology*, 95(3), 417–430. <https://doi.org/10.1189/jlb.0813468>

- Kogel, T. (2010). Distinct roles of myosin Va in membrane remodeling and exocytosis of secretory granules. *Traffic.*, *11*, 637–650.
- Kukimoto-Niino, M., et al., *Structural basis for the exclusive specificity of Slac2-a/melanophilin for the Rab27 GTPases*. *Structure*, 2008. **16**(10): p. 1478-90.
- Kural, C., Serpinskaya, A. S., Chou, Y.-H., Goldman, R. D., Gelfand, V. I., & Selvin, P. R. (2007). Tracking melanosomes inside a cell to study molecular motors and their interaction. *Proceedings of the National Academy of Sciences*, *104*(13), 5378–5382. <https://doi.org/10.1073/pnas.0700145104>
- Kuroda, T. S., Ariga, H., & Fukuda, M. (2003). The Actin-Binding Domain of Slac2-a/Melanophilin Is Required for Melanosome Distribution in Melanocytes. *Molecular and Cellular Biology*, *23*(15), 5245–5255. <https://doi.org/10.1128/MCB.23.15.5245-5255.2003>
- Kuroda, T.S. and M. Fukuda, *Rab27A-binding protein Slp2-a is required for peripheral melanosome distribution and elongated cell shape in melanocytes*. *Nat Cell Biol*, 2004. **6**(12): p. 1195-203.
- Labarchives.com. (2012, May 21). Phenotypic Mutation “quicksilver.” Retrieved from <https://mynotebook.labarchives.com/share/Mutagenetix/MjA0LjF8MzA4My8xNTcvVHJlZU5vZGUVMTV8NTE4LjE=>
- Lowery, J., Kuczarski, E. R., Herrmann, H., & Goldman, R. D. (2015). Intermediate Filaments Play a Pivotal Role in Regulating Cell Architecture and Function. *Journal of Biological Chemistry*, *290*(28), 17145–17153. <https://doi.org/10.1074/jbc.R115.640359>
- Machery-Nagel, 2015/Rev.09. Plasmid DNA purification user manual. http://www.mnnet.com/Portals/8/attachments/Redakteure_Bio/Protocols/Plasmid%20DNA%20Purification/UM_pDNA_NS.pdf
- Makar, A. B., McMartin, K. E., Palese, M., & Tephly, T. R. (1975). Formate assay in body fluids: application in methanol poisoning. *Biochemical Medicine*, *13*(2), 117–126.
- Marks, M. S., & Seabra, M. C. (2001). The melanosome: membrane dynamics in black and white. *Nature Reviews. Molecular Cell Biology*, *2*(10), 738–748. <https://doi.org/10.1038/35096009>

- Martin-Fernandez ML, Clarke DT. Single molecule fluorescence detection and tracking in mammalian cells: The state-of-the-art and future perspectives. *Int J Mol Sci.* 2012; 13:14742–14765. [PubMed: 23203092]
- Matesic, L. E., Yip, R., Reuss, A. E., Swing, D. A., O’Sullivan, T. N., Fletcher, C. F., ... Jenkins, N. A. (2001). Mutations in *Mlph*, encoding a member of the Rab effector family, cause the melanosome transport defects observed in leaden mice. *Proceedings of the National Academy of Sciences of the United States of America*, 98(18), 10238–10243. <https://doi.org/10.1073/pnas.181336698>
- Nagarajan N, Custer K, Bajjalieh S. Regulated secretion. In: Segev N, editor. *Trafficking Inside Cells: Pathways, Mechanisms and Regulation*. Austin/New York: Landes Bioscience/Springer Science+Business Media; 2009. pp. 84–102.
- Natarajan, V. T., Ganju, P., Singh, A., Vijayan, V., Kirty, K., Yadav, S., ... Gokhale, R. S. (2014). IFN- γ signaling maintains skin pigmentation homeostasis through regulation of melanosome maturation. *Proceedings of the National Academy of Sciences*, 111(6), 2301–2306. <https://doi.org/10.1073/pnas.1304988111>
- Oda, T., Iwasa, M., Aihara, T., Maéda, Y., & Narita, A. (2009). The nature of the globular- to fibrous-actin transition. *Nature*, 457(7228), 441–445. <https://doi.org/10.1038/nature07685>
- Pruess M, Weidman P, Nielsen E. How we study protein transport. In: Segev N, editor. *Trafficking Inside Cells: Pathways, Mechanisms and Regulation*. Austin/New York: Landes Bioscience/Springer Science+Business Media; 2009. pp. 15–41
- Ramalho, J.S., et al. 2001. Chromosomal mapping, gene structure, and characterization of the human and murine *RAB27B* gene. *BMC Genet.* 2:2
- ,Seabra, M. C., Ho, Y. K., and Anant, J. S. (1995) *J. Biol. Chem.* 270, 24420–24427, <http://www.jbc.org/content/277/28/25423.full.pdf>
- Randhawa, M., Huff, T., Valencia, J. C., Younossi, Z., Chandhoke, V., Hearing, V. J., & Baranova, A. (2009). Evidence for the ectopic synthesis of melanin in human adipose tissue. *FASEB Journal: Official Publication of the Federation of American Societies for Experimental Biology*, 23(3), 835–843. <https://doi.org/10.1096/fj.08-116327>

- Ranganathan, S., Radhakrishnan, N., & Vijayachandra, K. (2007). Changing skin color: Evolution and modern trends. *Indian Journal of Dermatology*, 52(2), 71. <https://doi.org/10.4103/0019-5154.33282>
- Rink J, Ghigo E, Kalaidzidis Y, et al. Rab conversion as a mechanism of progression from early to late endosomes. *Cell*. 2005;122(5):735–49. [PubMed]
- Rizo, J., & Xu, J. (2015). The Synaptic Vesicle Release Machinery. *Annual Review of Biophysics*, 44, 339–367. <https://doi.org/10.1146/annurev-biophys-060414-034057>
- Robinson, Christopher L. (2016) *MyosinVa and dynamic actin oppose minus-end directed microtubule motors to drive anterograde melanosome transport*. PhD thesis, University of Nottingham.
- Ross, J. L., Ali, M. Y., & Warshaw, D. M. (2008). Cargo transport: molecular motors navigate a complex cytoskeleton. *Current Opinion in Cell Biology*, 20(1), 41–47. <https://doi.org/10.1016/j.ceb.2007.11.006>
- Sakamoto, T., Amitani, I., Yokota, E., & Ando, T. (2000). Direct observation of processive movement by individual myosin V molecules. *Biochem. Biophys. Res. Commun.*, 272, 586–590. <https://doi.org/10.1006/bbrc.2000.2819>
- Sakamoto, T., Webb, M. R., Forgacs, E., White, H. D., & Sellers, J. R. (2008). Direct observation of the mechanochemical coupling in myosin Va during processive movement. *Nature*, 455, 128–132. <https://doi.org/10.1038/nature07188>
- Schmoltdt, A., Benthe, H. F., & Haberland, G. (1975). Digitoxin metabolism by rat liver microsomes. *Biochemical Pharmacology*, 24(17), 1639–1641.
- Scott, G., Leopardi, S., Printup, S., & Madden, B. C. (2002). Filopodia are conduits for melanosome transfer to keratinocytes. *Journal of Cell Science*, 115(Pt 7), 1441–1451.
- Segev N, editor. *Trafficking Inside Cells: Pathways, Mechanisms and Regulation*. Austin: Landes Bioscience and Springer Science+Business Media; 2009. pp. 103–438.
- Semenova I, Burakov A, Berardone N, Zaliapin I, Slepchenko B, Kashina A, Rodionov V. (2008). Actin dynamics is essential for myosin-based transport of membrane organelles. *Curr Biol*;18(20): 1581-6.

- Sheets, L., et al., Zebrafish melanophilin facilitates melanosome dispersion by regulating dynein. *Curr Biol*, 2007. **17**(20): p. 1721-34
- Singh, S. K., Kurfurst, R., Nizard, C., Schnebert, S., Perrier, E., & Tobin, D. J. (2010). Melanin transfer in human skin cells is mediated by filopodia--a model for homotypic and heterotypic lysosome-related organelle transfer. *FASEB Journal: Official Publication of the Federation of American Societies for Experimental Biology*, *24*(10), 3756–3769. <https://doi.org/10.1096/fj.10-159046>
- Singh, S. K., Nizard, C., Kurfurst, R., Bonte, F., Schnebert, S., & Tobin, D. J. (2008). The silver locus product (Silv/gp100/Pmel17) as a new tool for the analysis of melanosome transfer in human melanocyte-keratinocyte co-culture. *Experimental Dermatology*, *17*(5), 418–426. <https://doi.org/10.1111/j.1600-0625.2008.00702.x>
- Sitaram, A., & Marks, M. S. (2012). Mechanisms of Protein Delivery to Melanosomes in Pigment Cells. *Physiology*, *27*(2), 85–99. <https://doi.org/10.1152/physiol.00043.2011>
- Snider, J., Lin, F., Zahedi, N., Rodionov, V., Yu, C. C., & Gross, S. P. (2004). Intracellular actin-based transport: How far you go depends on how often you switch. *Proceedings of the National Academy of Sciences*, *101*(36), 13204–13209. <https://doi.org/10.1073/pnas.0403092101>
- Sprague, B. L., Pego, R. L., Stavreva, D. A. and McNally, J. G. (2004). "Analysis of Binding Reactions by Fluorescence Recovery after Photobleaching." *Biophysical Journal* 86: 3473-3495.
- Staleva, L., Manga, P., & Orlow, S. J. (2002). Pink-eyed dilution protein modulates arsenic sensitivity and intracellular glutathione metabolism. *Molecular Biology of the Cell*, *13*(12), 4206–4220. <https://doi.org/10.1091/mbc.E02-05-0282>
- Stanley, A. C., & Lacy, P. (2010). Pathways for Cytokine Secretion. *Physiology*, *25*(4), 218–229. <https://doi.org/10.1152/physiol.00017.2010>
- Strom, M., Hume, A. N., Tarafder, A. K., Barkagianni, E., & Seabra, M. C. (2002). A family of Rab27-binding proteins. Melanophilin links Rab27a and myosin Va function in melanosome transport. *The Journal of Biological Chemistry*, *277*(28), 25423–25430. <https://doi.org/10.1074/jbc.M202574200>

- Südhof, T. C. (2013). A molecular machine for neurotransmitter release: synaptotagmin and beyond. *Nature Medicine*, *19*(10), 1227–1231. <https://doi.org/10.1038/nm.3338>
- Tarafder, A. K., Bolasco, G., Correia, M. S., Pereira, F. J. C., Iannone, L., Hume, A. N., ... Seabra, M. C. (2014). Rab11b Mediates Melanin Transfer between Donor Melanocytes and Acceptor Keratinocytes via Coupled Exo/Endocytosis. *Journal of Investigative Dermatology*, *134*(4), 1056–1066. <https://doi.org/10.1038/jid.2013.432>
- Taruho S. Kuroda, Hiroyoshi Ariga, & Mitsunori Fukuda (2003). The Actin-Binding Domain of Sla2-a/Melanophilin is required for melanosome distribution in melanocytes. *Molecular Biology and cellular Biology*.
- Ronald D. Vale. (2003). Myosin V motor proteins: marching stepwise towards a mechanism. *J Cell Biology*. *163*(3): 445-450.
- Van Den Bossche, K., Naeyaert, J.-M., & Lambert, J. (2006). The quest for the mechanism of melanin transfer. *Traffic (Copenhagen, Denmark)*, *7*(7), 769–778. <https://doi.org/10.1111/j.1600-0854.2006.00425.x>
- Van Gele, M., Dynoodt, P., & Lambert, J. (2009). Griscelli syndrome: a model system to study vesicular trafficking. *Pigment Cell & Melanoma Research*, *22*(3), 268–282. <https://doi.org/10.1111/j.1755-148X.2009.00558.x>
- Vershinin, M., Carter, B. C., Razafsky, D. S., King, S. J., & Gross, S. P. (2007). Multiple-motor based transport and its regulation by Tau. *Proceedings of the National Academy of Sciences*, *104*(1), 87–92. <https://doi.org/10.1073/pnas.0607919104>
- Wachsmuth, M., Weidemann, T., Muller, G., Hoffmann-Rohrer, U. W., Knoch, T. A., Waldeck, W. and Langowski, J. (2003). "Analyzing Intracellular Binding and Diffusion with Continuous Fluorescence Photobleaching." *Biophys. J.* *84*(5): 3353-3363.
- Warshaw, D. M. (2005). Differential labeling of myosin V heads with quantum dots allows direct visualization of hand-over-hand processivity. *Biophys. J.*, *88*, L30–L32. <https://doi.org/10.1529/biophysj.105.061903>
- Wasmeier, C., Hume, A. N., Bolasco, G., & Seabra, M. C. (2008). Melanosomes at a glance. *Journal of Cell Science*, *121*(24), 3995–3999. <https://doi.org/10.1242/jcs.040667>

- Wäster, P., Eriksson, I., Vainikka, L., Rosdahl, I., & Öllinger, K. (2016). Extracellular vesicles are transferred from melanocytes to keratinocytes after UVA irradiation. *Scientific Reports*, *6*, 27890. <https://doi.org/10.1038/srep27890>
- Watanabe, T. M., & Higuchi, H. (2007). Stepwise Movements in Vesicle Transport of HER2 by Motor Proteins in Living Cells. *Biophysical Journal*, *92*(11), 4109–4120. <https://doi.org/10.1529/biophysj.106.094649>
- Wickstead, B., & Gull, K. (2011). The evolution of the cytoskeleton. *The Journal of Cell Biology*, *194*(4), 513–525. <https://doi.org/10.1083/jcb.201102065>
- Wilson, S.M., et al., *A mutation in Rab27a causes the vesicle transport defects observed in ashen mice*. Proc Natl Acad Sci U S A, 2000. **97**(14): p. 7933-8.
- Wu, S. K., Zeng, K., Wilson, I. A., & Balch, W. E. (1996). Structural insights into the function of the Rab GDI superfamily. *Trends in Biochemical Sciences*, *21*(12), 472–476.
- Wu, X., & Hammer, J. A. (2014). Melanosome transfer: it is best to give and receive. *Current Opinion in Cell Biology*, *29*, 1–7. <https://doi.org/10.1016/j.ceb.2014.02.003>
- Wu, X. S., Masedunskas, A., Weigert, R., Copeland, N. G., Jenkins, N. A., & Hammer, J. A. (2012). Melanoregulin regulates a shedding mechanism that drives melanosome transfer from melanocytes to keratinocytes. *Proceedings of the National Academy of Sciences of the United States of America*, *109*(31), E2101-2109. <https://doi.org/10.1073/pnas.1209397109>
- Wu, X. S., Rao, K., Zhang, H., Wang, F., Sellers, J. R., Matesic, L. E., ... Hammer, J. A. (2002). Identification of an organelle receptor for myosin-Va. *Nature Cell Biology*, *4*(4), 271–278. <https://doi.org/10.1038/ncb760>
- Xufeng Wu, John A Hammer (2014). Melanosome transfer: it is best to give and receive. *Current opinion in Cell Biology*. Volume 29, pages <https://doi.org/10.1016/j.ceb.2014.02.003>
- Xufeng Wu, Fei Eang, Kang Rao, James R. Sellers and John A. Hammer (2002). Rab27a is an essential component of melanosome receptor for myosin Va. *Cell*, *13*(5): 1735-1749.
- Yamaguchi, Y., & Hearing, V. J. (2009). Physiological factors that regulate skin pigmentation. *BioFactors*, *35*(2), 193–199. <https://doi.org/10.1002/biof.29>

- Yasuda, T., Saegusa, C., Kamakura, S., Sumimoto, H., & Fukuda, M. (2012). Rab27 effector Slp2-a transports the apical signaling molecule podocalyxin to the apical surface of MDCK II cells and regulates claudin-2 expression. *Molecular Biology of the Cell*, 23(16), 3229–3239. <https://doi.org/10.1091/mbc.E12-02-0104>
- Yasuda, T., S. Mrozowska, P., & Fukuda, M. (2015). Functional Analysis of Rab27A and Its Effector Slp2-a in Renal Epithelial Cells. In G. Li (Ed.), *Rab GTPases* (Vol. 1298, pp. 127–139). New York, NY: Springer New York. Retrieved from http://link.springer.com/10.1007/978-1-4939-2569-8_11
- Zhang, W.-B., Yao, L.-L., & Li, X. (2016). The Globular Tail Domain of Myosin-5a Functions as a Dimer in Regulating the Motor Activity. *Journal of Biological Chemistry*, 291(26), 13571–13579. <https://doi.org/10.1074/jbc.M116.724328>